For Reference

NOT TO BE TAKEN FROM THIS ROOM

Ex libris
universitatis
albertaensis

The University of Alberta
Printing Department
Edmonton, Alberta

Digitized by the Internet Archive
in 2024 with funding from
University of Alberta Library

https://archive.org/details/Vermeulen1973

THE UNIVERSITY OF ALBERTA

BEVERAGE ANTENNAS FOR BIO-TELEMETRY

by

© HENRY WILLIAM RICHARD VERMEULEN

A THESIS
SUBMITTED TO THE FACULTY OF GRADUATE STUDIES AND RESEARCH
IN PARTIAL FULFILMENT OF THE REQUIREMENTS FOR THE DEGREE
OF MASTER OF SCIENCE

DEPARTMENT OF ELECTRICAL ENGINEERING

EDMONTON, ALBERTA

FALL, 1973

ABSTRACT

The use of a long Beverage receiving antenna for wildlife telemetry is investigated. The antenna consists of long wires (0.8 miles) spanned at several heights above the ground, in both double-wire and ground-return configurations. Theoretical expressions are developed for losses along the antenna and for the signal coupled to the line from a small radiating loop used to simulate a radio-tagged animal. Experimental measurements made at frequencies of 29, 51 and 95 MHz on the Beverage antenna are compared both theoretically and experimentally with the signal received on an omnidirectional ground-plane antenna for the same frequencies and heights of 8, 22 and 38 feet. Good agreement between the theoretical and experimental results is achieved. It is shown that the Beverage antenna provides larger signals out to a distance that is dependent on the height of both antennas. However, in many low-power telemetry applications this cross-over point occurs well beyond the limiting range of the tower-mounted antenna and in such cases the Beverage antenna can significantly increase the system's range.

Although the signal coupled to the Beverage antenna decreases rapidly with distance from the wire, a grid of such wires can provide satisfactory coverage. Moreover, it is shown that the position of the loop antenna can be accurately located within this grid by measuring signals on the various wires of the grid. The wire-grid system is, however, only economical when small areas have to be covered; the increasing number of wires will rapidly outweigh the

investment necessary to locate a transmitter using triangulation from two or more directional tower-mounted antennas.

ACKNOWLEDGEMENTS

The author wishes to express his appreciation to his supervising professor, Dr. F.S. Chute, and to Mr. P. Harding for their help and encouragement throughout the course of this work.

Sincere thanks are also extended to the technical staff of the Electrical Engineering Department, especially to Mr. I. Grisch and Mr. N. Burtch for their support, and to Mr. A. Aasen and his staff of the Agricultural Engineering Department at the University Farm Ellerslie, Alberta.

Thanks are also expressed to Mr. B. Barrett and Mr. D. Sekora for their aid in conducting the field tests.

The financial support provided by the Alberta Government Telephone Centennial Fellowship during the years 1971 to 1973 is gratefully acknowledged.

To Mrs. B. Gallaiford, my sincere thanks for the final typing of this report.

In addition I would like to thank my wife, Helen, for her assistance in completing this work.

TABLE OF CONTENTS

CHAPTER PAGE

I. INTRODUCTION 1

II. THEORETICAL DEVELOPMENT OF THE BEVERAGE RECEIVING SYSTEM 9

2.1 Background 9

2.2 The Line Impedance 14

2.2.1 The Single-Line Impedance 15

2.2.2 The Double-Line Impedance 19

2.3 Loop to Wire Coupling 22

2.3.1 The Mutual Inductance between Loop and Single-Wire Line 31

2.3.2 The Mutual Inductance between Loop and Double-Wire Line 33

2.4 Signal Dependence on Orientation and Lateral Displacement 35

2.5 Attenuation along the Wire Line 35

2.5.1 Ground Loss along the Wire Line 38

2.5.2 Conductor Loss along the Wire Line 44

2.5.3 Dielectric Loss along the Wire Line 45

III. EXPERIMENTAL INVESTIGATION OF THE BEVERAGE RECEIVING SYSTEM 49

3.1 Introduction 49

3.2 The Loop Antenna 53

3.2.1 The Design 53

3.2.2 The Efficiency 58

CHAPTER PAGE

3.3 The Signal Generation 64

3.4 The Wire Line 65

3.5 Results for the Single-Wire Line 72

3.6 Results for the Double-Wire Line 81

3.7 Lateral Loop Displacement 83

3.8 The Wire Grid 86

IV. OMNI-DIRECTIONAL, TOWER-MOUNTED RECEIVING SYSTEM 93

4.1 Introduction 93

4.2 Theoretical Analysis 94

4.3 Experimental Measurements 94

V. SUMMARY AND CONCLUSIONS 105

5.1 Introduction 105

5.2 Scaling the Results 109

5.3 Relative Systems Range 111

5.4 Wire Grid System versus Directional Antenna 114

5.5 Conclusions 118

REFERENCES 120

APPENDIX A POWER TRANSFER BETWEEN TWO ANTENNAS 123

LIST OF FIGURES

Figure — Page

1. Conventional Antenna System 3
2. Beverage Antenna System 5
3. Single-Wire (Ground Return) System 10
4. Double-Wire System 11
5. Single Wire and Image 16
6. Double Wire and Images 20
7. Equivalent Circuit (Loop-Transmission Line) 23
8. Magnetic Field of the Single Wire 32
9. Magnetic Field of the Double Wire 34
10. Loss Area along the Wire Line 37
11. Attenuation versus Frequency 43
12. Experimental System 51
13. Loop-Antenna Matching 56
14. Loop-Antenna Design 57
15. Efficiency Test 59
16. Single-Wire Line Taper 66
17. Double-Wire Line Taper 67
18. Wire-Line Matching Network 70
19. Results for 6-foot, Single-Wire Line at 29 MHz 73
20. Results for 6-foot, Single-Wire Line at 51 MHz 74
21. Results for 6-foot, Single-Wire Line at 95 MHz 75
22. Results for 3-foot, Single-Wire Line at 51 MHz 80
23. Results for 6-foot, Double-Wire Line at 51 MHz 82

Figure Page

24. Lateral Signal Loss of 6-foot, Single-Wire Line at 29, 51, and 95 MHz 84

25. Lateral Signal Loss of 6-foot, Double-Wire Line at 51 MHz 85

26. Loop Location and Received Signal Strength 87

27. Wire-Grid System 88

28. Small Oscillator Circuit 89

29. Typical Wire-Grid Results 91

30. Ground-Plane Antenna 95

31. Matching Networks for Ground-Plane Antenna 98

32. Received Voltage from Elevated Ground-Plane Antenna at 29 MHz 100

33. Received Voltage from Elevated Ground-Plane Antenna at 51 MHz 101

34. Received Voltage from Elevated Ground-Plane Antenna at 95 MHz 102

35. Systems Comparison (theoretical) at 51 MHz 106

36. Systems Comparison (practical) at 51 MHz 113

37. Wire-Star System 115

38. Wire-Grid Locating System 117

39. Antenna Transmission 125

40. Reflected Vertically Polarized E-Wave 126

41. Receiving System 134

LIST OF PHOTOGRAPHIC PLATES

Plate	DESCRIPTION	Page
1.	Ground-Plane Antenna for 29 MHz at 8.1 foot height	7
2.	Ground-Plane Antenna for 51 MHz at 38.8 foot height	7
3.	Loop Antenna on Wooden Rails Transmitting to Single-Wire Line (Beverage Antenna)	8
4.	100 by 100 foot Wire-Grid System	8

CHAPTER I

INTRODUCTION

The use of radio telemetry to obtain information about animals in their natural state began in 1957 with the monitoring of the temperature of a penguin egg [1]. Since that time the techniques used in the tracking of toads, rabbits, eagles, deer, wolves, grizzly bears, etc. have become common knowledge. However, improvements regarding the reliability, cost, location techniques, and the monitoring of certain bodily functions offer a wide area of possible involvement.

One of the most critical links in the telemetering problem is the radio transmitter carried by the animal under observation. The transmitter has to be constructed so that the animal transporting it is not disturbed or restricted in its movements. Usually each specific case requires special equipment designed for a certain assignment and animal to obtain the desired data. For practical battery weights, the range and lifetime of the telemetry link are usually severely limited, even when the transmitter lifetime has been increased by intermittent transmission of signals.

The transmitting antenna has to be designed for the specific animal carrying it. Short, straight wire antennas have shown advantages for use in bird-tracking, whereas, loop antennas are mainly utilized on mammals. In the latter, a collar antenna with attached transmitter pack seems to be most practical [2, 3, 4]. The diameter of the loop depends on the kind of animal, but is normally small compared to a wave-

length. When such a loop is mounted around the neck of an animal, the radiation efficiency is usually less than one percent. This poor radiation efficiency and battery-pack weight restrictions severely limit the range of the telemetry link.

Another factor affecting the animal monitoring system is the nature of wave propagation. Wave propagation can be influenced by the frequency used, the medium of transmission, and the height of the receiving antenna. Frequencies from 100 KHz to 300 MHz have been used in actual field tests [1, 2]. The observation of an animal has to be done in its natural habitat and whatever uncertainties exist, due to the specific environment, have to be accepted in general.

Receivers used for wildlife telemetry usually incorporate very limited bandwidth and low noise preamplification in order to obtain acceptable signal to noise ratios. Although it has been found advantageous to use portable receivers with attached loop antennas for close-range field work, the receiver is usually in a fixed location with rather elaborate receiving antenna systems. To compensate for the low efficiency of the radiating antenna, it has been found necessary in most cases to use elevated receiving antennas. Towers (50 to 150 feet high) are necessary just to obtain sufficient signal for ranges of the order of one mile. Typically a receiving antenna system will consist of two or more highly directional antennas mounted on high towers in such a way that they may be rotated from a remote location. The transmitter position can then be obtained by triangulation. It is obvious that such antenna installations as shown in Figure 1 can be quite

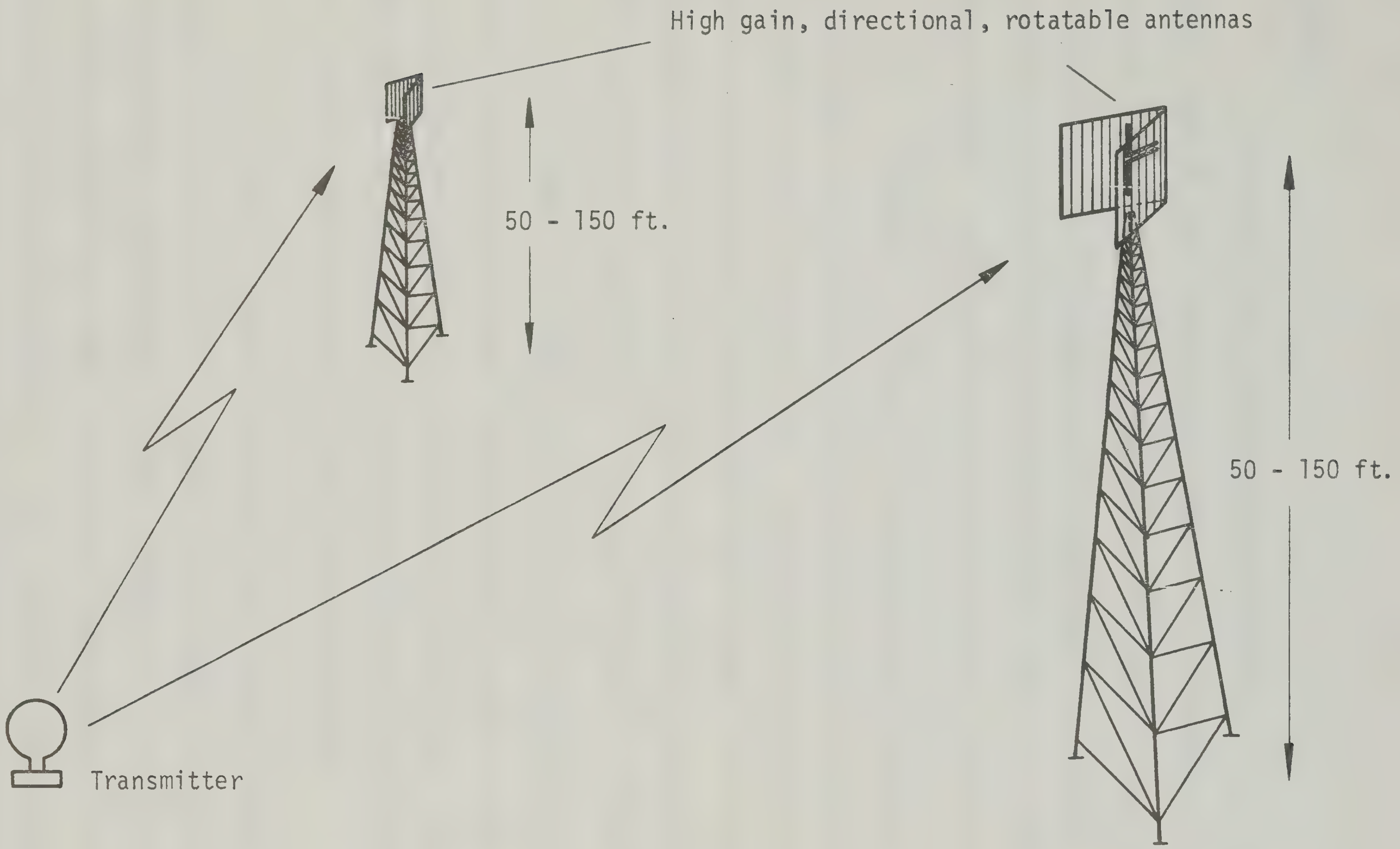

Figure 1. Conventional Antenna System

costly.

The present study investigates the theoretical and experimental behavior of a long Beverage antenna as an alternative to the complex tower installations. The antenna investigated consists of a long horizontal wire terminated in its characteristic impedance. The transmitter consists of an oscillator feeding a small loop antenna, which induces a signal into the free-hanging wire as shown in Figure 2.

In Chapter II, theoretical expressions are developed for losses along the antenna and for the amount of signal coupled to the line from the small radiating loop. Experimental measurements made at frequencies of 29, 51, and 95 MHz, and for several wire heights, show good agreement with the theoretically predicted signal strength. The experimental investigation is described in detail in Chapter III.

Although the signal coupled to the Beverage antenna decreases rapidly with distance from the antenna, a grid of such wires is shown to provide satisfactory coverage. Moreover, it is found that the position of the radiating loop can be accurately located within this grid by measuring signals on the various grid wires.

In order to assess the merits of the Beverage antenna system relative to more conventional antennas, a theoretical study (supported by experimental measurements) is made in Chapter IV, of an omnidirectional antenna mounted on a tower. The relative performance of the two systems is discussed in Chapter V. It is shown that the Beverage antenna provides larger signals out to some distance, which depends on the height of both antennas. Beyond this range the tower antenna

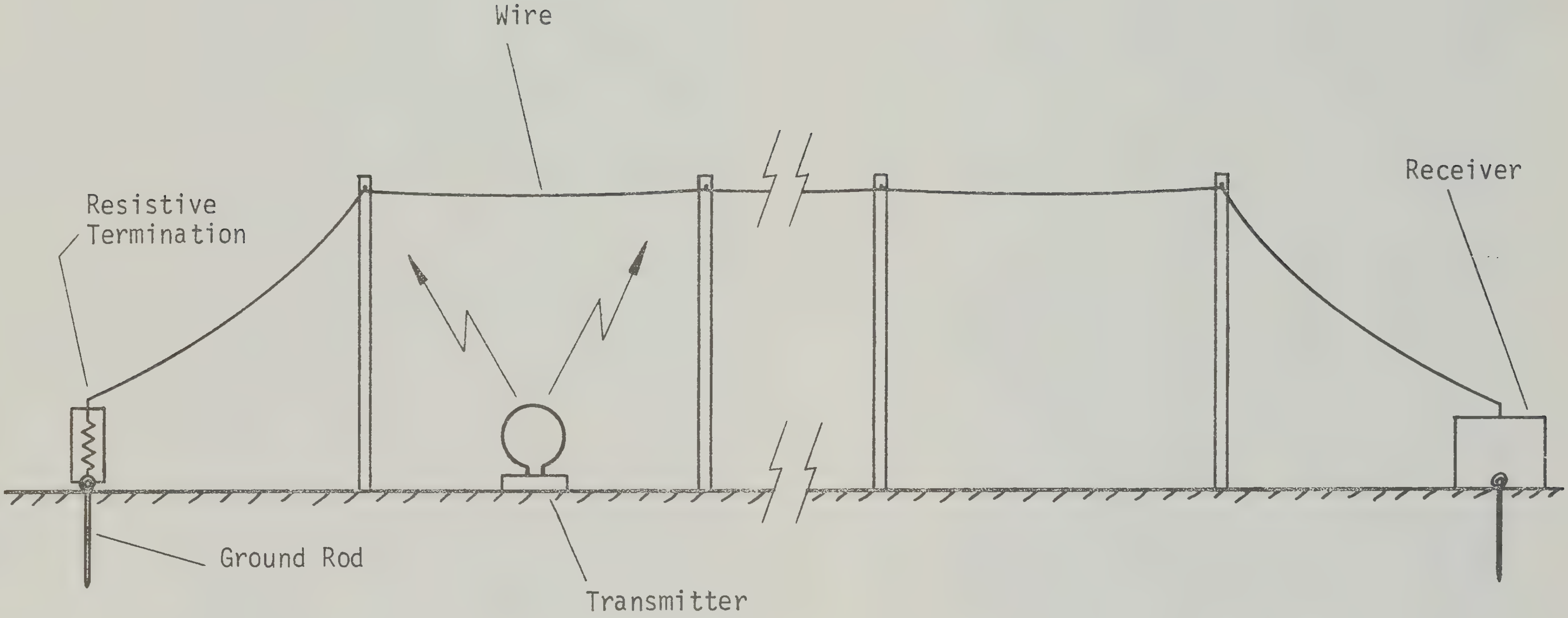

Figure 2. Beverage Antenna System

provides greater signals. However, in many low power telemetry applications this crossover point occurs well beyond the limiting range of the tower antenna, and in such cases the Beverage antenna can significantly increase the system's range.

Possible applications are also discussed, and include monitoring the activity of small rodents such as rabbits, ground squirrels, mice and lemmings whose mobility is usually confined to a rather small area.

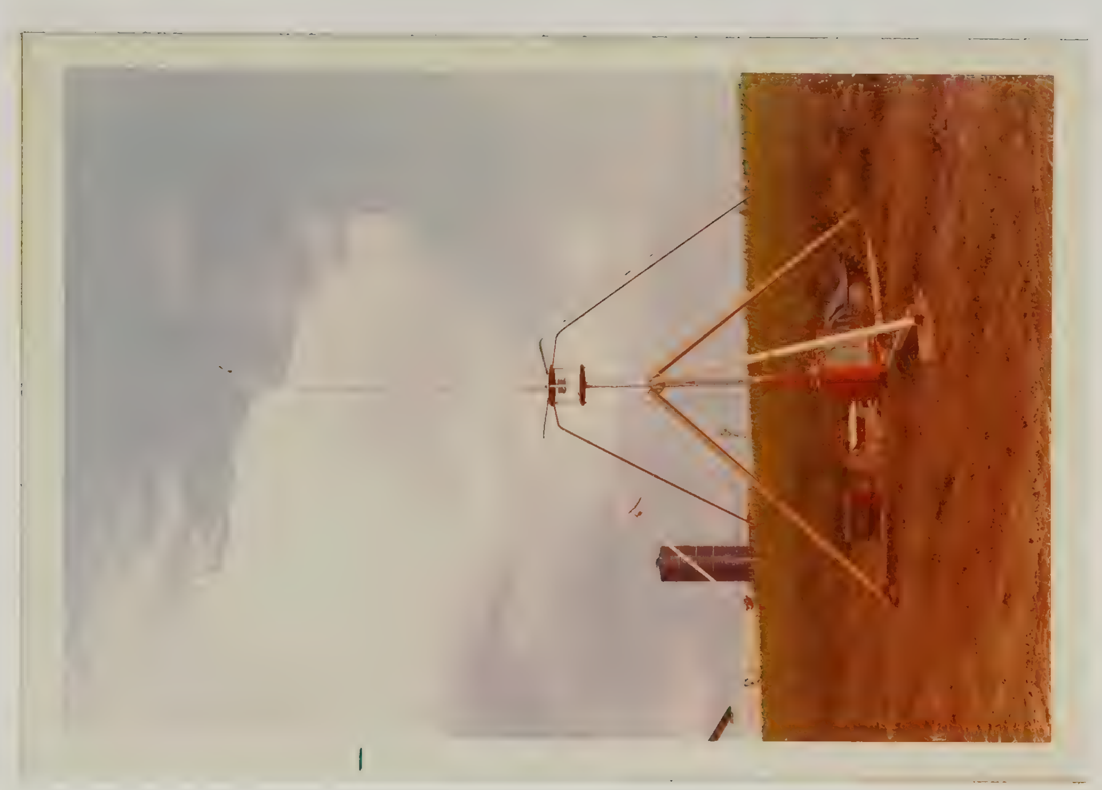

Plate 1. Ground-Plane Antenna for 29 MHz at 8.1 foot height

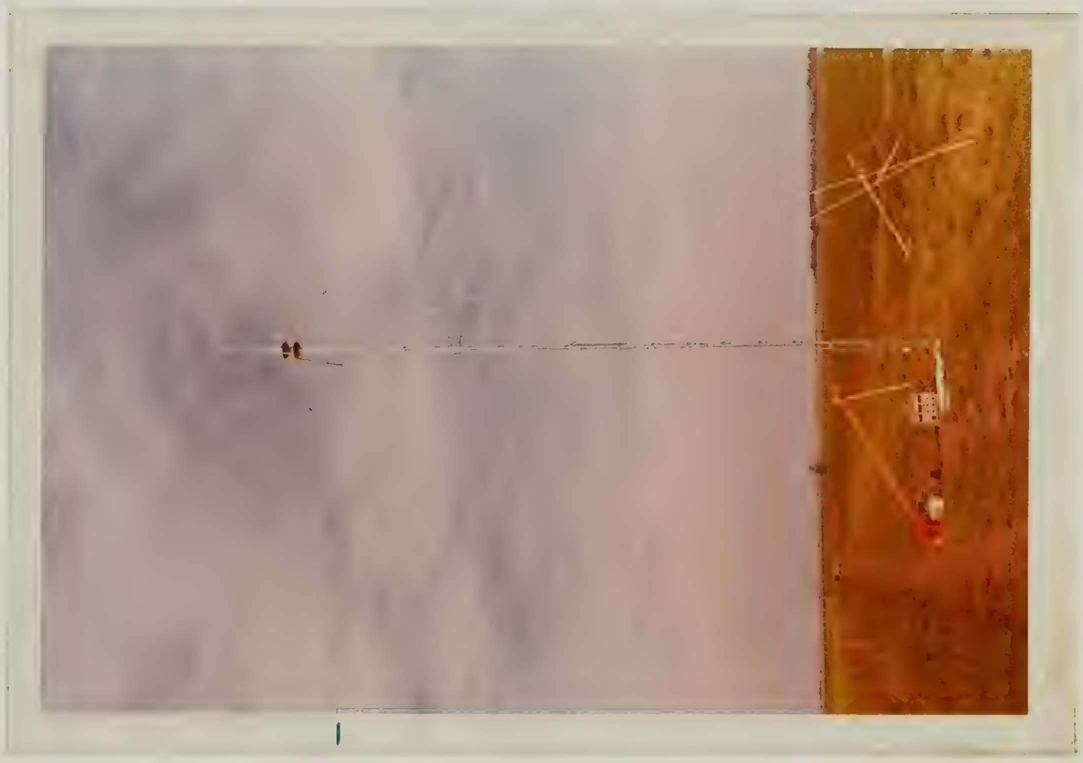

Plate 2. Ground-Plane Antenna for 51 MHz at 38.8 foot height

Plate 3. Loop Antenna on Wooden Rails Transmitting to Single-Wire Line (Beverage Antenna)

Plate 4. 100 by 100 foot Wire-Grid System

CHAPTER II

THEORETICAL DEVELOPMENT OF THE BEVERAGE RECEIVING SYSTEM

2.1 Background

The Wave or Beverage antenna was developed as a receiving antenna for transatlantic radio communication in the low and medium frequency range. In its elementary form the wave antenna consists of a single, straight horizontal conductor supported several feet above the ground and in the order of one wave length long. The wire is aligned parallel to the direction of propagation of the incoming signal. The receiver is located at the end farthest from the sending station, while the end nearest the sending station is grounded through a resistance of a value such as to establish a travelling wave current distribution along the wire. The first work with such horizontal antennas appears to have been done in the pioneer days of radio by Marconi, Braun and Secher [5].

As suggested in Chapter I, it is proposed that the Beverage antenna, used singly or as part of a grid, can be employed as a receiving antenna for monitoring radio-tagged animals. In such applications the frequencies used will generally be much higher than is common for a Beverage antenna, which results in a greater overall length of receiving system in terms of wave length. Two possible basic configurations are shown in Figures 3 and 4.

In this application the Beverage antenna can be considered to act like a transmission line, locally excited by the radiating loop antenna. Indeed, when the receiver and the terminating resistance

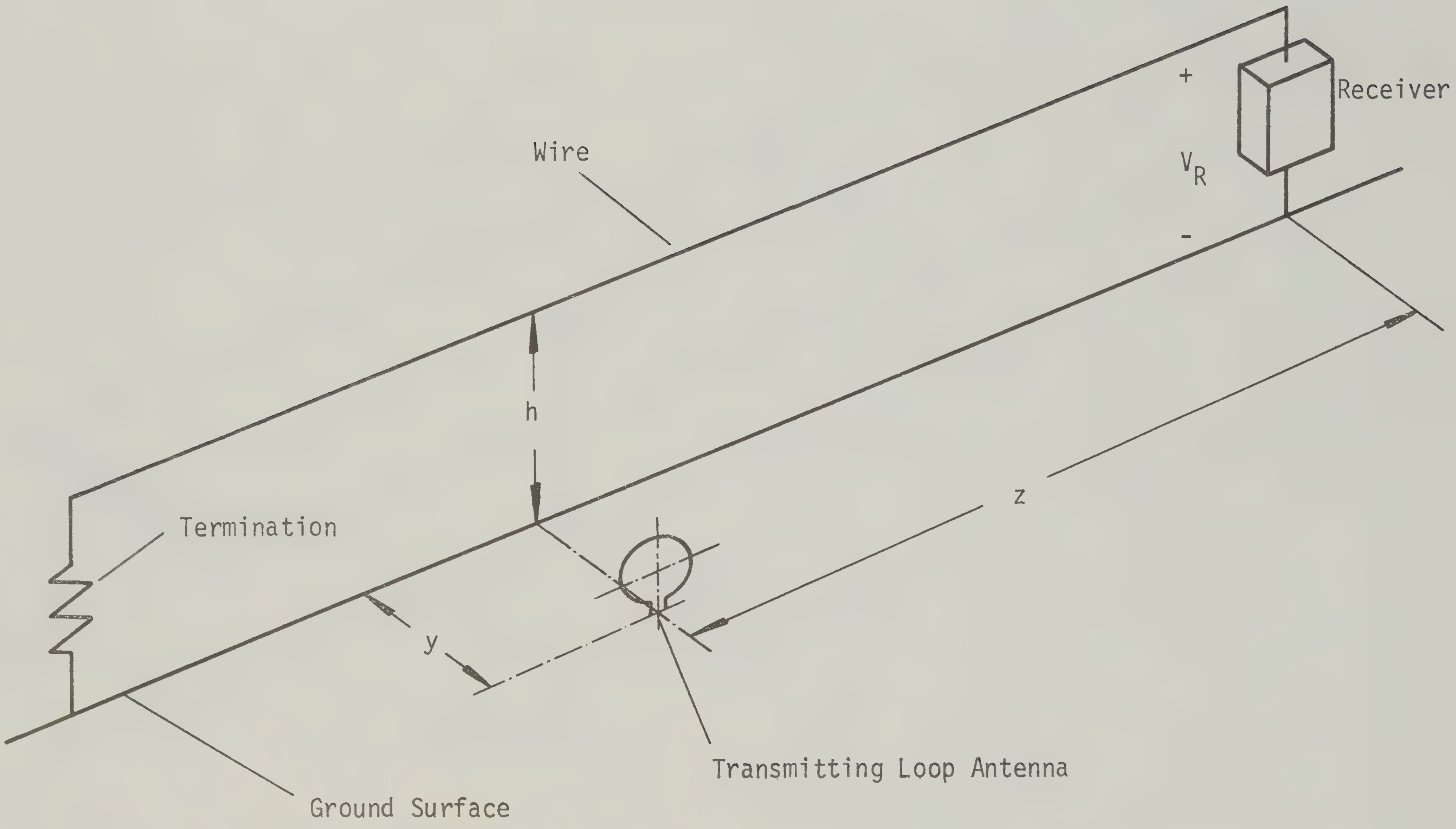

Figure 3. Single Wire (Ground Return) System

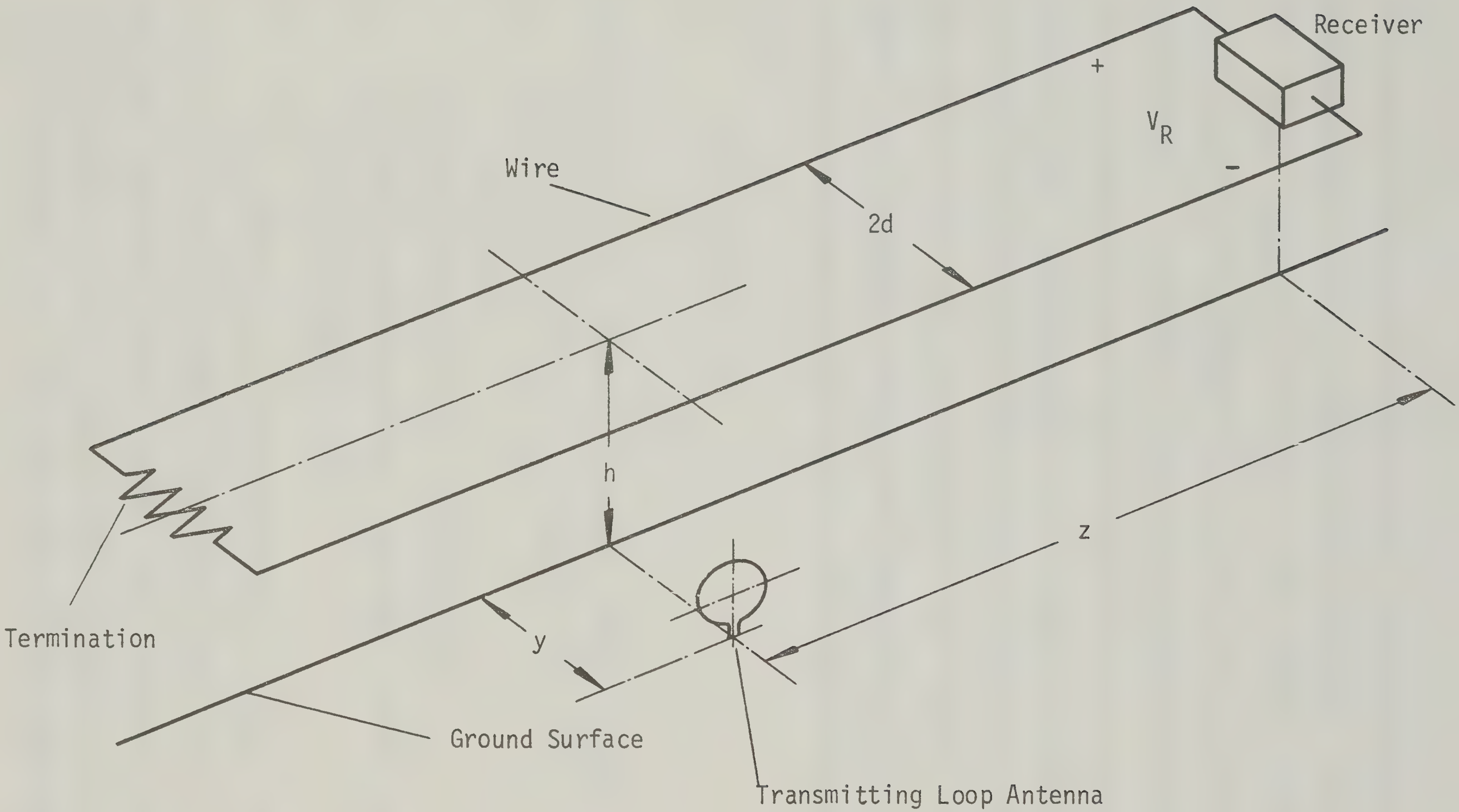

Figure 4. Double-Wire System

are properly matched to the characteristic impedance of the line, energy coupled from the loop will be conveyed without reflection to the receiver. However, as the signal travels towards the receiver it will be significantly attenuated by the Ohmic loss in the wire and in the ground. In addition it can be expected that some energy will be lost through reradiation from the Beverage antenna. The theoretical behavior of this receiving system can be treated conveniently by first calculating the magnitude of the received voltage in the absence of any loss along the line. The attenuation factor for the Beverage antenna can be obtained separately and the magnitude of the actual received voltage can be expressed with sufficient accuracy as

$$|V_R| = |V_o| \; e^{-\alpha z} \quad , \qquad (2.1)$$

where $|V_R|$ is the rms value of the actual received voltage,

$|V_o|$ is the rms value of the received voltage when no loss is experienced,

α is the attenuation factor of the antenna,

z is the distance between the transmitter and the receiver as indicated in Figures 3 and 4.

In Section 2.3, a simple expression for $|V_o|$ is developed, using a quasi-static approach that expresses the voltage in terms of the mutual inductance between the loop and the antenna, the characteristic impedance of the line, and the power delivered to the terminals of the transmitting loop. The expressions for the characteristic

impedance of the single and double-wire lines are derived separately in Section 2.2. The decrease in received voltage with increasing lateral distance, y, is investigated in Section 2.4.

The problem of the attenuation of a long wire over ground carrying a high-frequency signal has been discussed numerous times in the literature [5 to 20]. Theoretical and practical results have been obtained with sufficient accuracy for engineering design. However, with one exception, the published results have not established the functional dependence of α on the ground constants, the frequency, the height of the wire above ground and the wire diameter. The attenuation factor must be evaluated by lengthy numerical integrations for specific examples. Only the work of Knight [11] has led to a closed form expression for α.

In Section 2.5 an analogous but much simpler expression for α is derived in an entirely different manner. The approach is based on a direct calculation of the power absorbed in the ground and appears valid up to frequencies between 50 MHz and 100 MHz. Values of α calculated from this expression agree closely with Knight's results over a wide range of ground and antenna parameters. The power losses in the wire itself and in the dielectric coating on the wire are also calculated in Section 2.5.

In addition the method has been employed to calculate α for two parallel wires supported above ground, and it is shown that the attenuation is much less than for the single wire with a ground return.

2.2 The Line Impedance

For the general case of a transmission line with loss, the characteristic impedance is known to be

$$Z_o = \sqrt{\frac{R + j\omega L}{G + j\omega C}}\ , \tag{2.2}$$

where R = series resistance per unit length

G = shunt conductance per unit length

L = distributed inductance per unit length

C = distributed capacitance per unit length

ω = $2\ \pi$ frequency

However, as will be seen from the experimental results in Chapter III, the power loss per unit length along the Beverage antenna is small in which case,

$$R \ll \omega L$$

$$G \ll \omega C$$

and

$$Z_o = \sqrt{\frac{L}{C}}\ . \tag{2.3}$$

In the following sections values of L, C, and Z_o for both the single and the double-wire lines will be derived assuming the ground acts as a perfect conducting plane. Although somewhat empirical, it will be shown in Chapter III, that this treatment of the ground produces results which are in satisfactory agreement with the experiment. Actually, a study of electromagnetic plane waves reflected from a ground surface with loss, shows that over a wide range of ground

constants the surface acts much like a perfect conductor at all frequencies [21]. Only for very dry rocky terrain will the perfect conductor approximation be unacceptable. However, even in this case the approximation is valid at frequencies below a few megahertz.

2.2.1 The Single-Line Impedance

As seen in Figure 5 the wire above ground will produce an image below the ground surface carrying a current of opposite polarity. The wire and its image together can now be treated as a transmission line with a conductor spacing of twice the wire height.

Referring to Figure 5, the magnetic fields B_c and B_i caused by the current in the wire and its image give rise to a total magnetic flux, ψ_t, threading the area A above the ground, which in turn equals the product of the current and the inductance per unit length. Thus,

$$L\ I = \psi_t = \int_a^h (\overline{B}_c + \overline{B}_i) \cdot \overline{n}\, dr \quad . \tag{2.4}$$

From the Biot-Savart Law the components of $\overline{B}_c$ and $\overline{B}_i$, normal to the area A, at a distance r from the wire become

$$\overline{B}_c \cdot \overline{n} = \frac{\mu_o I}{2\pi r} \tag{2.5}$$

and

$$\overline{B}_i \cdot \overline{n} = \frac{\mu_o I}{2\pi (2h-r)} \tag{2.6}$$

where μ_o is the permeability of free space. The resulting magnetic flux due to current in the conductor is

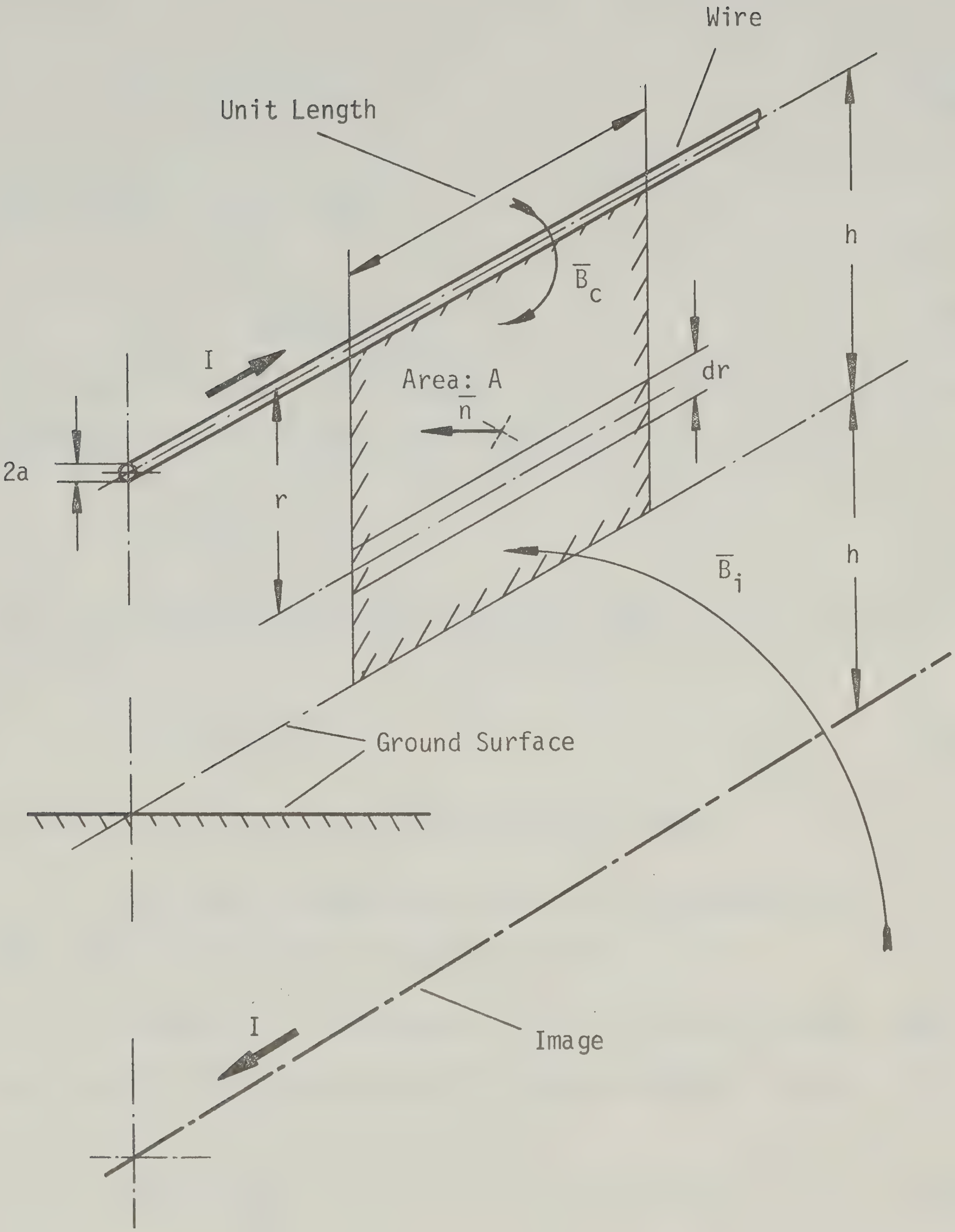

Figure 5. Single Wire and Image

$$\psi_c = \int_a^h \frac{\mu_o I}{2\pi r} \, dr \quad , \tag{2.6a}$$

and similarly for the image,

$$\psi_i = \int_a^h \frac{\mu_o I}{2\pi(2h-r)} \, dr \quad . \tag{2.6b}$$

The integrated result will, assuming the wire diameter to be negligible compared to the wire height, yield the total flux of

$$\psi_t = \frac{\mu_o I}{2\pi} \ln \frac{2h}{a} \quad . \tag{2.7}$$

Thus, employing equation (2.4), it follows that

$$L = \frac{\mu_o}{2\pi} \ln \frac{2h}{a} \tag{2.8}$$

is the line inductance per unit length of the line.

In a similar manner it is possible to determine the capacitance of the assumed transmission line.

Consider q the charge of the line per unit length. Then the electric field around the wire is given by Gauss's Law as

$$E_r = \frac{q}{2\pi\varepsilon_o r} \quad , \tag{2.9}$$

and is directed radially away from the wire. ε_o is the permittivity of free space. Hence, the potential difference between the conductor and the ground due to this charge on the wire can be expressed as

$$V_{cg} = \int_a^h \frac{q}{2\pi\varepsilon_o r}\, dr \quad . \tag{2.10a}$$

The image charge also contributes to the potential difference between the conductor and the ground, with the result that,

$$V_{ig} = \int_h^a \frac{-q}{2\pi\varepsilon_o(2h-r)}\, dr \quad . \tag{2.10b}$$

The voltage between the single wire and the ground is the sum of the two contributions of potential difference due to the charge on the wire and its image.

Employing the same integration and approximations as used to obtain equation (2.7),

$$V = \frac{q}{2\pi\varepsilon_o} \ln \frac{2h}{a} \quad . \tag{2.11}$$

Since

$$q = C \cdot V \quad , \tag{2.12}$$

it follows that

$$C = \frac{2\pi\varepsilon_o}{\ln \frac{2h}{a}} \quad , \tag{2.13}$$

is the transmission line capacitance per unit length.

The required characteristic impedance, Z_o, of the single wire line can therefore be easily obtained by using equation (2.3), which yields

$$Z_o = 60 \ln \frac{2h}{a} \quad . \tag{2.14}$$

2.2.2 The Double-Line Impedance

For the case of the double-wire antenna as shown in Figure 6, the derivation of the characteristic line impedance is executed in a similar way as in the previous section for the single-wire line. However, it can be seen that in this situation the geometrical configuration consists of four current lines - two wires and two images.

The total magnetic flux, linking the area A of unit length, can be expressed as the sum of the fluxes produced individually by each wire and its associated image. The appropriate fluxes can be obtained, by analogy, from equations (2.6a) and (2.6b). Thus,

$$\psi_{\text{line 1}} = \psi_{\text{line 2}} = \frac{\mu_o I}{2\pi} \ln \frac{2d}{a} \quad . \tag{2.15a}$$

The contributions of the two image currents are equal as well and are given by

$$\psi_{\text{image 1}} = \psi_{\text{image 2}} = -\frac{\mu_o I}{2\pi} \ln \frac{\sqrt{(2h)^2 + (2d)^2}}{2h} \quad . \tag{2.15b}$$

The inductance of the parallel wire pair, $L_{1,2}$, is thus obtained as

$$L_{1,2}\, I = \psi_{\text{total}} = 2\psi_{\text{line}} + 2\psi_{\text{image}} \quad . \tag{2.16}$$

Hence,

$$L_{1,2} = \frac{\mu_o}{\pi} \ln \frac{2d}{a} \left(\frac{1}{1 + (\frac{d}{h})^2} \right)^{\frac{1}{2}} \quad . \tag{2.17}$$

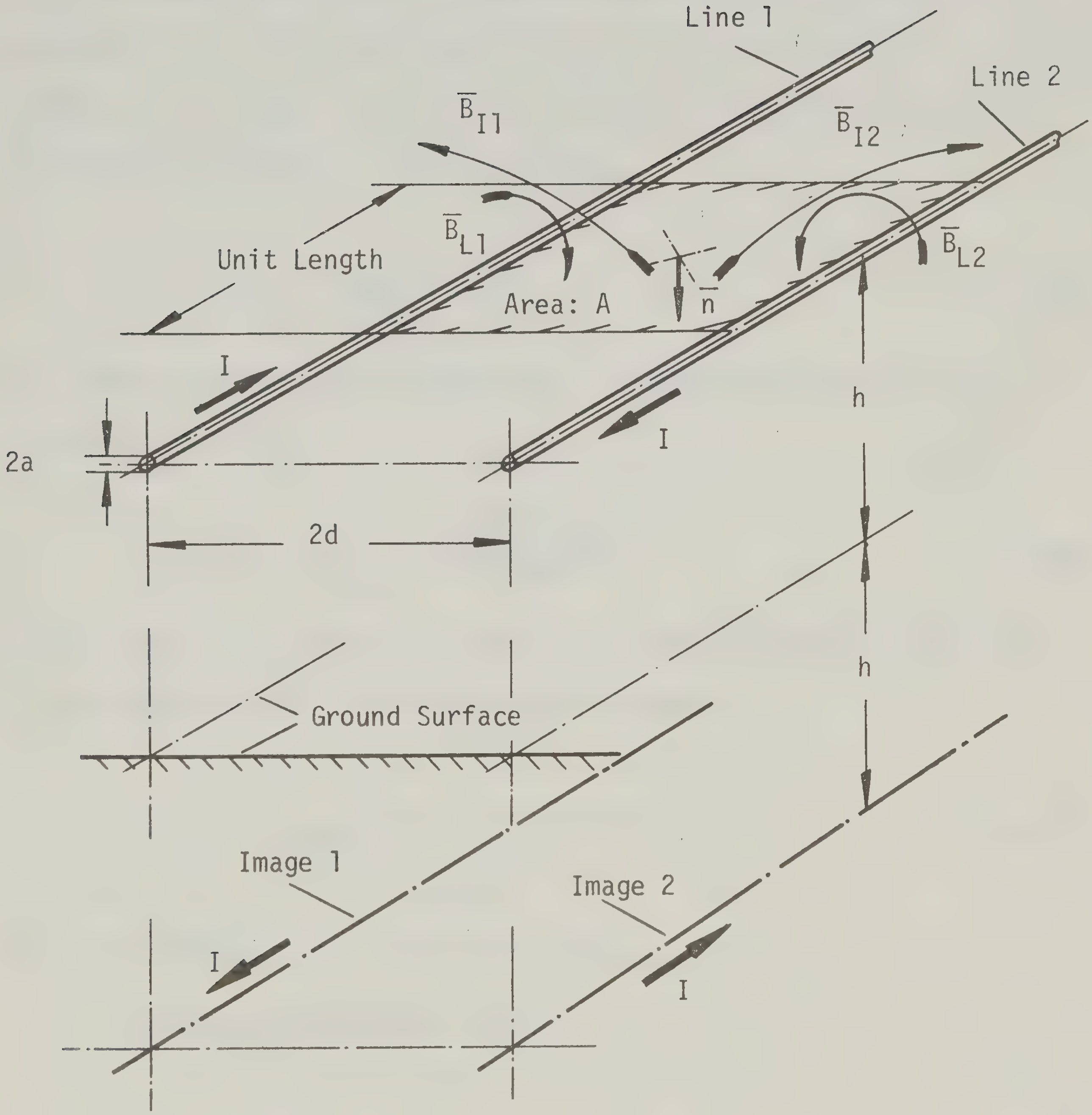

Figure 6. Double Wire and Images

The line capacitance per unit length can be developed in an analogous manner. Again, q is the charge of the line segment of unit length and the electric field surrounding a wire is given by equation (2.9). The contribution to the electrical potential between wire one and two due to the charges on the two wires is, by analogy to equations (2.10a) and (2.10b),

$$V_1 = V_2 = \frac{q}{2\pi\varepsilon_o} \ln \frac{2d}{a} \ . \tag{2.18a}$$

The images will produce a similar pair of equal contributions of potential given by

$$V_3 = V_4 = \frac{-q}{2\pi\varepsilon_o} \ln \frac{\sqrt{(2h)^2+(2d)^2}}{2h} \ . \tag{2.18b}$$

Summing these contributions to find the total voltage and then using equation (2.12), the line capacitance becomes

$$C_{1,2} = \frac{\pi\varepsilon_o}{\ln \frac{2d}{a}\left(\frac{1}{1+(\frac{d}{h})^2}\right)^{\frac{1}{2}}} \tag{2.19}$$

per unit length of the double-wire line.

Hence, by equation (2.3),

$$Z_o = 120 \ln \frac{2d}{a} \left(\frac{1}{1+(\frac{d}{h})^2} \right)^{\frac{1}{2}} \tag{2.20}$$

for the double-wire line above ground.

2.3 Loop to Wire Coupling

As pointed out in Chapter I, the transmitting antenna consists of a loop of small diameter. The question arises, how much signal power is coupled from the transmitter loop to the wire line illustrated in Figures 3 and 4? The purpose of this section is to derive an expression for the voltage across the receiver in terms of the power delivered to the loop terminals for the case where the transmission line is without loss.

One way of approaching the coupling problem is to treat the loop and the Beverage antenna system in terms of the equivalent circuit shown in Figure 7. Terminal plane 0 represents the input to the receiver and terminal plane i represents the input to the wire at the loop - wire coupling point, while the terminal plane T represents the input to the transmitting loop antenna. It will be assumed in the following derivation that the receiver is matched to the transmission line and that the terminating impedance on the Beverage antenna equals the characteristic impedance of the line.

The first step in the derivation will be to find the parameters of the equivalent circuit. They may be found in a straight forward manner by suitable open-circuit measurements at the receiver and the loop terminal planes.

The parameter Z_1

Consider setting $I_T = 0$. Then, referring to Figure 7, the equivalent generator $a \cdot I_T$ is zero, and the impedance presented

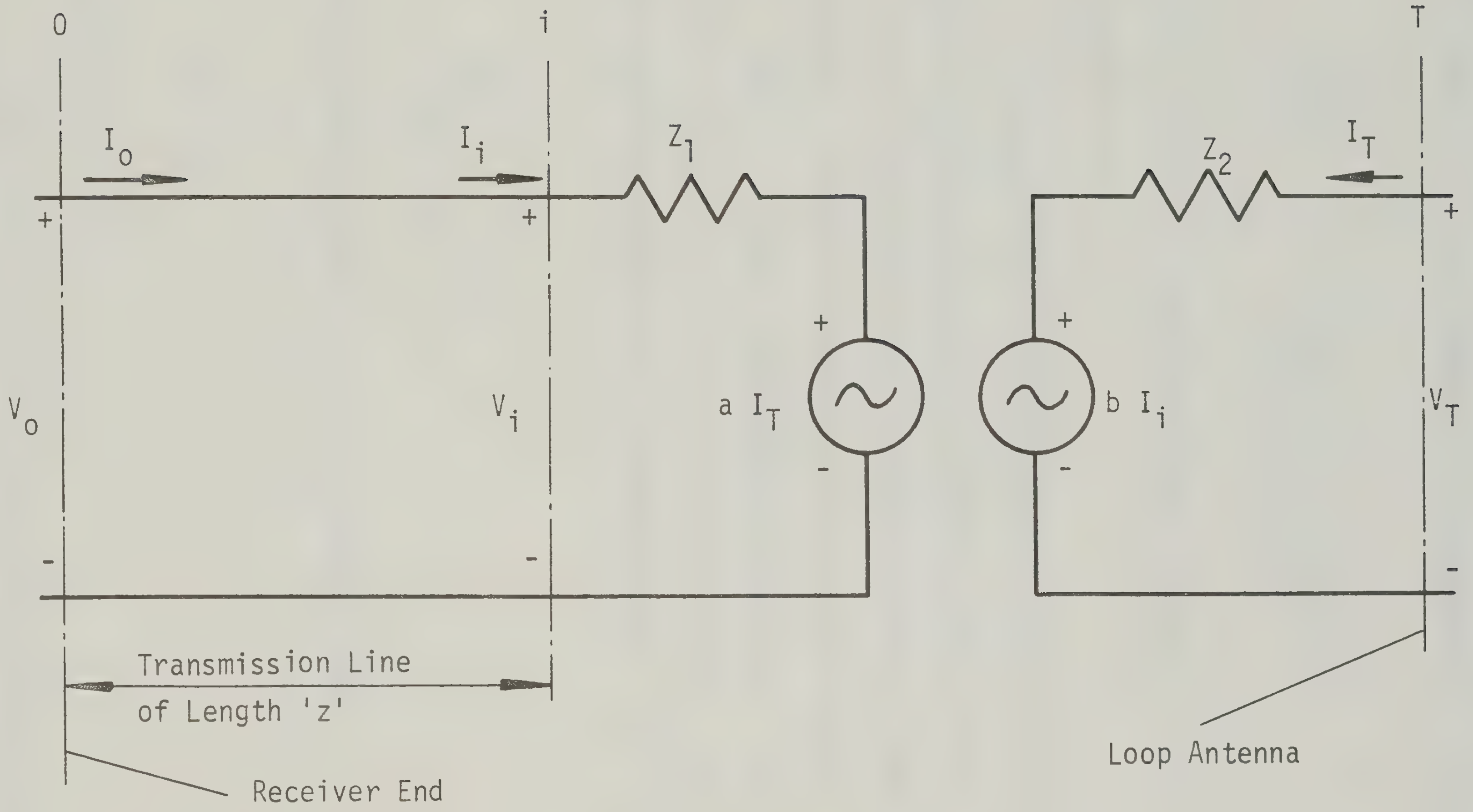

Figure 7. Equivalent Circuit (Loop - Transmission Line)

at the receiver terminals is simply that of a section of transmission line of length z, terminated in the impedance Z_1. Thus

$$\left.\frac{V_o}{I_o}\right|_{I_T = 0} = \frac{Z_o(Z_1 + j\, Z_o \tan kz)}{(Z_o + j\, Z_1 \tan kz)} , \tag{2.21a}$$

where, $k = \omega\sqrt{L\,C}$, is the propagation constant for the transmission line without loss.

Alternatively, it is possible to calculate the input impedance of the Beverage antenna directly when the loop current is zero. In this case, the small perturbing effect of the loop on the transmission line can be ignored since the loop is small compared to both λ and h. Thus, on the actual antenna V_o and I_o represent the voltage and current on a lossless transmission line terminated in its characteristic impedance. In other words,

$$\left.\frac{V_o}{I_o}\right|_{I_T = 0} = Z_o . \tag{2.21b}$$

Equating (2.21a) and (2.21b), it is apparent that

$$Z_1 = Z_o . \tag{2.22}$$

The parameter b

Also, when $I_T = 0$, it is possible to show that the ratio of the open-circuit voltage at the loop to the current at the receiving

terminal is given by

$$\left.\frac{V_T}{I_o}\right|_{I_T = 0} = \frac{b \cdot I_i}{I_o} \quad . \tag{2.23a}$$

However, in this case, the transmission line currents, I_o and I_i, are related as

$$I_o = I_i \cos kz + j \frac{I_i Z_1}{Z_o} \sin kz \quad , \tag{2.23b}$$

with the result that

$$\left.\frac{V_T}{I_o}\right|_{I_T = 0} = \frac{b\ Z_o}{Z_o \cos kz + jZ_1 \sin kz} \quad . \tag{2.23c}$$

Since, from equation (2.22), $Z_1 = Z_o$, this expression reduces to

$$\left.\frac{V_T}{I_o}\right|_{I_T = 0} = b\ e^{-j\ kz} \quad . \tag{2.23d}$$

However, the open-circuit voltage induced in the loop by currents in the Beverage antenna can easily be determined from Faraday's Law as

$$V_T = j\ \omega\ \psi = j\ \omega\ M\ I_i \quad . \tag{2.24}$$

ψ is the magnetic flux linking the loop as the result of the current, I_i, flowing on the transmission line adjacent to the loop. M is the

mutual inductance between the loop and the line. (A similar result for the voltage in a small loop has been used by Saha [22] to study the radio interference of overhead transmission lines.). The current I_i, adjacent to the loop, is related to the receiving terminal current I_o as

$$I_i = I_o e^{-j kz} , \tag{2.25}$$

if the perturbing effect of the open-circuited loop is ignored. Hence, equation (2.23d) may also be expressed as

$$\left. \frac{V_T}{I_o} \right|_{I_T = 0} = j \omega M e^{-j kz} . \tag{2.26}$$

Equating (2.23d) and (2.26) the parameter, b, becomes

$$b = j \omega M . \tag{2.27}$$

The parameter a

To determine a , consider the voltage V_i (indicated in Figure 7) when $I_o = 0$ and the loop is driven by a current I_T. Since the open-circuited receiver terminals reflect an impedance of $- j Z_o \cot kz$ at terminal plane i , V_i can be expressed as

$$V_i = - \frac{j Z_o \cot kz}{Z_1 - j Z_o \cot kz} \cdot a \cdot I_T . \tag{2.28a}$$

Recognizing that V_i is related to the open-circuit voltage at the receiver terminals as

$$V_i = V_o \cos k z \quad , \tag{2.28b}$$

the ratio of open-circuit voltage to current in the loop can be written as

$$\left.\frac{V_o}{I_T}\right|_{I_o = 0} = - \frac{j Z_o \cot kz \cdot a}{(Z_1 - j Z_o \cot kz) \cos kz} \quad . \tag{2.29a}$$

For $Z_1 = Z_o$ this relationship becomes

$$\left.\frac{V_o}{I_T}\right|_{I_o = 0} = a e^{-j kz} \quad . \tag{2.29b}$$

Now, the Reciprocity Theorem requires that

$$\left.\frac{V_o}{I_T}\right|_{I_o = 0} = \left.\frac{V_T}{I_o}\right|_{I_T = 0} \quad . \tag{2.29c}$$

Hence, from equations (2.26) and (2.29b),

$$a = j\omega M \quad . \tag{2.30}$$

The parameter Z_2

On the basis of the equivalent circuit of Figure 7, Z_2 is

the input impedance of the loop when the current $I_i = 0$. In practice I_i can be set to zero by breaking the transmission line adjacent to the loop. In this case, provided the loop is small compared to λ and h, a satisfactory approximation for Z_2 is simply

$$Z_2 = Z_{loop} \quad . \tag{2.31}$$

Z_{loop} is the input impedance of the loop in the absence of the wire. During the course of the experimental measurements, it was found that the input impedance of the loop did not change significantly in the presence of the wire.

It is now possible to calculate V_o in terms of the power delivered to the loop. Referring to Figure 7 the loop voltage can be written as

$$V_T = I_T Z_2 + b \, I_i \quad . \tag{2.32}$$

Or using equations (2.27) and (2.31),

$$V_T = I_T Z_{loop} + j\omega M \, I_i \quad . \tag{2.33}$$

When the receiver is matched to the wire line, the voltage and current at the terminal plane i are related as

$$V_i = - I_i Z_o \quad . \tag{2.34}$$

The negative sign arises from the assumed positive direction for I_i .

Thus, from Figure 7,

$$- I_i Z_o = I_i Z_1 + a I_T \quad . \tag{2.35}$$

Making use of equation (2.22) and (2.30),

$$I_i = - \frac{j\omega M I_T}{2 Z_o} \quad . \tag{2.36}$$

Substituting for I_i in equation (2.33),

$$V_T = I_T Z_{loop} + \frac{(\omega M)^2 I_T}{2 Z_o} \quad . \tag{2.37}$$

Now multiply both sides of this equation by the complex conjugate of I_T. Thus,

$$V_T I_T^* = Z_{loop} |I_T|^2 + \frac{(\omega M)^2}{2Z_o} |I_T|^2 \quad . \tag{2.38}$$

When V_T and I_T^* are expressed as rms quantities, the power delivered to the loop is

$$P_{loop} = \text{Real } [V_T I_T^*] \quad . \tag{2.39}$$

Hence, from equations (2.38) and (2.39),

$$P_{loop} = |I_T|^2 \left[R_{loop} + \frac{(\omega M)^2}{2Z_o} \right] \tag{2.40}$$

where R_{loop} is the resistive portion of the loop-input impedance. From equation (2.36),

$$P_{loop} = \left| \frac{2Z_o}{\omega M} \right|^2 \left[R_{loop} + \frac{(\omega M)^2}{2Z_o} \right] |I_i|^2 \quad . \tag{2.41}$$

Now since the receiver is matched to the line,

$$|I_i| = |I_o| = \frac{|V_o|}{Z_o} \ . \tag{2.42}$$

Thus, equation (2.41) becomes

$$P_{loop} = \left| \frac{2}{\omega M} \right|^2 \left[R_{loop} + \frac{(\omega M)^2}{2Z_o} \right] |V_o|^2 \ . \tag{2.43}$$

Finally,

$$|V_o| = \frac{\omega M}{2} \sqrt{\frac{P_{loop}}{R_{loop} + \frac{(\omega M)^2}{2Z_o}}} \tag{2.44}$$

where V_o is the rms voltage across the wire line at the receiver end.

Usually it is necessary to transform the actual receiver impedance in order to match the line, in which case the actual voltage measured on the receiver will differ from V_o . Indeed, when the line is matched the measured voltage, V_o' , is

$$V_o' = \sqrt{\frac{Z_R}{Z_o}} \ V_o \tag{2.45}$$

where Z_R is the input impedance of the receiver. Then equation (2.44) becomes

$$|V_o'| = \frac{\omega M}{2} \sqrt{\frac{Z_R \ P_{loop}}{Z_o \ (R_{loop} + \frac{(\omega M)^2}{2Z_o})}} \ . \tag{2.46}$$

The above derivation is equally valid for single and

double-wire Beverage antennas provided the appropriate values of Z_o and M are used.

2.3.1 The Mutual Inductance between Loop and Single-Wire Line

Referring to Figure 8, when the loop is small compared to h and λ, the magnetic field, produced by a current I in the wire, can be assumed to be uniform across the loop area and of magnitude equal to the field strength at the ground surface.

It follows from the Biot-Savart Law that the component of the magnetic field normal to the loop and hence tangent to the ground is

$$B_y = \frac{\mu_o \, I \cos\theta}{\pi \, (h^2+y^2)^{\frac{1}{2}}} \quad . \tag{2.47}$$

In this case the magnetic flux threading the loop is approximately

$$\begin{aligned} \psi &= B \cdot \text{(area of the loop)} \\ &= \frac{\mu_o \, I \, h}{\pi(h^2+y^2)} \text{ (area of the loop)} \end{aligned} \tag{2.48}$$

since

$$\cos\theta = \frac{h}{(h^2+y^2)^{\frac{1}{2}}} \quad . \tag{2.49}$$

From $\psi = M \cdot I$, the mutual inductance between the loop and the wire becomes

$$M = \frac{\mu_o h}{\pi(h^2+y^2)} \text{ (area of the loop)} \quad . \tag{2.50}$$

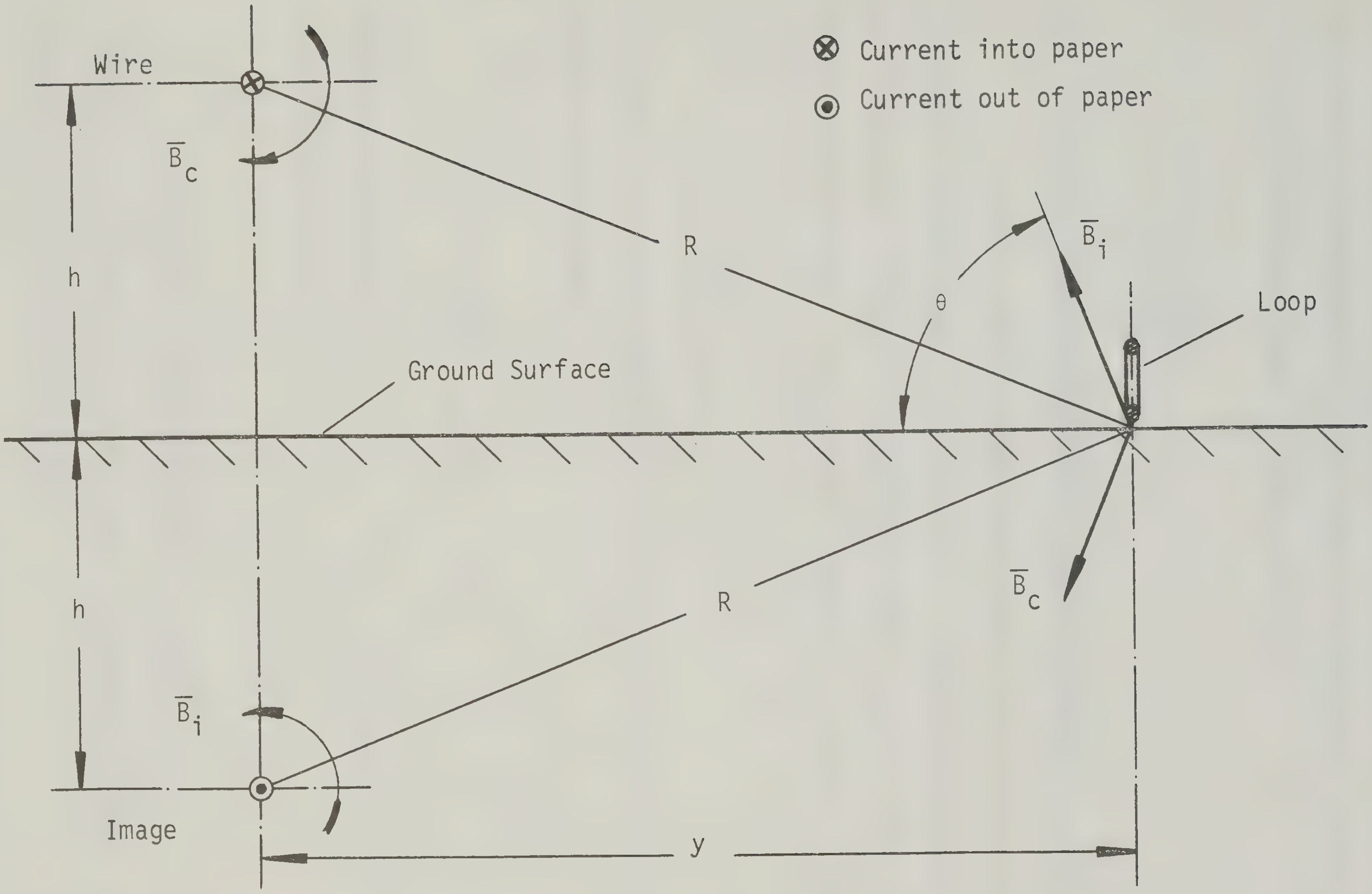

Figure 8. Magnetic Field of the Single Wire

Note that with the above approximations, the value of the mutual inductance is independent of the shape of the loop. For the circular-loop antenna used in this work,

$$M = \frac{\mu_o\, h\, d_{loop}^2}{4\,(h^2+y^2)} \quad . \tag{2.51}$$

2.3.2 The Mutual Inductance between Loop and Double-Wire Line

For the example of the double-wire line, the magnetic field may be visualized as in Figure 9. From the Biot-Savart Law and the geometry shown, the magnetic fields caused by line 1 and image 1 are additive. They produce together at point Y a value of

$$B_{y1} = \frac{\mu_o\, I}{\pi\, R_1} \cos\theta_1 \quad . \tag{2.52a}$$

Similarly, line 2 and image 2 give rise to a magnetic field of opposite sign, namely,

$$B_{y2} = -\frac{\mu_o\, I}{\pi\, R_2} \cos\theta_2 \; . \tag{2.52b}$$

Substituting for R_1 , θ_1 , R_2 , θ_2 , the total field at Y, normal to the loop, is

$$B_y = \frac{\mu_o \quad 4\, I\, d\, h\, y}{\pi[h^2 + (y-d)^2][h^2 + (y+d)^2]} \quad . \tag{2.53}$$

Assuming again that the magnetic field is uniform over the small loop area on the ground, so that

$$\psi_{DW} = M_{DW} \cdot I = B_y \text{ (area of the loop)} , \tag{2.54}$$

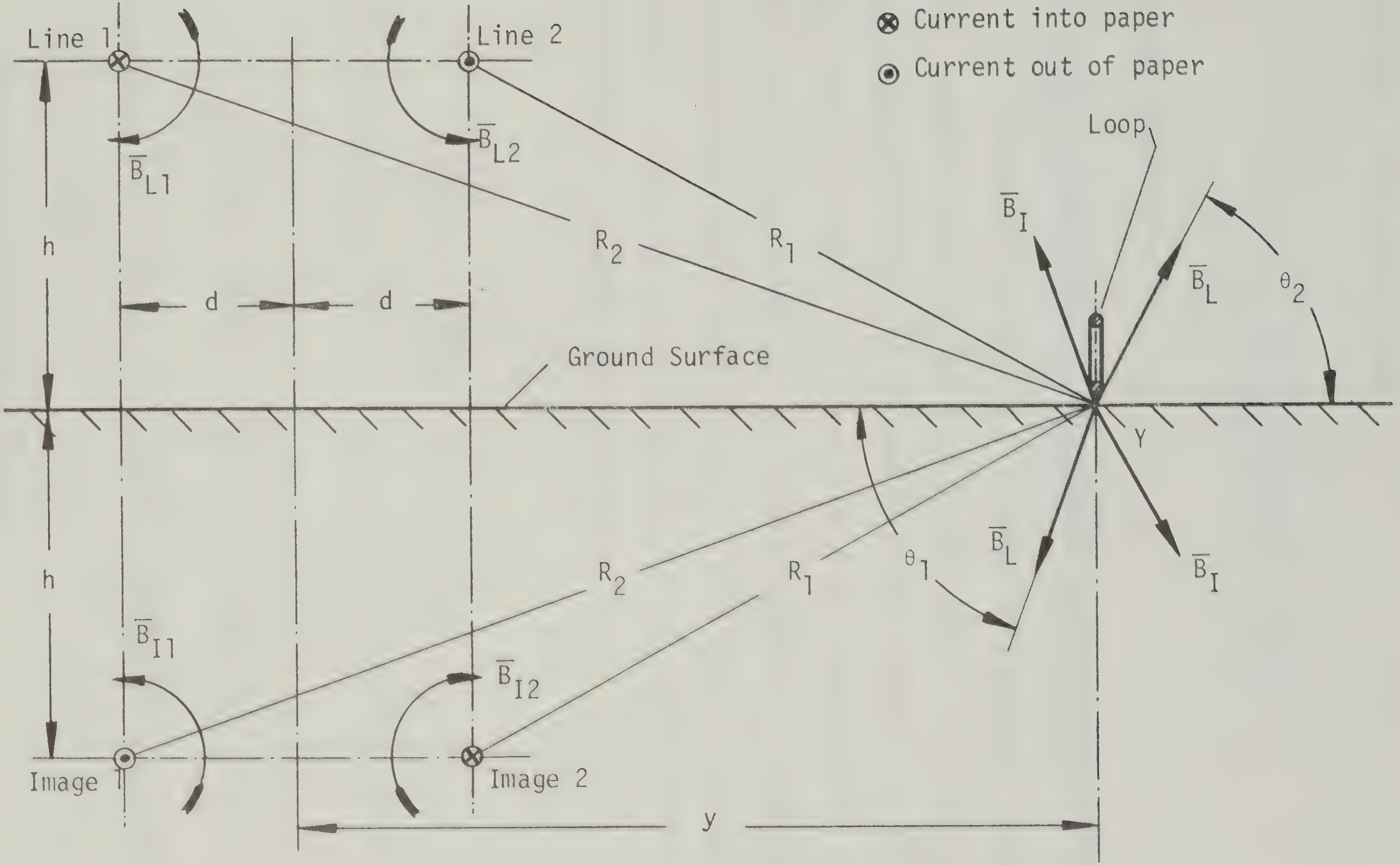

Figure 9. Magnetic Field of the Double Wire

the mutual inductance becomes

$$M_{DW} = \frac{\mu_o \; d \; h \; y \; d_{loop}^2}{[h^2 + (y - d)^2] \; [h^2 + (y + d)^2]} \qquad (2.55)$$

for the double-wire line.

2.4 Signal Dependence on Orientation and Lateral Displacement

Equations (2.46), (2.51), and (2.55) describe how the loop-wire coupling changes as the loop is positioned at various distances and orientations from the overhead wire line. When $\omega M << 2 \; Z_o$, the induced voltage in the wire can be seen, from equation (2.46), to be directly proportional to M . This inequality is true for the loop dimensions and frequencies used in this study. Thus, the rate at which the coupled signal decreases with increasing lateral displacement of the loop can be expressed as

$$\frac{V_o(y)}{V_o(y=0)} = \frac{M(y)}{M(y=0)} = \frac{1}{1 + (\frac{y}{h})^2} \; . \qquad (2.56)$$

For the double-wire line it is convenient to take the ratio as

$$\frac{V_o(y)}{V_o(y=d)} = \frac{M(y)}{M(y=d)} = \frac{y \; h^2 \; [h^2 + 4 \; d^2]}{d[h^2 + (y-d)^2][h^2 + (y+d)^2]} \; . \qquad (2.57)$$

Experimental verification of equations (2.56) and (2.57) will be presented in Chapter III.

2.5 Attenuation along the Wire Line

Although the Beverage antenna, seen as a transmission line,

is considered of low loss, certain attenuation factors cannot be neglected and shall be described in the following.

As a first approximation, the major effect of small but finite losses is to introduce an exponential multiplier to the expressions for voltage and current in the lossless case [23]. Thus, in the presence of loss, the line voltage and current are given by

$$V = V_i \, e^{-\alpha z} e^{-jkz} \tag{2.58}$$

and

$$I = I_i \, e^{-\alpha z} \, e^{-jkz} \, , \tag{2.59}$$

where V_i and I_i are as defined in Figure 7 and Figure 10. z is the distance along the line from the loop antenna towards the receiver. α is the attenuation factor in nepers per meter.

The average power transferred along the line is thus

$$P = \text{Real} \;\; V \cdot I^* = e^{-2\alpha z} \, \text{Real} \; V_i \;\; I_i^* \tag{2.60a}$$

or

$$P = |I_i|^2 \, Z_o \;\; e^{-2\alpha z} \, , \tag{2.60b}$$

since the wire line is matched.

The rate of decrease of this average power with distance along the line must correspond to the average power loss in the line per unit length, P_L. Thus,

$$-\frac{\partial P}{\partial z} = P_L = 2 \, \alpha \, e^{-2\alpha z} \, |I_i|^2 \, Z_o \tag{2.61}$$

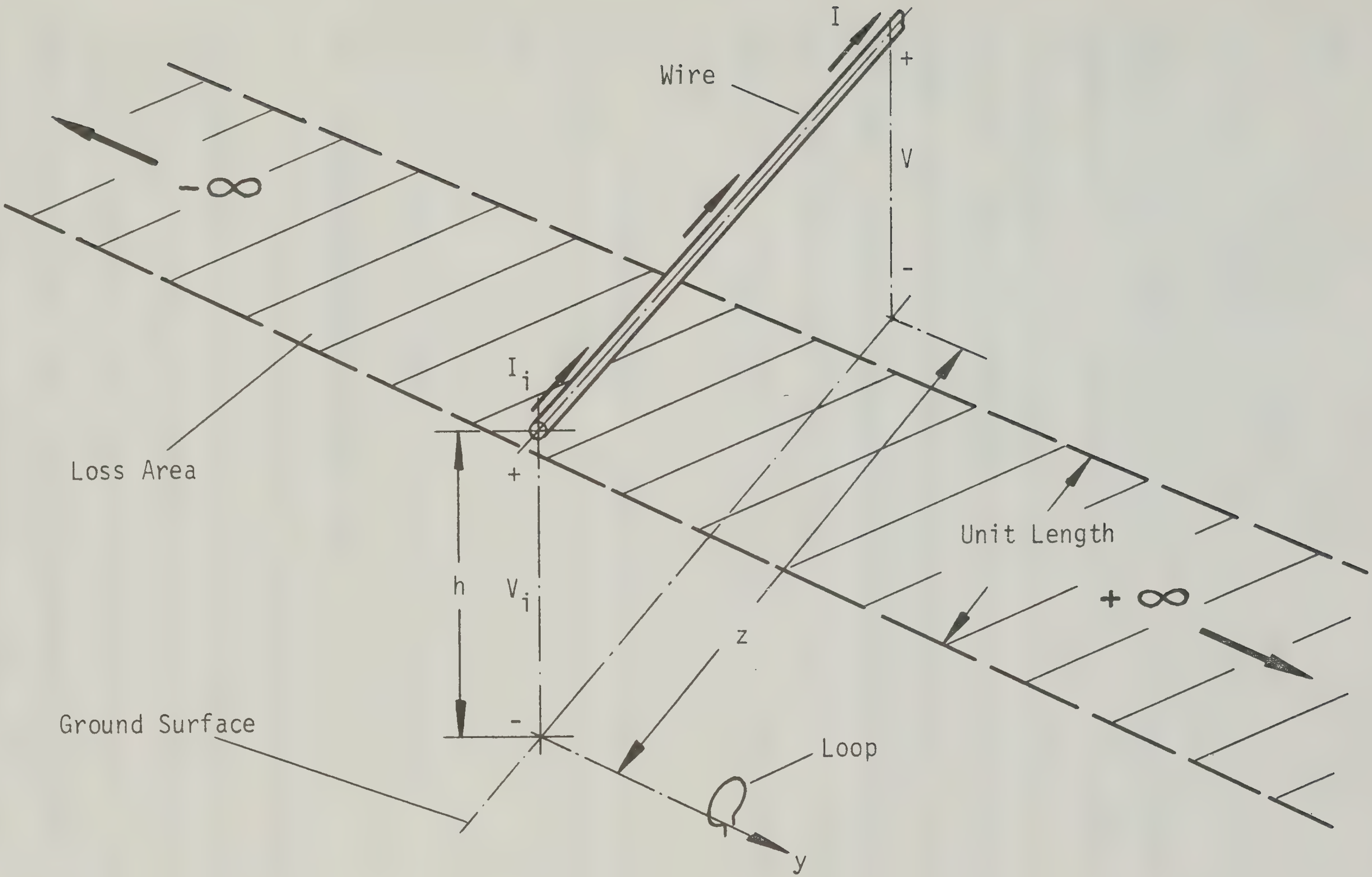

Figure 10. Loss Area along the Wire Line

and

$$\alpha = \frac{P_L}{2Z_o|I_i|^2} \quad e^{2\alpha z} \quad . \tag{2.62}$$

Since P_L will depend on z, as $e^{-2\alpha z}$ this expression will be independent of z. The problem of finding α thus reduces to finding the power losses per unit length at any distance z along the line. The most significant contribution to the attenuation factor arises from the losses related to the induced ground currents below the line. In addition, materials utilized in the insulated wire line will contribute conductor and dielectric losses. The radiation loss from the wire has been shown to be negligible compared to the other losses [7 to 10].

The power losses per unit length from each of these sources are additive with the result that the attenuation factor can be evaluated as

$$\alpha_{total} = \alpha_{ground} + \alpha_{conductor} + \alpha_{dielectric} \quad . \tag{2.63}$$

2.5.1 Ground Loss along the Wire Line

As previously pointed out, the ground behaves much like a good conductor over a wide range of ground constants and frequencies. In such cases, the magnetic field tangential to the surface of the ground is nearly the same as the field that would exist if the ground were perfectly conducting. The small component of electric field tangential to the ground, which would be identically zero for a perfect conductor, can then be estimated from this ideal value of the magnetic field as [24]

$$\overline{E}_{tang} = \eta_g \, \overline{H}_{tang} \quad , \tag{2.64}$$

where $\overline{H}_{tang}$ is obtained from equations (2.47) for the single-wire line or from equation (2.53) for the double-wire line. The characteristic impedance of the ground, η_g, is given by

$$\eta_g = \sqrt{\frac{j \, \omega \, \mu_o}{\sigma_g + j \, \omega \, \varepsilon_g}} \quad , \tag{2.65}$$

where ε_g is the permittivity of the ground and σ_g is the conductivity of the ground. It has also been assumed that the ground is non-magnetic and hence that $\mu_o = \mu_g$. Equation (2.64) is valid provided [24]

$$\left| \frac{1}{\frac{\varepsilon_g}{\varepsilon_o} + j \, \frac{\sigma_g}{\omega \varepsilon_o}} \right| \ll 1 \quad . \tag{2.66}$$

This inequality is satisfied for most ground conditions at all frequencies, and for rocky or sandy soils at frequencies below a few megacycles [21].

Using Poynting's Theorem it is now possible to estimate the power lost to the shaded ground area per unit length, shown in Figure 10, as

$$P_L = \text{Real} \int_{-\infty}^{\infty} (\overline{E}_{tang} \times \overset{\star}{\overrightarrow{H}}_{tang}) \;\; dy \quad , \tag{2.67}$$

where $\overline{E}_{tang}$ and $\overline{H}_{tang}$ are taken to be rms phasors. Thus from equation (2.64),

$$P_L = \text{Real} \int_{-\infty}^{\infty} \eta_g \; |\overline{H}_{tang}|^2 \; dy \quad . \tag{2.68}$$

For a single wire along a perfectly conducting ground, H_{tang} can be obtained from equation (2.47) as

$$H_y = H_{tang} = \frac{I\ h}{\pi\ (h^2+y^2)} \quad , \tag{2.69}$$

where I is now interpreted as the current in the wire line at the position z . Thus, in terms of the current I_i the field is written as

$$H_{tang} = \frac{I_i\ e^{-\alpha z}\ e^{-jkz}\ h}{\pi\ (h^2+y^2)} \quad . \tag{2.70}$$

Substituting this value of H_{tang} in equation (2.68) will result in

$$P_L = \text{Real}\ \eta_g \int_{-\infty}^{\infty} \frac{|I_i|^2\ h^2\ e^{-2\alpha z}}{\pi^2\ (h^2+y^2)^2}\ dy \quad . \tag{2.71}$$

Changing the variables will yield, with the aid of Figure 8,

$$y = h \tan \theta$$

and

$$dy = \frac{h\ d\theta}{\cos^2\theta} \quad ;$$

also

$$\cos\ \theta = \frac{h}{\sqrt{h^2+y^2}}$$

and

$$\cos^4 \theta = \frac{h^4}{(h^2+y^2)^2} \quad .$$

Hence, equation (2.71) becomes

$$P_L = \text{Real } \eta_g \frac{|I_i|^2 e^{-2\alpha z}}{\pi^2 h} \int_{-\frac{\pi}{2}}^{\frac{\pi}{2}} \cos^2\theta \, d\theta \quad , \tag{2.72}$$

which may be integrated to yield

$$P_L = \frac{|I_i|^2 e^{-2\alpha z}}{2\pi h} \text{ Real } \eta_g \quad . \tag{2.73}$$

Thus, from equations (2.62) and (2.73), the contribution to the attenuation from the ground losses for the single wire becomes

$$\alpha_g = \frac{\text{Real} \sqrt{\dfrac{j \omega \mu_o}{\sigma_g + j\omega\varepsilon_g}}}{4 \pi Z_o h} \quad . \tag{2.74}$$

It is interesting to note that Knight [11], using a generalization of the Compensation Theorem, states that to first order,

$$\alpha = \text{Real} \left[j\omega\sqrt{\mu_o\varepsilon_o} \left(1 - j \frac{\eta_g}{2 \pi h Z_o \omega\sqrt{\mu_o\varepsilon_o}} \right)^{\frac{1}{2}} \right] \quad ,$$

which reduces to exactly equation (2.74) when

$$\left| \frac{\eta_g}{2 \pi h Z_o} \right| << \omega \sqrt{\mu_o\varepsilon_o} \quad .$$

Equation (2.74) also agrees well with the numerical results of Kikuchi [15, 16]. Only a partial comparison is possible because of the

lack of data provided. Kikuchi plots attenuation against frequency for a wire height of 5 meters for the case $\sigma_g = 0.01$ mhos/meter and $\varepsilon_g = 10\ \varepsilon_0$. The radius of the wire is given as $a = 2.5$ mm . This graph is reproduced in Figure 11 along with a curve of attenuation versus frequency calculated from equation (2.74). There is close agreement at lower frequencies but between 10 MHz and 200 MHz, Kikuchi predicts a drop in attenuation, while equation (2.74) indicates a continued increase. Kikuchi demonstrates that this reduction in the attenuation is associated with a gradual transition from a transmission line mode of propagation along the wire to a surface wave, dissociated from the ground, and guided by the wire. The behaviour of the attenuation for this surface wave can be determined by the theory of Sommerfeldt - Gobaü. The respective curve, in Figure 11, was adopted from Kikuchi's work. Kikuchi's results also indicate that the transition takes place at increasingly higher frequencies as the wire height is decreased. Indeed it seems that provided $h \leq \lambda/4$, the transmission line mode dominates and equation (2.74) can be expected to yield satisfactory results for the attenuation along the line. For the wire heights used in the experimental study in Chapter III, equation (2.74) should be valid up to about 50 MHz. The experimental results in Chapter III are consistent with Kikuchi's predicted decrease in attenuation at sufficiently high frequencies.

The method of the evaluation of α_g for the double line is very similar to the previous derivation. However, the value of H_{tang} is obtained from equation (2.53) and is substituted into equation (2.68),

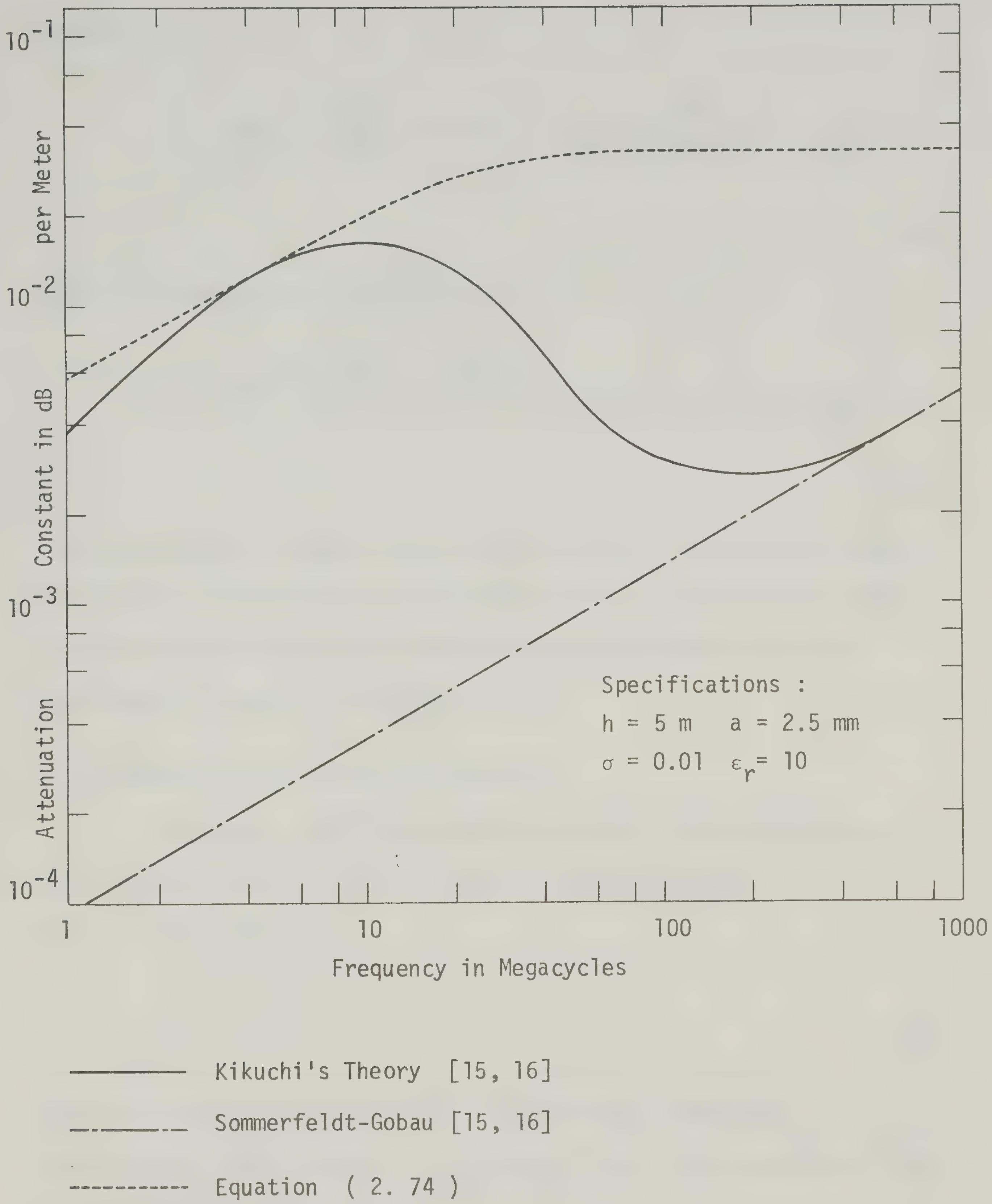

Figure 11. Attenuation versus Frequency

so that

$$P_L = \text{Real}\ \eta_g \frac{|I_i|^2}{\pi^2} h^2 d^2 16 \int_{-\infty}^{\infty} \frac{y^2\, e^{-2\alpha z}}{[h^2+(y-d)^2]^2[h^2+(y+d)^2]^2}\, dy\ . \tag{2.75}$$

Thus, from equations (2.62) and (2.75),

$$\alpha_g = \text{Real} \sqrt{\frac{j\omega\mu_o}{\sigma_g + j\omega\varepsilon_g}}\ \frac{16h^2d^2}{\pi^2\ Z_o} \int_0^{\infty} \frac{y^2}{[h^2+(y-d)^2]^2[h^2+(y+d)^2]^2}\, dy \tag{2.76}$$

for the attenuation factor caused by the ground loss under the double-wire line. No closed form solution was found for this integral and the expression is evaluated numerically for comparison with the experimental results in Chapter III.

2.5.2 Conductor Loss along the Wire Line

The ohmic loss in the conductor itself also contributes to the attenuation of the signal along the Beverage antenna. This loss is given simply as

$$P_L = |I|^2 R\ , \tag{2.77}$$

where R is the resistance of the line per unit length and I is the current at some distance z along the line. From equation (2.59), P_L may be written as

$$P_L = |I_i|^2 R\, e^{-2\alpha z}\ . \tag{2.78}$$

Thus, using equation (2.62), the contribution to the attenuation from conductor losses becomes

$$\alpha_c = \frac{R}{2Z_o} \quad . \tag{2.79}$$

For good conductors the flow of current is confined to within approximately the first skin depth, where in terms of σ_c, the conductivity of the conductor, the skin depth is

$$\delta = \sqrt{\frac{2}{\omega \, \mu_o \, \sigma_c}} \quad . \tag{2.80}$$

Providing $\delta << a$, the resistance per unit length of the round conductor is given approximately by

$$R = \frac{1}{2\pi \, a \, \delta \, \sigma_c} = \frac{1}{2\pi a} \sqrt{\frac{\omega\mu_o}{2\sigma_c}} \quad . \tag{2.81}$$

Using equations (2.79) and (2.81),

$$\alpha_c = \frac{1}{4\pi \, a \, Z_o} \sqrt{\frac{\omega\mu_o}{2\sigma_c}} \quad . \tag{2.82}$$

For the double-wire line, there are two such conductors and the resulting attenuation will be double the value given by equation (2.82). Of course, in this latter case the value of Z_o must be taken as that of the double-wire line.

2.5.3 Dielectric Loss along the Wire Line

For the insulated wire line, losses occur within the dielectric insulation of the wire. The loss per unit length can be

calculated as

$$P_L = \sigma_d \int |E|^2 \; dv \quad , \tag{2.83}$$

where σ_d is the conductivity of the dielectric and E is the electric field in the dielectric surrounding the wire. The integration is taken over the volume of the dielectric per unit length.

A thin coating of dielectric will have little effect on the potential between the signal-wire line and the ground. Thus, from equation (2.11), the potential at a distance z along the line is

$$V = \frac{q}{2 \pi \varepsilon_o} \ln \frac{2h}{a} \quad . \tag{2.11}$$

However, from Gauss's Law the total electric field close to the conductor and within the dielectric coating is approximately

$$E_r = \frac{q}{2 \pi \varepsilon_d r} \quad , \tag{2.84}$$

which is directed radially away from the wire. ε_d is the permittivity of the dielectric coating. Then, using equations (2.11), (2.58) and (2.84),

$$E_r = \left(\frac{\varepsilon_o}{\varepsilon_d} \right) \frac{V_i}{r \ln \frac{2h}{a}} \; e^{-\alpha z} \; e^{-jkz} \quad . \tag{2.85}$$

The power loss per unit length thus becomes

$$P_L = \sigma_d \left(\frac{\varepsilon_o}{\varepsilon_d} \right)^2 \frac{|V_i|^2 \, e^{-2\alpha z}}{(\ln \frac{2h}{a})^2} \int_0^{2\pi} \int_a^b \frac{1}{r} \, dr \, d\phi \quad , \tag{2.86a}$$

and further

$$P_L = 2\pi\ \sigma_d \left(\frac{\varepsilon_o}{\varepsilon_d}\right)^2 \frac{|V_i|^2}{(\ln \frac{2h}{a})^2}\ e^{-2\alpha z} \ln \frac{b}{a}\ , \tag{2.86b}$$

where b is the outer radius of the coated wire. Then, since

$$|V_i|^2 = |I_i|^2\ Z_o^2\ , \tag{2.87}$$

the dielectric attenuation factor of the single-wire line becomes, using equations (2.62) and (2.86b),

$$\alpha_d = 60\ \pi\ \sigma_d \left(\frac{\varepsilon_o}{\varepsilon_d}\right)^2 \frac{\ln \frac{b}{a}}{\ln \frac{2h}{a}}\ . \tag{2.88}$$

Use has been made of the fact that for the single-wire line

$$Z_o = 60 \ln \frac{2h}{a}\ . \tag{2.14}$$

Similarly, the dielectric attenuation factor for the double wire may be calculated. For thin coating the potential is approximately the same as obtained from equations (2.18a) and (2.18b). Thus, at some distance z along the line,

$$V = \frac{q}{\pi\varepsilon_o} \ln \frac{2d}{a} \left(\frac{1}{1 + (\frac{d}{h})^2}\right)^{\frac{1}{2}} \tag{2.89}$$

for the double-wire line. Again equation (2.84) is valid for the electric field near the wires which may be expressed, using equation (2.89) as

$$E_r = \frac{\varepsilon_o}{\varepsilon_d} \frac{V_i\ e^{-\alpha z}\ e^{-jkz}}{2r \ln \frac{2d}{a} \left(\frac{1}{1 + (\frac{d}{h})^2}\right)^{\frac{1}{2}}}\ . \tag{2.90}$$

The power loss per unit length thus becomes

$$P_L = 2\,\sigma_d \left(\frac{\varepsilon_o}{\varepsilon_d}\right)^2 \frac{|V_i|^2\, e^{-2\alpha z}}{4\left[\ln\frac{2d}{a}\left(\frac{1}{1+(\frac{d}{h})^2}\right)^{\frac{1}{2}}\right]^2} \int_o^{2\pi}\int_a^b \frac{1}{r}\,dr\,d\phi \qquad (2.91)$$

since there are two wires. Or,

$$P_L = \pi\,\sigma_d \left(\frac{\varepsilon_o}{\varepsilon_d}\right)^2 \frac{|V_i|^2\, e^{-2\alpha z}}{\left[\ln\frac{2d}{a}\left(\frac{1}{1+(\frac{d}{h})^2}\right)^{\frac{1}{2}}\right]^2}\ \ln\frac{b}{a}\,. \qquad (2.92)$$

As before, using

$$Z_o = 120\,\ln\frac{2d}{a}\left(\frac{1}{1+(\frac{d}{h})^2}\right)^{\frac{1}{2}}\,, \qquad (2.20)$$

the dielectric attenuation for the double-wire line can be written as

$$\alpha_d = 60\,\pi\,\sigma_d \left(\frac{\varepsilon_o}{\varepsilon_d}\right)^2 \frac{\ln\frac{b}{a}}{\ln\frac{2d}{a}\left(\frac{1}{1+(\frac{d}{h})^2}\right)^{\frac{1}{2}}}\,. \qquad (2.93)$$

CHAPTER III

EXPERIMENTAL INVESTIGATION OF THE BEVERAGE RECEIVING SYSTEM

3.1 Introduction

To test the validity of the theoretical derivations developed in Chapter II, a 4250-foot long Beverage antenna was constructed. For this purpose a relatively level location was selected at the University of Alberta Farm, Ellerslie, Alberta. The area was comparatively free of surrounding obstructions, such as buildings, wire fences and nearby roads with heavy car traffic. Thus, unwanted reflections as well as electrical interference were minimal.

The operating frequencies were chosen to be 29, 51, and 95 MHz. These values were selected in order to cause negligible interference with commercially used frequencies, and at the same time to provide a spread of values around frequencies already in use in actual bio-telemetric tracking experiments conducted by the Department of Electrical Engineering at the University of Alberta.

The noise interference within the planned band of frequencies depends on the location and the time of day, and may be the result of atmospheric static, man-made noise, cosmic noise or circuit noise.

The man-made noise is caused primarily by the operation of electrical switches, as for example ignition noise, and is usually the controlling factor at frequencies between 10 and 400 MHz in urban

areas. Radio transmission in this frequency range is primarily tropospheric and man-made noise is relatively unimportant beyond 10 to 20 miles from the source. Thus, interference from the nearby city of Edmonton was not an important factor.

In rural areas, such as the farm, the controlling factor can either be circuit noise or cosmic noise. Cosmic and solar noise represent thermal interference of extraterrestrial origin. Its practical importance as a limitation on communication circuits seems to be in the 20 to 80 MHz range, and hence is of significance for this experiment [25].

The external noise level and the bandwidth of the calibrated selective voltmeter, used for measuring the received power levels, determined the required transmitting power. To keep the received signal above the noise at all times, and yet to limit the radiated fields to the vicinity of the farm, the transmitter power was set to approximately 1 Watt.

Figure 12 shows the system as used in the actual experiment. The construction of the wire antenna consisted of a straight-spanned wire (#18 GA multi-strand, copper, PVC insulated), supported at 50 foot intervals by 2" by 2" wooden poles. The line length was limited to 4250 feet. Provision was made to adjust the height of the wire between 0 and 6 feet. For the double-wire line, a second wire was set up at 6 feet distance parallel to the first line.

The wire line was connected at one end to a receiving system (Brüel and Kjaer Heterodyne Voltmeter Type 2006) by means of

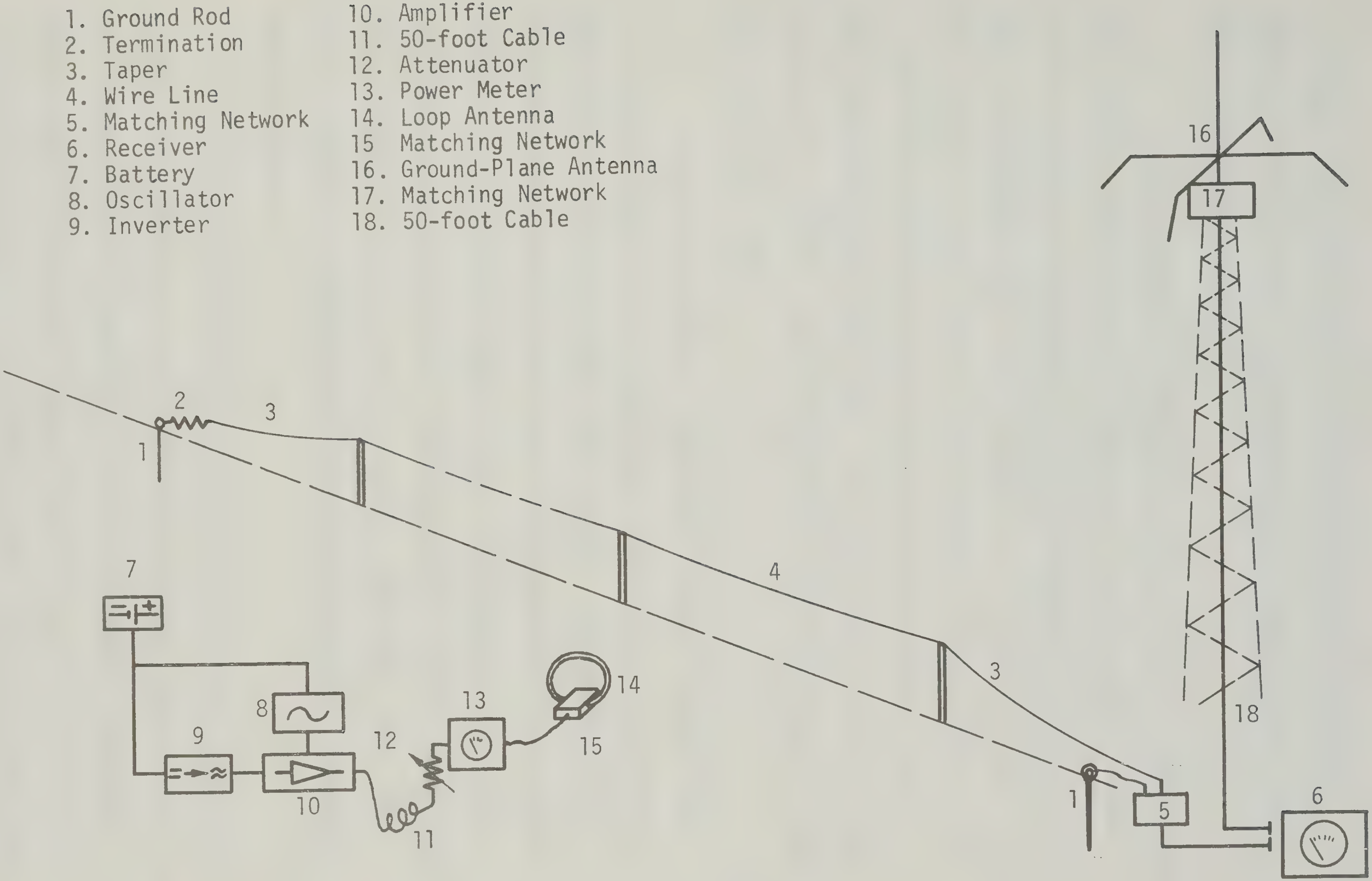

Figure 12. Experimental System

an impedance matching network. The transformation of the wire impedance to the 50 ohms of the measuring instrument avoids signal losses due to reflections.

It was planned to conduct tests at distances of 500 to 4000 feet from the receiving end of the wire. Thus, a movable transmitting apparatus was required. For this purpose, two 12 volt 70 AH lead acid batteries were used to power a solid-state inverter (Terado Mark II Model 50-132), which in turn provided 115 volt at 60 Hz to a tunable high-frequency power amplifier (Hewlett-Packard 230 A, Signal Generator Power Amplifier). The latter amplified the signal generated by a 12 volt crystal oscillator, whose amplitude was adjustable over a wide range.

A variable attenuator (Weinschel Engineering Model 905, 0 - 10 dB) allowed for a fine adjustment of the power, and finally the use of a feedthrough power meter (Philco - Sierra 164B, Bi-directional Power-monitor) permitted the observation of the signal strength, as well as the amount of the reflected power. The power fed into the small loop antenna was kept constant during the course of the experiment. The loop antenna itself, representing the transmitting animal, was matched again to the instrumentation impedance level of 50 ohms.

For the actual tests the complete transmitting equipment was moved by a car to the required locations along the wire line. The loop antenna then was connected to the high-frequency source and lined up under the wire for maximum coupling into the line. The use of a 50-foot long coaxial cable for the above connection allowed the

power amplifier and the vehicle to be stationed sufficiently far from the wire line that effects of interference caused by the reflecting car body were negligible.

Two or three single measurements were taken at each point and recorded at the receiving end of the line. A two-way radio transmitter allowed for constant consultation between transmitting and receiving stations.

3.2 The Loop Antenna

3.2.1 The Design

In order to match the loop antenna to the transmitter output impedance of 50 ohms, it was necessary to determine the driving-point impedance of the loop. This impedance is also required for the theoretical determination of the signal coupled to the line which was determined in Section 2.3 of Chapter II. The loop impedance has in general both resistive and reactive parts. The reactive part arises from the surrounding induction fields, because these fields give rise to a reactive energy storage in the region surrounding the antenna. The resistive part of the input impedance has contributions from all physical mechanisms that give cause to a loss of energy from the antenna. The radiated power is the desired loss mechanism, but other losses, for example ohmic losses are unavoidable.

The radiation resistance of the antenna is a fictitious resistance which, when substituted for the antenna, will consume the same amount of power that is actually radiated. The radiation resistance for a balanced-loop antenna in free space is given as [26]

$$R_{rad} = 31200 \left(\frac{A_L}{\lambda^2} \right)^2 , \qquad (3.1)$$

where A_L is the area of the loop. Since the current along the loop is distributed sinusoidally with a peak opposite the feed terminals [27], the radiation resistance referred to the loop input terminals becomes

$$R_{11} = \frac{1}{\cos^2 \frac{k\rho}{2}} \quad 31200 \left(\frac{A_L}{\lambda^2} \right)^2 , \qquad (3.2)$$

where ρ is the circumference of the loop.

The reactance of the loop is approximated by an equivalent short-circuited transmission line [28] as

$$j\, X_{loop} = j\, 120 \ln \frac{r}{a} \tan k\, \rho\, \frac{1}{2} , \qquad (3.3)$$

where a is the radius of the tubing used to construct the loop and r is the radius of the loop itself.

Both equations (3.2) and (3.3) are valid only with the restriction that the loop diameter is smaller than $\lambda/10$. In addition, it may be noted that for an antenna right above the ground, as planned for the experiment, the input impedance must be multiplied by a factor of two to account for the image of the antenna.

The calculated input impedance of the loop antenna, ignoring losses, showed a negligible resistance compared to the value of the inductance. Nevertheless, the values permitted the estimation of a first approximation of the required capacitances to tune out the inductance of the actual antenna, and at the same time, to match the

loop to a 50 ohm line as shown in Figure 13. The series capacitor at the top of the loop consisted of a 25 pf adjustable air capacitor. A 550 pf adjustable capacitor with plastic insulation was shunted across the feeding terminals of the antenna.

Initial tuning was accomplished with the aid of a vector impedance meter (Hewlett - Packard, Model 4815A). The loop antenna proved to have a high Q , and the final tuning had to be done on the ground under conditions approximately the same as those on the University Farm. The capacitors used proved to be quite unstable in their set adjustment, which resulted in frequency detuning of the loop. As a result, the variable capacitors were replaced by a small coaxial cable (RG 174/U Type 50) of 50 ohm impedance cut to a specific length, in parallel with a fixed-value mica capacitor. The tuning of the loop could be accomplished easily by the trimming of the coaxial cable. Final tuning of the loop was conducted with the aid of an in-line wattmeter capable of measuring both incident and reflected power. A signal of the required frequency was fed to the loop and the matching capacitors, while the reflected power was adjusted to a minimum by changing the capacitances in value. Care had to be taken, since trimming the cable too short meant repeating the entire tuning process. In the actual experiment, the reflected power could be dropped to about 1% of the incident power.

Three separate loops of the same dimensions as shown in Figure 14, were constructed and were tuned for 29, 51 and 95 MHz. The loops were found to remain matched for the duration of the

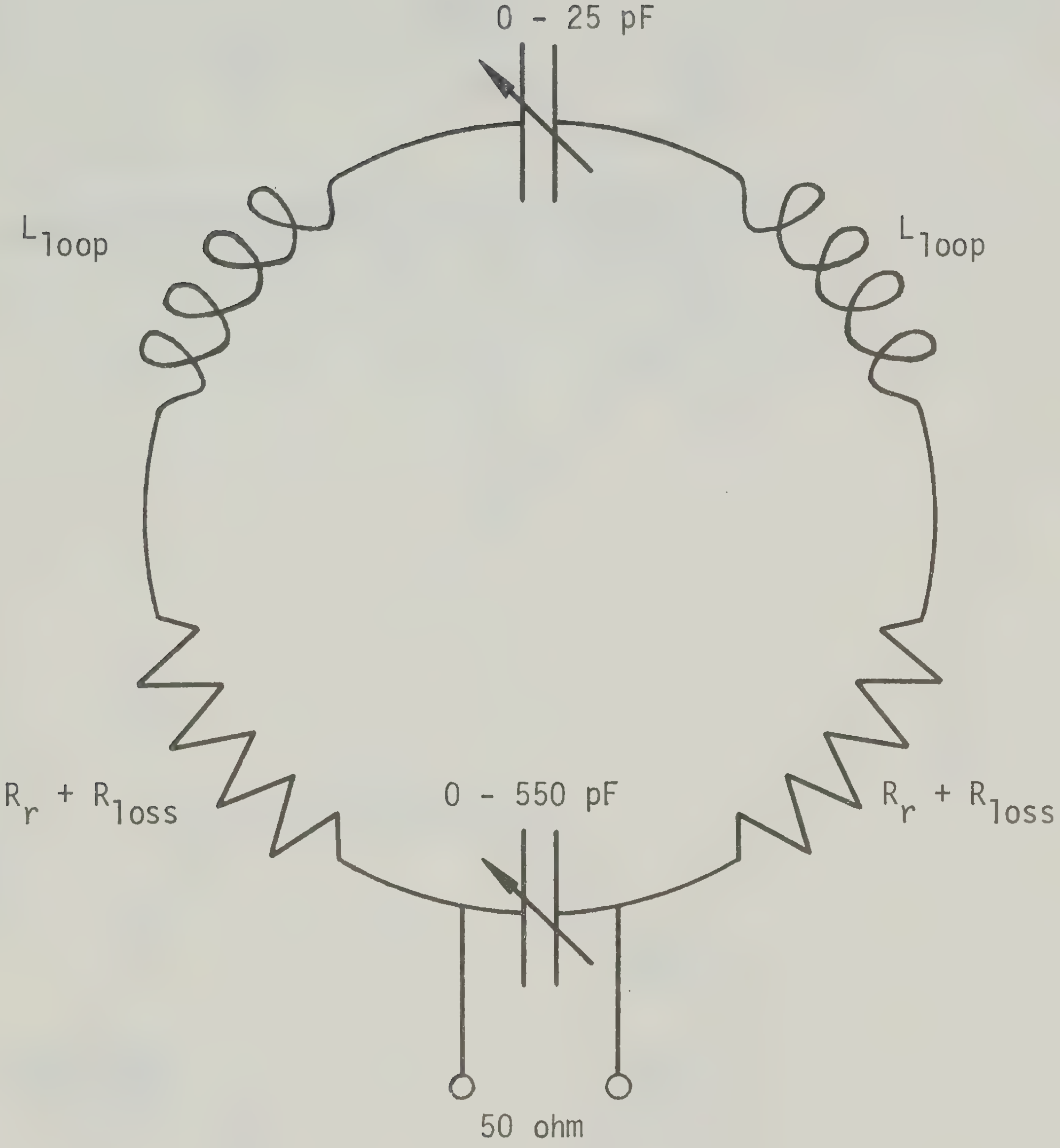

Figure 13. Loop-Antenna Matching

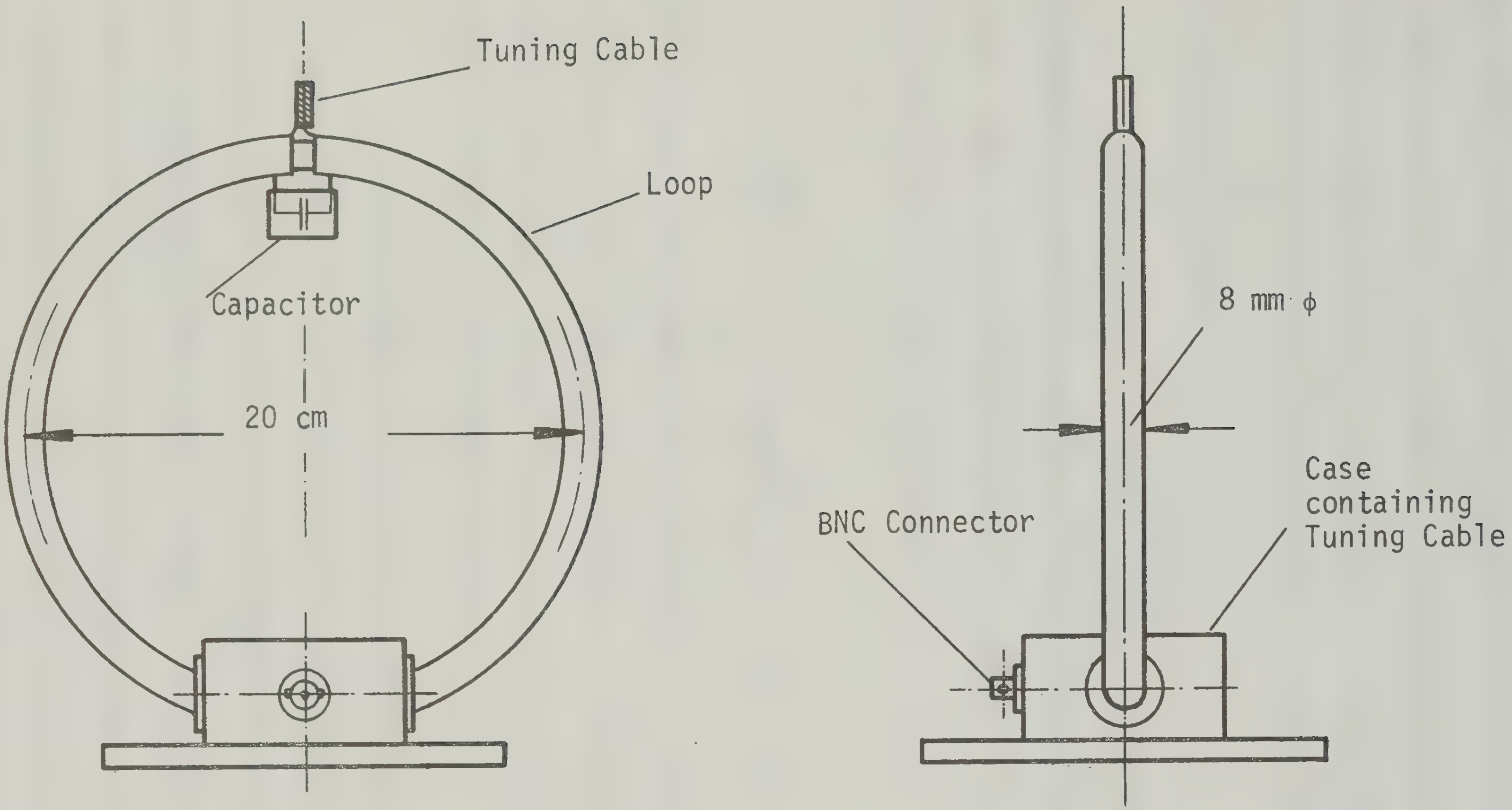

Figure 14. Loop-Antenna Design

experiment, though placing the loop at different locations on the ground occasionally increased the reflected power by up to three percent. An increase of the power delivered towards the loop by an equal amount resulted in effectively a constant radiated power.

3.2.2 The Efficiency

An important parameter of the loop antenna, which unfortunately cannot be calculated with sufficient accuracy because of ground losses, is the radiation efficiency. In order to calculate this efficiency, which is defined as

$$\frac{P_{rad}}{P_{in}} = \eta \doteq \frac{R_A}{R_A + R_{loss}} \quad 100 \quad \text{in } \% \quad , \qquad (3.4)$$

the following experiment was conducted. R_A represents the radiation resistance of the loop in the presence of the ground, referred to the antenna terminals. R_{loss} is the sum of the conductor and ground losses referred to the antenna terminals.

Three different antennas were set up as shown in Figure 15. The loop antenna (#1 in Figure 15) consisted of the antenna discussed above and was positioned with the direction of maximum gain towards the transmitting ground-plane antenna. The receiving ground-plane antenna (#2 in Figure 15) is further discussed in Chapter IV, and for the present discussion it is only of importance that its height was set to 8.12 feet. Finally, the transmitting antenna consisted of a ground-plane antenna located directly on the ground (#3 in Figure 15). While the latter antenna was only tuned in an approximate way, both

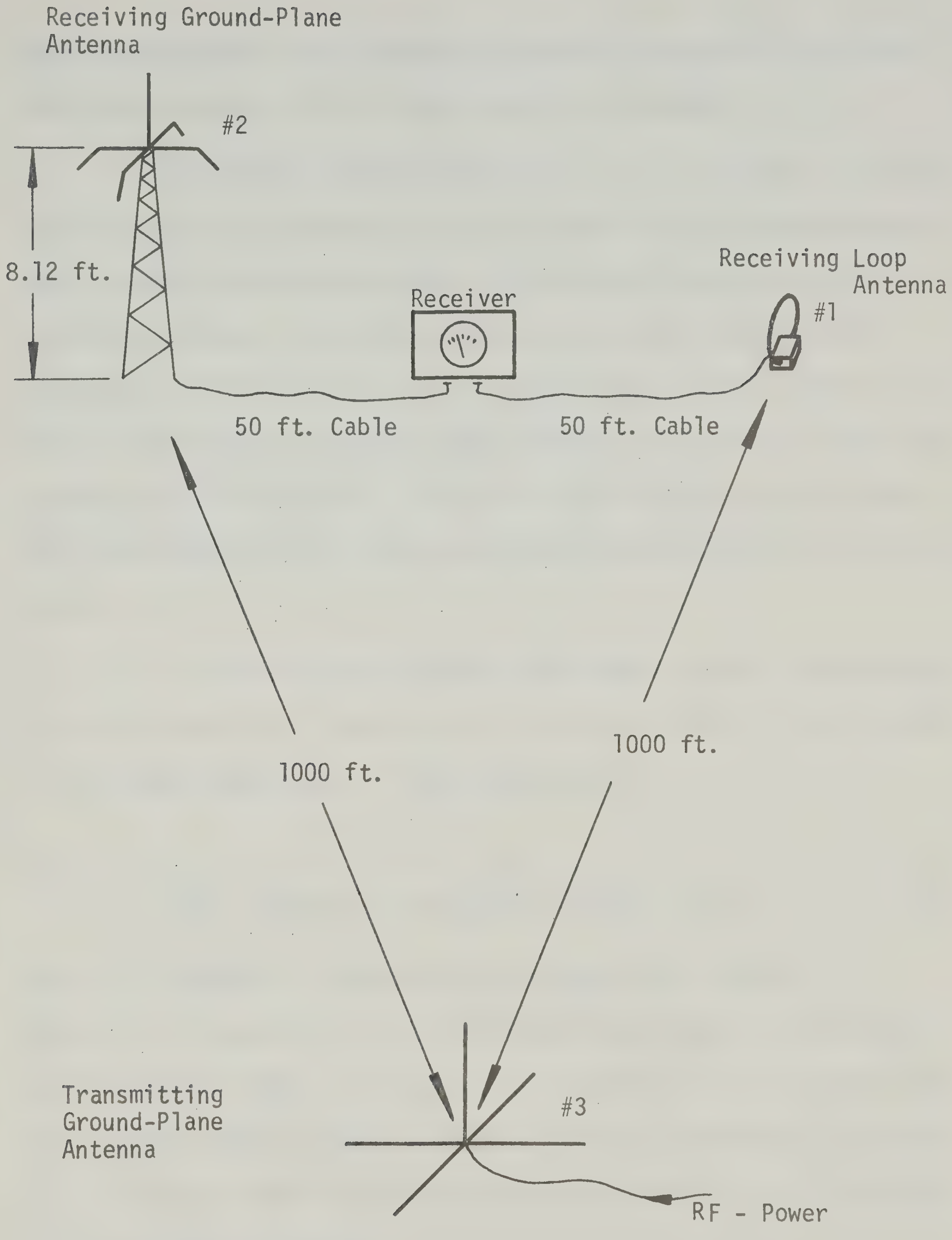

Figure 15. Efficiency Test

receiving antennas were trimmed by a matching network to 50 ohms, the input impedance of the tuned receiving voltmeter.

By sending a signal from antenna (#3) and keeping the power level constant, a comparison of the received signal strength between the elevated ground-plane antenna (#2) and the loop antenna (#1) could be obtained. Since the ground-plane antenna (#2) and the associated matching network can be approximated with an efficiency of close to 100%, an estimation of the radiation efficiency of the loop antenna (#1) was possible. It should be pointed out that the above efficiency prediction for the ground-plane antenna will be justified in Chapter IV.

For the evaluation of the efficiency, results from Appendix A will be employed. Equation (A.51) gives the ratio of the received to the transmitted power of two antennas as

$$\frac{P_{rx}}{P_{tx}} = \frac{1}{s^4} g_1 \, g_2 \, \eta_1 \, \eta_2 \frac{R_{11}}{R_{A1}} \frac{R_{22}}{R_{A2}} \left|(h_2 h_o - j \, h_o^2)\right|^2 , \qquad (3.5)$$

where all elements of the equation are explained in detail in Appendix A. Equation (3.5) is valid when one antenna is at ground level while the other is elevated. In Appendix A it was assumed that the antenna labelled with a subscript "2" was elevated at a height h_2 . If both antennas are at ground level, that is, $h_2=0$, equation (3.5) can still be applied.

Two transmission cases may be discussed; firstly, ground-plane antenna (#3) to ground-plane antenna (#2); and secondly, ground-

plane antenna (#3) to loop antenna (#1). It is possible to form the ratio of the power received by the loop antenna (#1) to the power received by the ground-plane antenna (#2).

All variables associated with the transmitting antenna (#3), as well as the transmitting distance will cancel out, leaving the result as

$$\frac{P_{rx\ loop}}{P_{rx\ grdpl}} = \frac{g_1}{g_2}\,\frac{\eta_1}{\eta_2}\,\frac{R_{11}}{R_{A1}}\,\frac{R_{A2}}{R_{22}}\;\frac{|(h_1 h_o - j\,h_o^2)|^2}{|(h_2 h_o - j\,h_o^2)|^2}\ , \qquad (3.6)$$

where the subscripts now refer to the antennas as labelled in Figure 15.

The following approximate values may be used:

Gain : $g_1 = g_2 = 1.5$

Efficiency : $\eta_2 = 1$

Impedance ratio : $\frac{R_{22}}{R_{A2}} = 1$ and $\frac{R_{11}}{R_{A1}} = \frac{1}{2}$.

The ground-plane antenna (#2) is located sufficiently far above ground that the effect of the ground on the input impedance is negligible. The loop antenna, however, rests directly on the ground and the resulting image current in the ground has the effect of doubling the radiation resistance.

Physical height : $h_1 = 0$

$h_2 = 8.12$ feet .

Making use of the above designations results in

$$\frac{P_{rx\ loop}}{P_{rx\ grdpl}} = N^2 = \frac{\eta_1}{2}\;\frac{|h_o|^4}{|h_o(h_2 - j\,h_o)|^2}\ . \qquad (3.7)$$

The received signal voltage ratio N was measured in the actual experiment, and so η_1 , the power efficiency, can be approximated from

$$\eta_1 = \frac{2\ N^2 |h_o(h_2 - j\ h_o)|^2}{|h_o|^4} \quad . \tag{3.8}$$

It can be shown that the law of reciprocity may be applied for receiving and transmitting from the same antenna at the same frequency. The more efficient the antenna is for transmitting, the more effective it will also be for receiving. Directivity and gain properties will be the same for both cases. Also, impedance will likewise be identical, whether the energy is fed directly to an antenna from the transmitter or whether it is picked up from passing waves of the same frequency. This property of reciprocity will permit the use of equation (3.8) to calculate the transmitting efficiency of the loop even though equation (3.8) was developed as the receiving efficiency.

For the three employed frequencies, the experimental values of N^2 were determined as

29 MHz $N^2 = 0.0115$
51 MHz $N^2 = 0.0259$
95 MHz $N^2 = 0.0169$.

Using values of $\varepsilon_r = 15$ and $\sigma_g = 0.008$ mhos/m, the values of h_o at 29 MHz, 51 MHz and 95 MHz may be calculated from equation (A.9), (A.12) and (A.28) in Appendix A. Substituting the resulting values of h_o into equation (3.8) gives

η_1 at 29 MHz $= 0.024$

η_1 at 51 MHz $= 0.068$

η_1 at 95 MHz $= 0.081$.

It is now possible to determine the approximate resistance of the loop antenna, which will be required in the estimation of the loop to wire signal coupling in equation (2.46). From equation (3.4),

$$\eta_1 = \frac{R_{A1}}{R_{A1} + R_{\text{loss }1}} \quad . \tag{3.9}$$

However, $R_{A1} + R_{\text{loss }1}$ is only the resistive portion of the driving-point impedance of the loop antenna, $R_{\text{loop }1}$. Thus, from equation (3.9),

$$R_{\text{loop }1} = \frac{R_{A1}}{\eta_1} \quad . \tag{3.10}$$

Since $R_{A1} = 2\,R_{11}$, the loop resistance may be written as

$$R_{\text{loop}} \simeq \frac{62400}{\cos^2 \frac{k\rho}{2}} \left(\frac{A_L}{\lambda^2} \right)^2 \frac{1}{\eta_1} \quad . \tag{3.11}$$

With the previously calculated values of η_1 the approximate values of the loop resistance become

R_{loop} for 29 MHz loop $\simeq$ 0.23 ohms

R_{loop} for 51 MHz loop $\simeq$ 0.84 ohms

R_{loop} for 95 MHz loop $\simeq$ 11.6 ohms .

3.3 The Signal Generation

For the experiment an unmodulated frequency was transmitted. The source of the signal consisted of a crystal oscillator. A tunable power amplifier was available (Hewlett - Packard 230 A, Signal Generator Power Amplifier) with a fixed gain of about 20 to 30 dB and a 50 ohm output impedance. Provisions were made to limit the oscillator output to about 2 mW into a 50 ohm load, and to allow for a rough signal amplitude adjustment.

Three different oscillators for 29, 51 and 95 MHz respectively were built for the tests. Since the oscillators were excellent with respect to drift and amplitude variations, a minimum of retuning of the heterodyne voltmeter at the receiving station was required. Although the 12 volt solid-state power inverter, providing 115 volt at 60 Hz, created a supply voltage more like a square wave, there was no problem with noise.

Because signal losses occurred in the 50-foot feeding line to the antenna, the feed-through power meter (Philco - Sierra 164 B, Bi - directional Power Monitor) was stationed directly before the radiating loop antenna and preceded by a variable attenuator, (Weinschel Engineering Model 905, 0 - 10 dB). It was possible to set the power level for the radiating loop antenna very accurately by keeping the difference between the power delivered to the loop and the reflected power at some constant level. Depending on the ground condition, the reflected power varied between zero and 3% at most.

To allow for possible power variations, the one-watt scale

of the meter was used and the transmitted power to the loop antennas was set to 0.7 watts. This value represented only a relative reading, because the scale of the power meter must be multiplied by a correction factor that depends on the frequency. Power meter calibration curves were obtained for all frequencies used.

3.4 The Wire Line

The constructed wire line consisted of one or two copper wires (#18 GA multistrand, PVC insulated) running parallel to a 4250-foot long previously surveyed line. The height of the wire could be adjusted up to 6 feet and the wire was supported by 2" by 2" wooden poles. To obtain a good ground-reference connection, one 6-foot ground rod was installed at each end of the line. Both the single and the double-wire lines are illustrated in Figures 16 and 17.

Considering the single wire first; it may be shown from equation (2.14), that the line impedance is approximately 512 ohms. The wire line is of finite length and an abrupt ending of it will give rise to standing waves along the wire itself. Coupling to the line will then be a function of distance along the line and losses at the receiving station will result.

Procedures to avoid these reflections were considered and an experimental method was developed to measure, and eventually to aid in the reduction of the standing waves. For this purpose, a signal of the desired frequency was fed to the terminals of what was to be the receiving end of the line. At the far end, the termination end of the wire, provisions were made for loading the line with

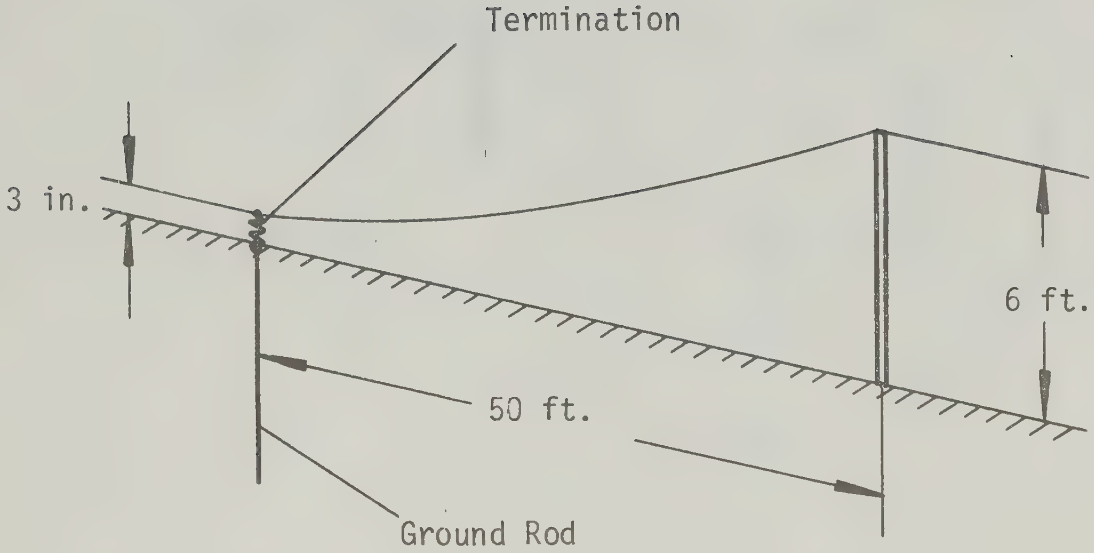

The Far End

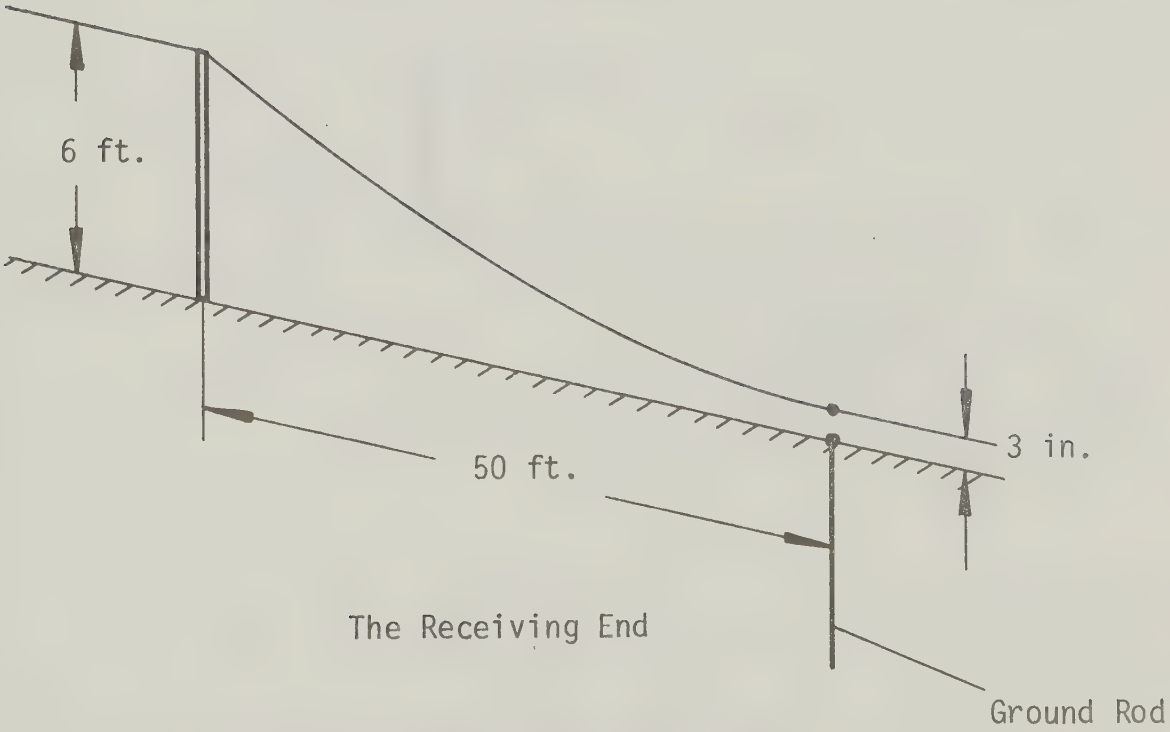

The Receiving End

Figure 16. Single-Wire Line Taper

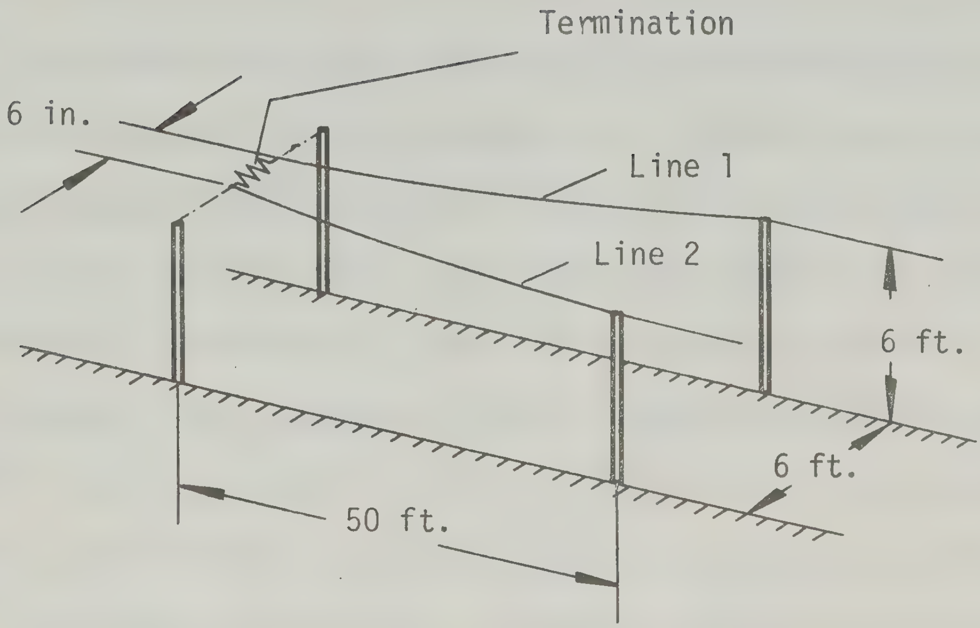

The Far End

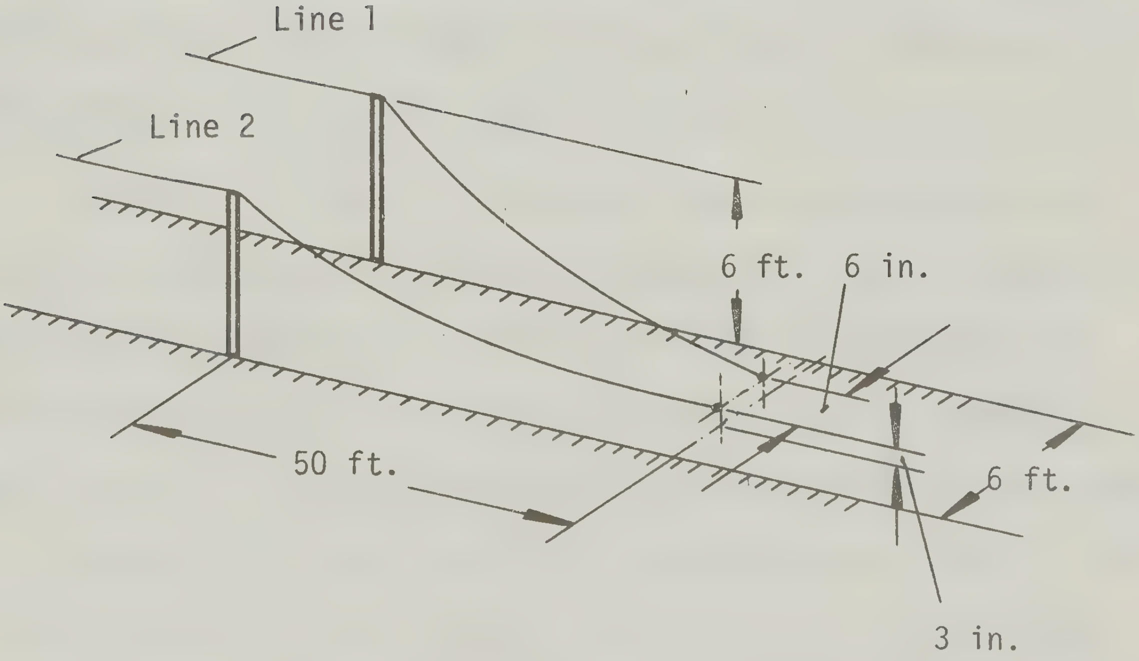

The Receiving End

Figure 17. Double-Wire Line Taper

ordinary ¼-watt resistors. At 4000 feet, (250 feet from the termination), a matched-loop antenna was placed directly under the line in maximum coupling position and connected by a 50-foot coaxial cable to a tuned voltmeter (Brüel and Kjaer Heterodyne Voltmeter Type 2006). Moving the loop antenna slowly along the line, keeping its orientation the same, the received signal varied through maximum and minimum values. The standing wave ratio (SWR) on the line was thus determined and the effect of various termination loads was immediately apparent. To match the line meant adjusting the load for a SWR of unity. To reduce irregularities in the SWR caused by uneven ground, the loop was mounted on wooden rails placed under the wire at ground level. The wire line was kept parallel to these rails with extra supporting poles. Plate 3 shows the loop antenna on wooden rails in transmitting position to the single-wire line.

Direct termination of the wire line in a selection of resistances did not result in the desired matching. It was found that a vertical wire connecting the line to the ground rod through the termination presented a discontinuity that could not be matched by a single resistor. It was not possible to arrive at a SWR of less than 2.5 . The next step was to avoid the discontinuity of the wire line by tapering the wire over a length of 50 feet from a 6-foot height to about 3 inches, as suggested by Figure 16. Now the results were more promising and it was possible to obtain SWR's down to 1.02 .

Next, an SWR measurement was made at 2000 feet. It showed however that the wire line was of such lossy character that the apparent SWR of about 1.15 was independent of the terminations at the far end, as for example, short or open circuit. Indeed, whenever a measurement

was made at distances greater than about 1000 feet from the end of the wire, the measured SWR was independent of the termination. The fact that at these remote locations the apparent SWR was higher than when measured near the terminating resistor is attributed to irregularities introduced by wire sag and heavy vegetation under the wire itself. In places growth up to 3 feet high was found. It was further observed that the maximum and minimum values of the received signal did not occur at the same location at all times. This result is also clearly an indication that changing, complex loads along the wire line were present.

To reduce the SWR near the termination to between 1.02 and 1.06 required load resistances of 220 to 330 ohms to be placed across the end of the tapered section. Note that the value of Z_o for the single-wire line at a height of 3 inches is given by equation (2.14) to be 332 ohms.

Determination of the far-end resistive load solved the problem, in principle, of the receiving-end termination. A tapered section was also inserted at the receiving end. Matching networks then were required which transformed the resistances of the wire line to the 50 ohm input impedance of the tuned-voltmeter receiver.

With the aid of a Smith Chart, three matching networks were designed. Figure 18 shows the final circuitry. It may be noted that the series inductance of the network was made slightly larger than required to allow for the addition of capacitor C1. The tuning of the device could then be accomplished by simply trimming the variable

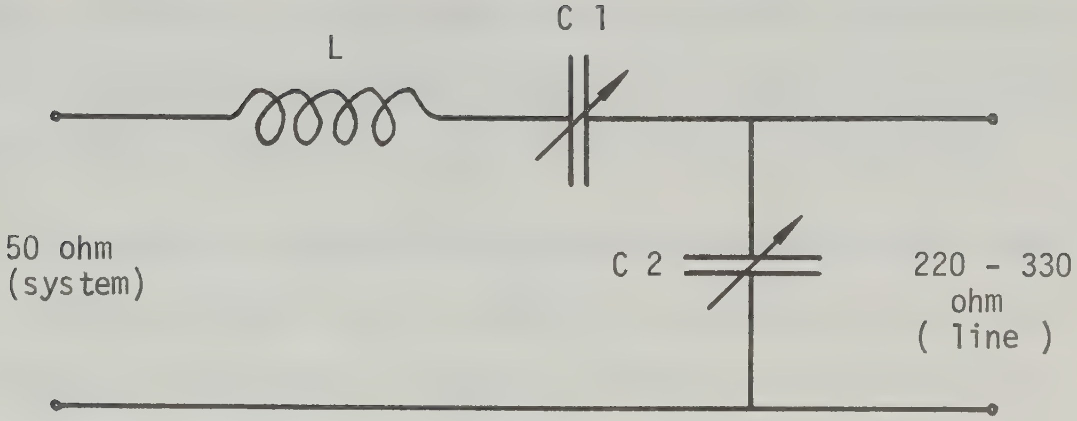

Frequency	L	C 1	C 2
29 MHz	0.686 µH	110 pF (0 - 150 pF)	15 pF (0 - 50 pF)
51 MHz	0.390 µH	25 pF (0 - 100 pF)	3 pF (0 - 50 pF)
95 MHz	0.209 µH	40 pF (0 - 50 pF)	2 pF (0 - 8 pF)

Figure 18. Wire-Line Matching Network

capacitors. Further, it may be seen from the circuit that since air capacitors were used, the greatest loss in the network occurs in the coil. This loss, however, is so small that it may be neglected.

The actual tuning of the device was conducted by the power method. That is, a signal at the required frequency was fed to the line by means of the matching network. Trimming the capacitors for a minimum reflected power from the matching network proved to be surprisingly simple. Reduction of reflections to less than about 1% of the input power was possible.

The same network was useful for all wire heights without the necessity of significant retuning. The tapered line compensated for all changes in the line impedance that depended on the wire height and the characteristic impedance of the line at the end of the taper remained constant.

Having solved the problem of line-matching for the single wire, the double line did not present any new difficulties. In fact, it was found that using the configuration of Figure 17, the receiving-end matching network could be used with only a small retuning. Only the far end of the line had to be equipped with a different resistive value. The method of finding it was the same as employed for the single line and resulted for

51 MHz in 750 ohms.

The SWR with this value was 1.13.

3.5 Results for the Single-Wire Line

Experimental data were obtained as described in the previous sections, and as mentioned earlier, it was necessary to create calibration curves for the bi-directional power meter. As a result, it was discovered that the following power levels were actually delivered to the antenna loops :

29	MHz	0.99 watts
51	MHz	1.17 watts
95	MHz	1.30 watts .

Before the different signals are compared, it is essential that the experimental results be normalized to a common transmitter power.

Equation (2.46) clearly shows that the received power is directly proportional to the power delivered to the loop. Thus, it is not difficult to bring the results at the different frequencies to a common denominator of 1 watt.

The normalized received voltages for the single wire are presented for the three frequencies in Figures 19, 20 and 21 respectively. The same graphs also show lines representing the results employing the theory of Chapter II.

The coupling between loop and wire presented in equation (2.46) and the attenuation of the travelling signal along the wire line, as given by equations (2.63), (2.74), (2.82) and (2.88), were used in preparing the theoretical curve. In each case, the loop was positioned directly under the wire and oriented for maximum coupling to the line.

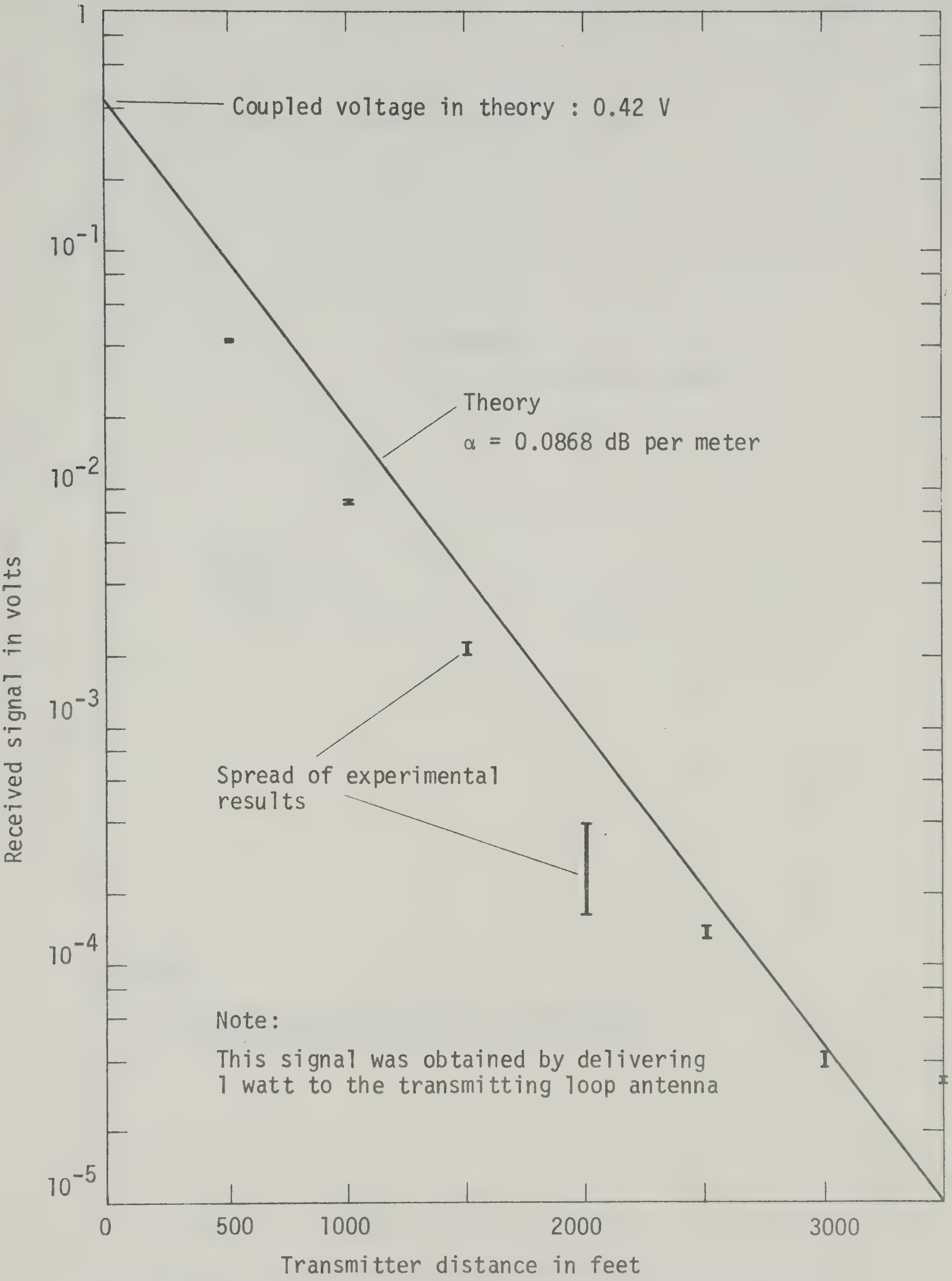

Figure 19. Results for 6-foot, Single-Wire Line at 29 MHz

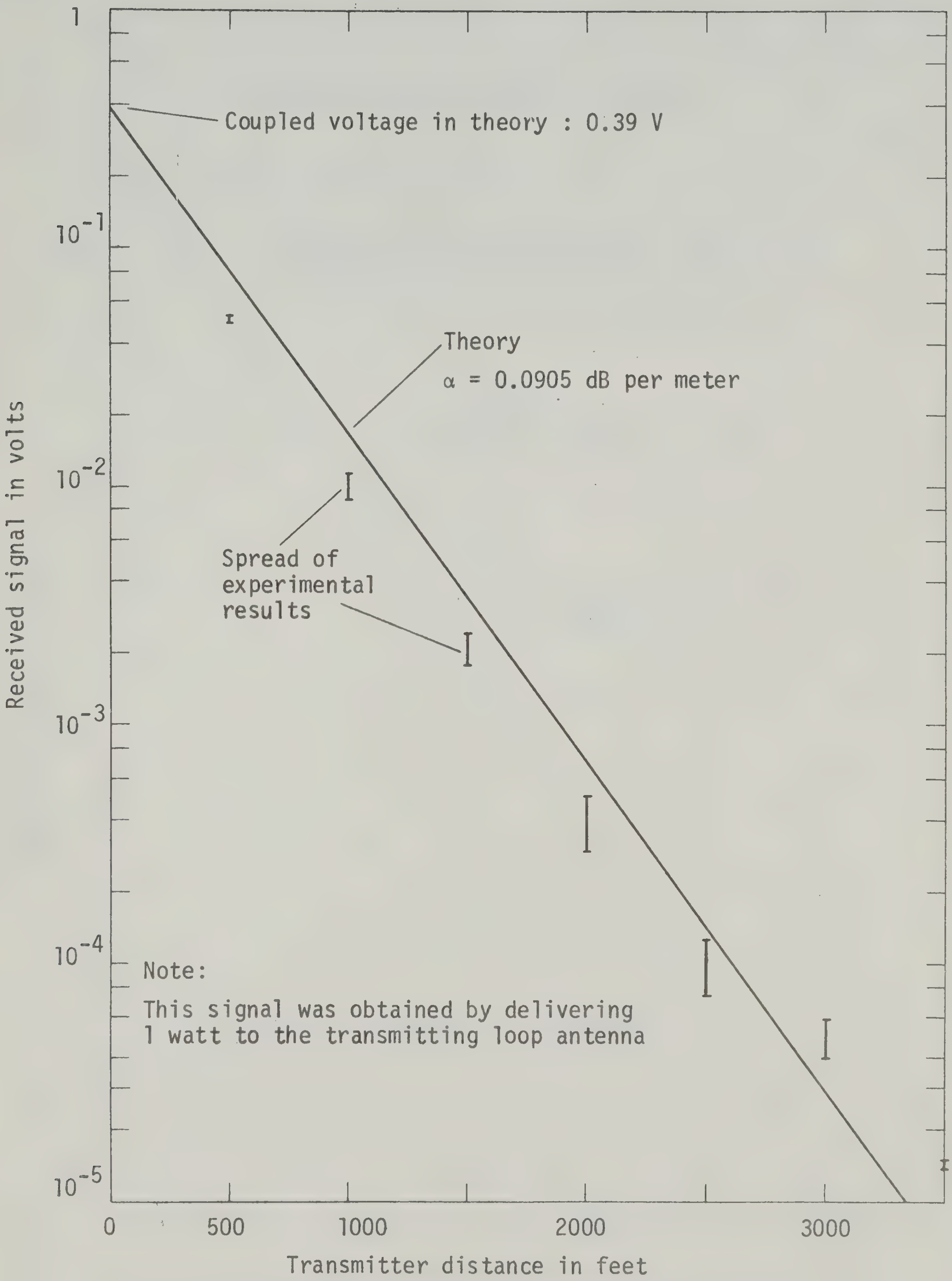

Figure 20. Results for 6-foot, Single-Wire Line at 51 MHz

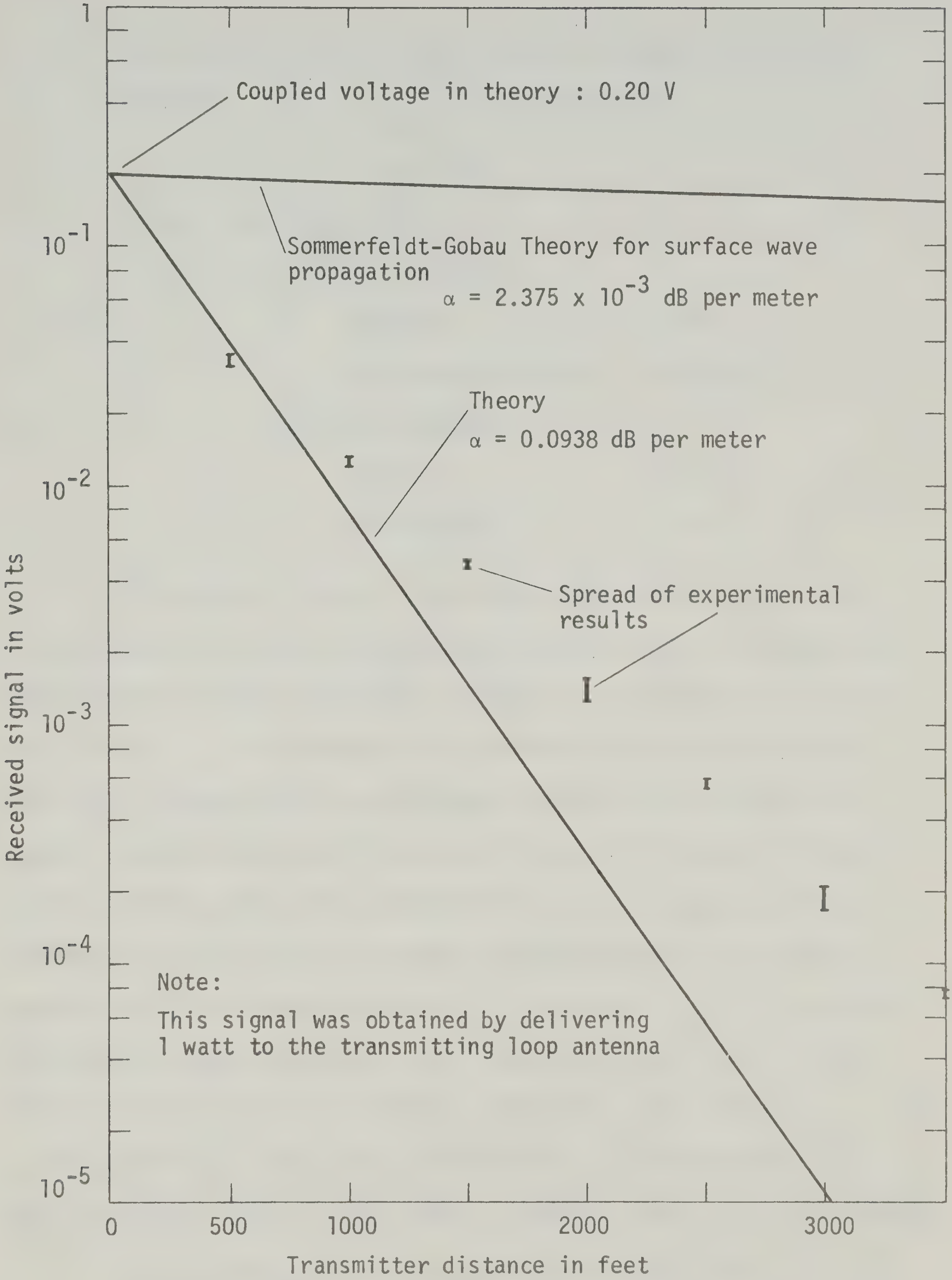

Figure 21. Results for 6-foot, Single-Wire Line at 95 MHz

For the calculations the following parameters were chosen:

Ground : $\sigma_g = 0.008$ mhos/meter

$\varepsilon_r = 15$

Wire : multistrand # 18 GA.

Height above ground:

average = 5 feet

at coupling points = 5.75 feet

Diameters (outside):

copper ø = 1.2 mm

insulation ø = 2.2 mm

The choice of these values needs some justification. The ground conductivity was estimated from data provided by the Department of Agriculture at the University of Alberta for the farm at Ellerslie. The value of ε_r was obtained on a somewhat trial and error basis. The loop to elevated tower experimental results to be discussed in Chapter IV were compared with the theoretical predictions of Appendix A. Since these results were dependent on ε_r , it was possible to estimate the value of this parameter that represented a satisfactory agreement with the experimental data. The value of $\varepsilon_r = 15$ obtained in this manner was then used in the theoretical calculations of the wire line propagation. It should be noted that these values of σ_g and ε_r are essentially the same as those given by "Reference Data for Radio Engineers" [29], for the type of farmland used in this experiment.

During the course of the experiments (summer 1971 and 1972) frequent rainfalls as well as dry periods were common. As a result,

the farm land showed changing plant growth. To give more specific values for the above mentioned constants would not be meaningful. Of course, it was also not possible to limit the experiments to times when the climate and growth conditions were approximately the same over short periods of time. The amount of physical work involved, the unpredictability of the elements, and the scheduling of work so as not to interfere with the work at the University farm - all these factors combined severely limited the available experimental time.

The differences in the wire heights used for the calculations have to be justified. At the points where the loop antenna was positioned to couple signal to the wire lines, the ground was cleared of all plant growth and the wire was supported with additional poles, such that an average wire height of about 5.75 feet above the ground could be maintained. At the points along the line where the wire was supported every 50 feet, a wire sag of about 6 inches could not be avoided. On the other side, all along and below the wire, a dense growth of vegetation was present. Though loose in its appearance, it effectively represented an elevated ground level. Another 6 inches was allowed for the influence of this vegetation, resulting in an effective wire height of 5 feet.

All approximations, of course, will have their effects on the calculated results and allowances must be made when comparing theory and practical experiment.

Comparing the results for 29 MHz and 51 MHz, it is apparent that the theoretical predictions are consistently high by about 4 dB

to 6 dB for ranges less than 2500 feet. The most probable cause for this discrepancy is in the determination of the efficiency of the loop antenna, and from it, the derivation of the value of the loop input resistance, R_{loop}, as described in Section 3.2. Undoubtedly a direct measurement of R_{loop} would have led to more accurate values, and thus, probably to a closer agreement between theory and experiment. However, such a measurement would have been difficult to obtain under actual field conditions with any reliability and it was decided that the indirect calculation of Section 3.2 would be sufficient to demonstrate the general validity of the theory. Beyond 2500 feet the experimental signal does not drop off as rapidly as predicted. As will be seen in discussing the results for a wire at a height of 3 feet, the attenuation can be expected to decrease to a value of 12 dB per octave, at distances large enough that the total attenuation of the signal along the line is greater than the attenuation of the signal directly radiated from the loop to the distant receiver. Moreover, an apparent decrease in attenuation will also result as the end of the line is approached because of an increase in the coupling.

Observing now that the spread of the experimental values varies up to 7.5 dB, the theoretical results clearly provide a satisfactory description of propagation along the wire at 29 MHz and 51 MHz.

Figure 21 shows the result for the 95 MHz transmission. In Chapter II it was pointed out that it is to be expected from the work of Kikuchi [15, 16] that the theory presented here will not hold true

at higher frequencies. Indeed, Figure 21 shows that at 95 MHz the attenuation is considerably less than expected, leading to the conclusion that the wave is propagating in some hybrid mode that is partly of a surface wave nature and partly of a transmission-line nature. As expected for such a situation, the attenuation lies between the two extremes predicted on the one hand by the Sommerfeldt-Gobau theory [30], and on the other hand, by the results of Chapter II.

Figure 22 shows the case of a 51 MHz signal transmitted along a wire elevated 3 feet above ground, or for reasons stated earlier, at an effective height of 2 feet. Both theory and experiment seem to agree quite well for ranges less than 1000 feet, although once again, the theoretical coupling appears to be somewhat high. Beyond 1000 feet the attenuation rapidly approaches a value of 12 db per octave. This value is what would be expected for the attenuation between two widely separated antenna systems whose heights above ground are much less than the distance between them (Appendix A). In other words, beyond 1000 feet, the total line attenuation is so severe that more signal is coupled to the receiver directly from the radiated fields of the loop antenna than is coupled via the overhead line. As a check on this suggestion, the wire line was removed except for a 50-foot section of 6-foot height, directly in front of the receiver. This short Beverage antenna was terminated in the same manner as the original 4000 foot antenna. Measurements of the received voltage were taken and the results are given by the dotted line in Figure 22. Although somewhat higher, these results clearly indicate that beyond

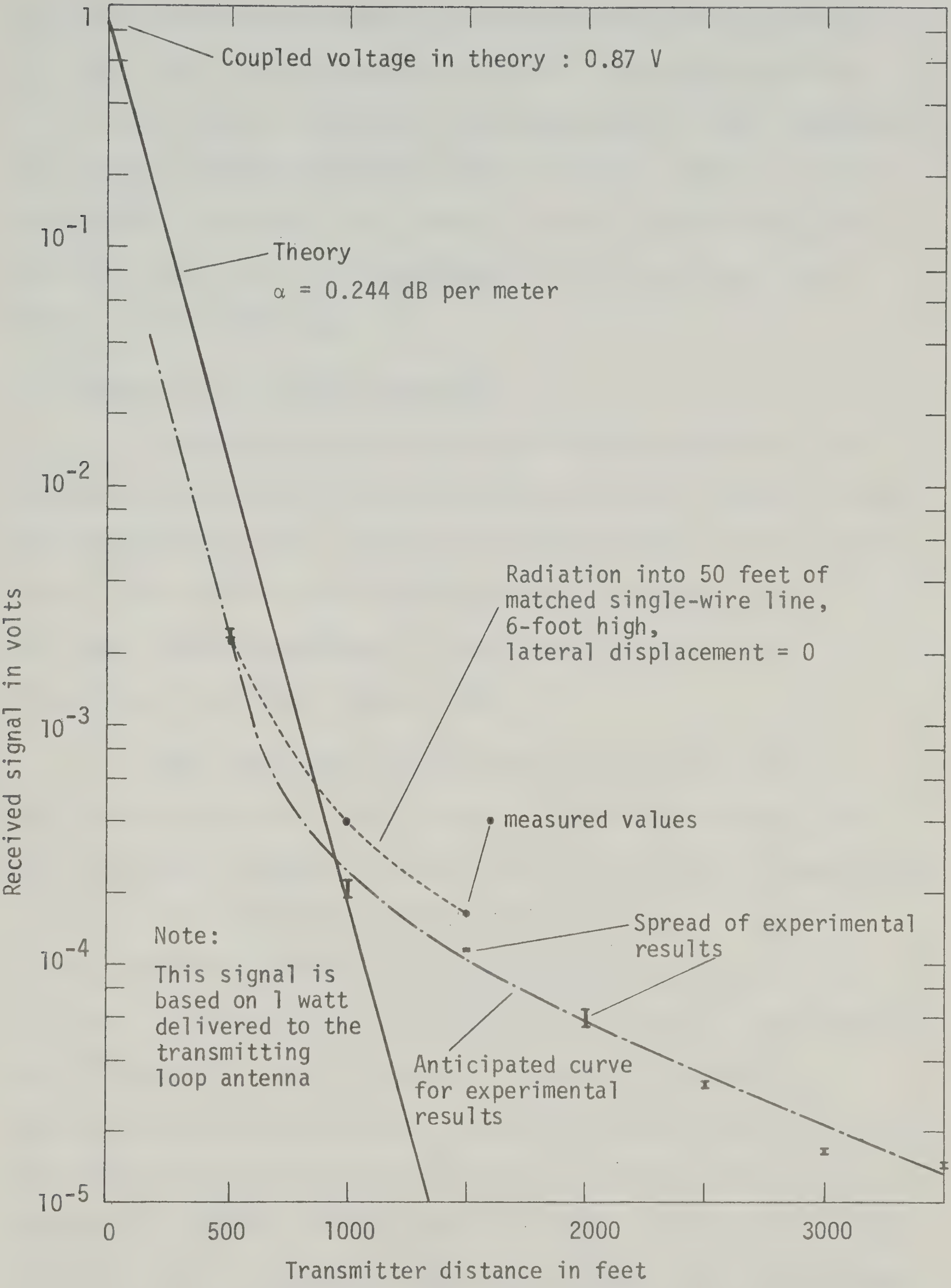

Figure 22. Results for 3-foot, Single-Wire Line at 51 MHz

1000 feet, the direct radiation is more important than the amount of signal that can be propagated along the 3-foot high wire line. As the wire height is increased, thus decreasing the line attenuation, the directly-coupled signal will not be important until the range is considerably increased. For example, Figures 19 and 20 show that for the 6-foot wire, direct radiation is significant only beyond ranges of about 3000 feet.

3.6 Results for the Double-Wire Line

In principle, all remarks regarding the assumptions and dimensions are valid also for the double-wire line. Figure 23 shows both calculated results, employing equations (2.46), (2.63), (2.76), (2.82) and (2.93) for the coupling and the attenuation along the line, and the experimental values normalized to one watt. Measurements were taken only at 51 MHz.

Again the signal coupled into the line is below the theoretically predicted value by about 4 dB. More important, the wave apparently attenuates somewhat more rapidly than is theoretically predicted. This difference in attenuation, of course, leads to increased separation between theory and practice as the range is increased. For the most part, this error can be traced to the assumption that the magnetic field at the earth's surface is the same as though the ground were a perfect conductor. In the single-wire case, this simplification led to quite accurate predictions for the attenuation. However, in the double-wire case the extra wire and its image give rise to a magnetic field that is nearly equal and opposite to the field produced by the first wire and its image at points

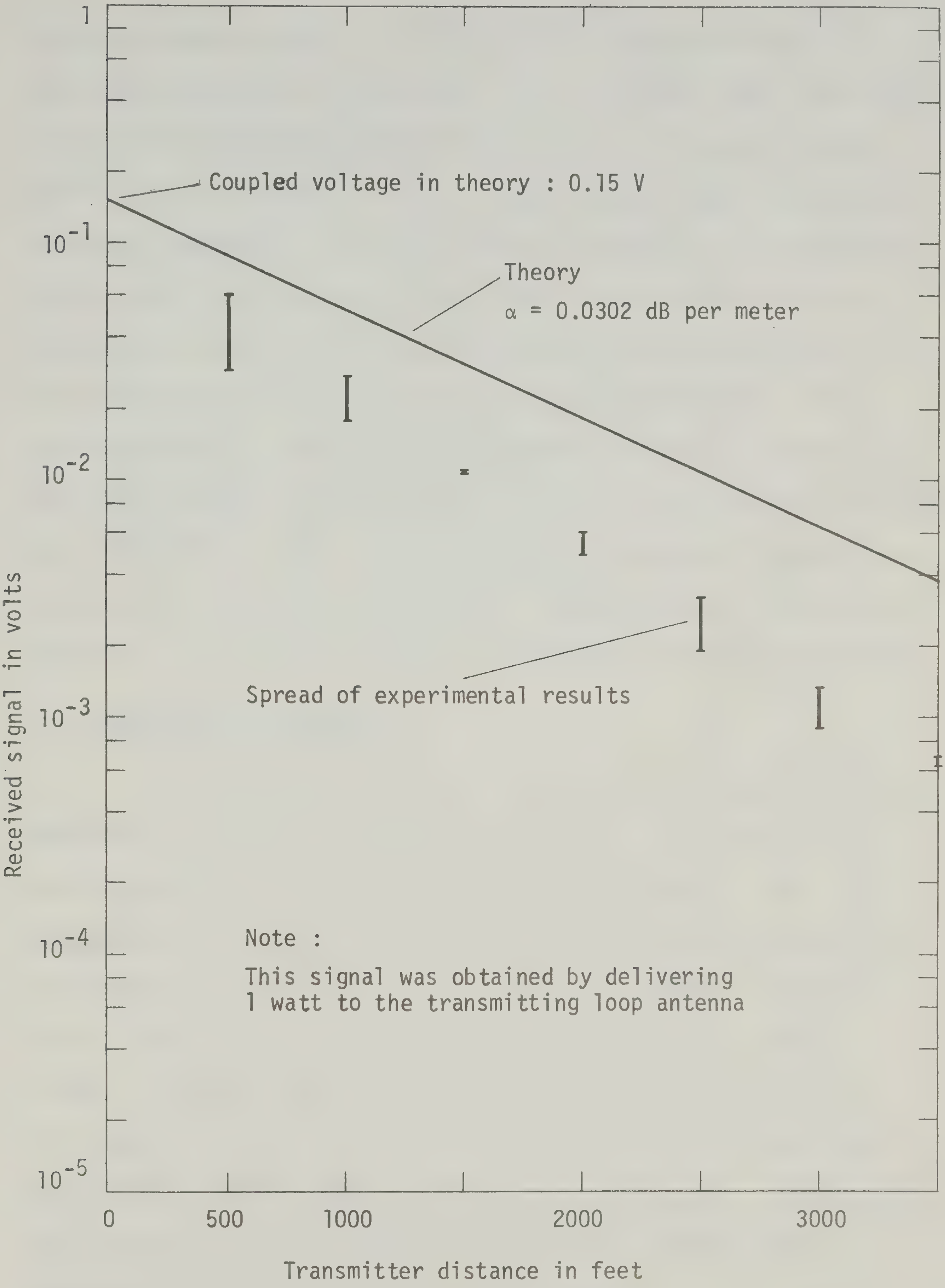

Figure 23. Results for 6-foot, Double-Wire Line at 51 MHz

along the ground surface. Thus, the net field when the ground is perfectly conducting is quite small. For a practical earth, this self-cancellation between the fields of the two wires is not as complete and the resulting magnetic field is significantly higher - leading to increased attenuation. Even with these discrepancies, the theoretical results still provide a satisfactory description of the wire-line propagation. It is important to note that with the double-wire line, the line attenuation is significantly reduced with respect to the single-wire line. Expressing the attenuation factor in decibels per 100 feet, the result for the double-wire line is approximately 0.93 dB per 100 feet at 51 MHz. The corresponding single-wire attenuation for the same wire height and frequency is approximately 2.75 dB per 100 feet; an increase of a factor 3 compared to the double-wire line.

3.7 Lateral Loop Displacement

As a check on the general nature of the coupling mechanism, measurements of received voltage were made at a fixed range as the loop was moved away from the wire line at right angles. The experimental results were then normalized as described in Section 2.4 and compared to the theoretical values given by equations (2.56) and (2.57). Figure 24 shows the results for the single-wire line at 29 MHz, 51 MHz and 95 MHz. Figure 25 shows the results for the double-wire line at 51 MHz. It is obvious that in both cases the correspondence between theory and practice is quite good. However, the experimental results for the single-wire line at 29 MHz are inexplicably high by about 6 dB.

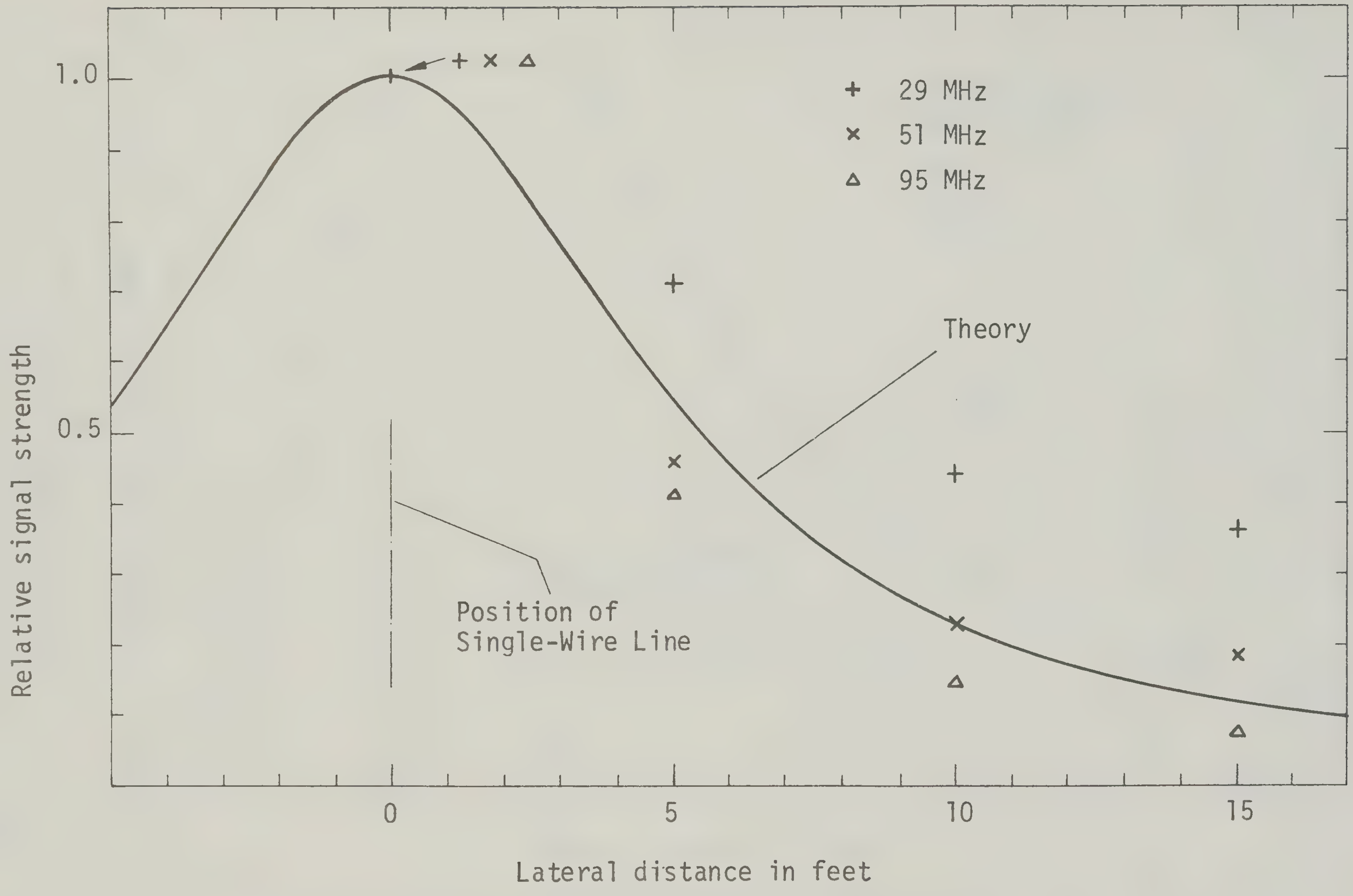

Figure 24. Lateral Signal Loss of 6-foot, Single-Wire Line at 29, 51 and 95 MHz

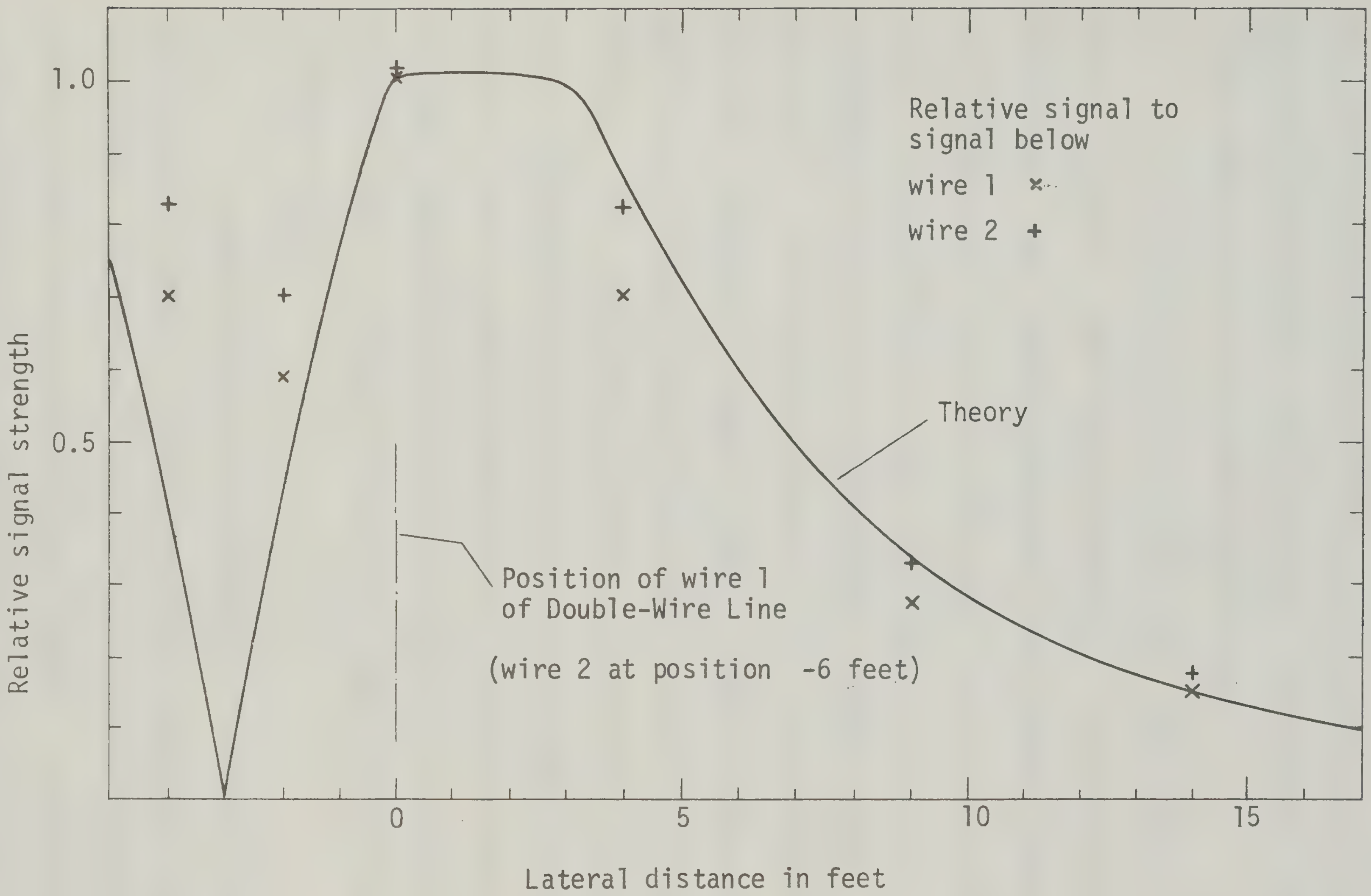

Figure 25. Lateral Signal Loss of 6-foot, Double-Wire Line at 51 MHz

3.8 The Wire Grid

From Figures 24 and 25, one may observe that the signal at a lateral displacement of 10 feet has dropped off to about one-fourth of its original value, and at the same time, the rate of change of the signal starts to decrease significantly.

It is now possible to imagine the case of several wires strung in parallel, each being terminated in the same way as the single-wire line. Placing a radiating loop between wires and observing the received voltage on each of them, should give an indication of the relative distance of the loop to any of the wires. The loop orientation itself will not influence the overall picture. The principle is illustrated in Figure 26. It is easy to expand this idea to a rectangular network of wires as shown in Figure 27. This grid was constructed with the dimensions indicated and is shown on Plate 4. Each single wire was terminated on one end in its characteristic line impedance and the other end was left open-circuited. A four-foot copper ground rod was placed at the ends of every line. The wires themselves were separated vertically by 6 inches at the crossover points to reduce the coupling between the two sets of orthogonal wires.

In order to test the effectiveness of the grid network in predicting the location of the transmitting loop, it was necessary to construct a small battery-operated portable oscillator that could readily be moved from one location to another. A circuit previously used by W. Cochran [3] was selected and is shown in Figure 28.

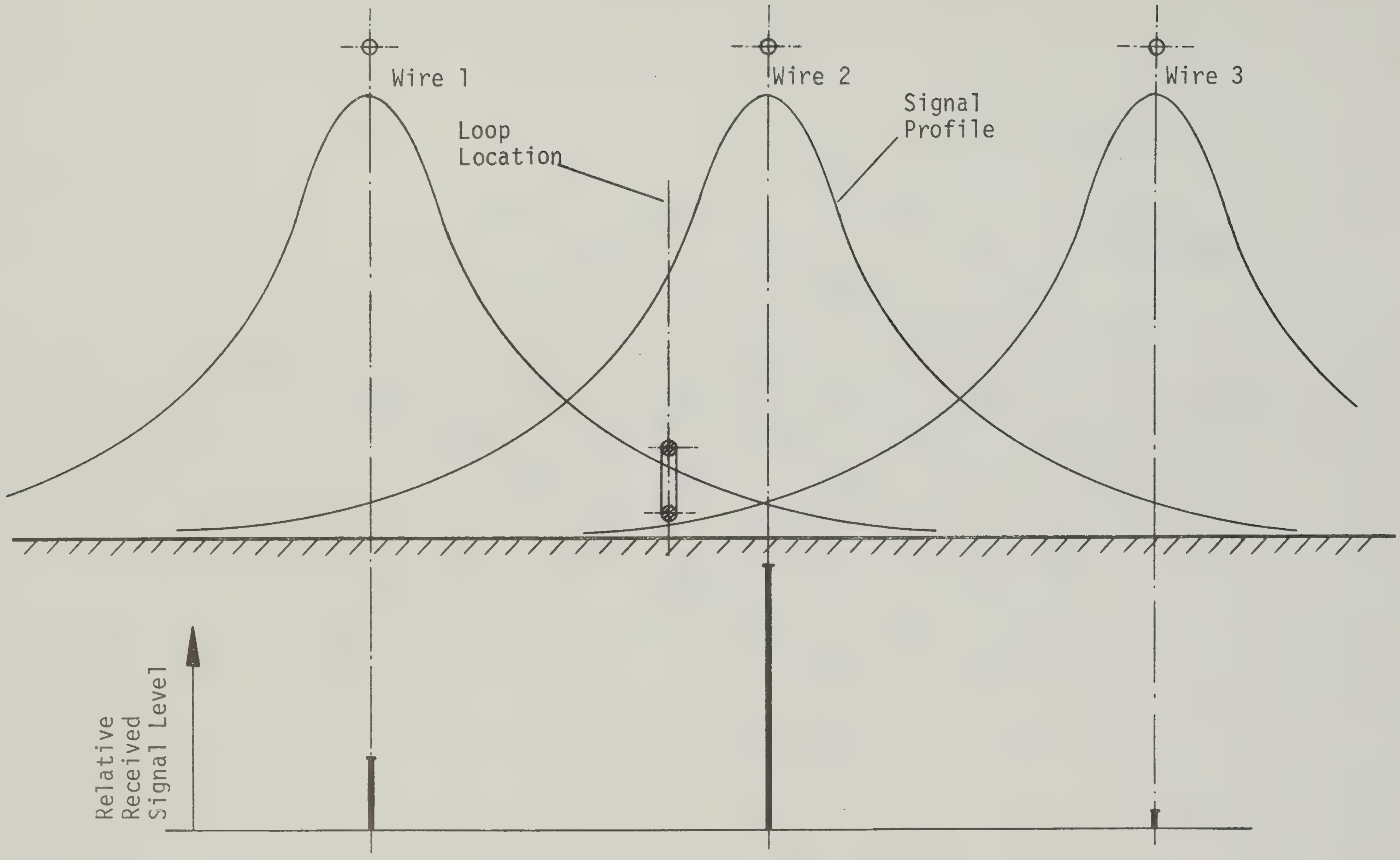

Figure 26. Loop Location and Received Signal Strength

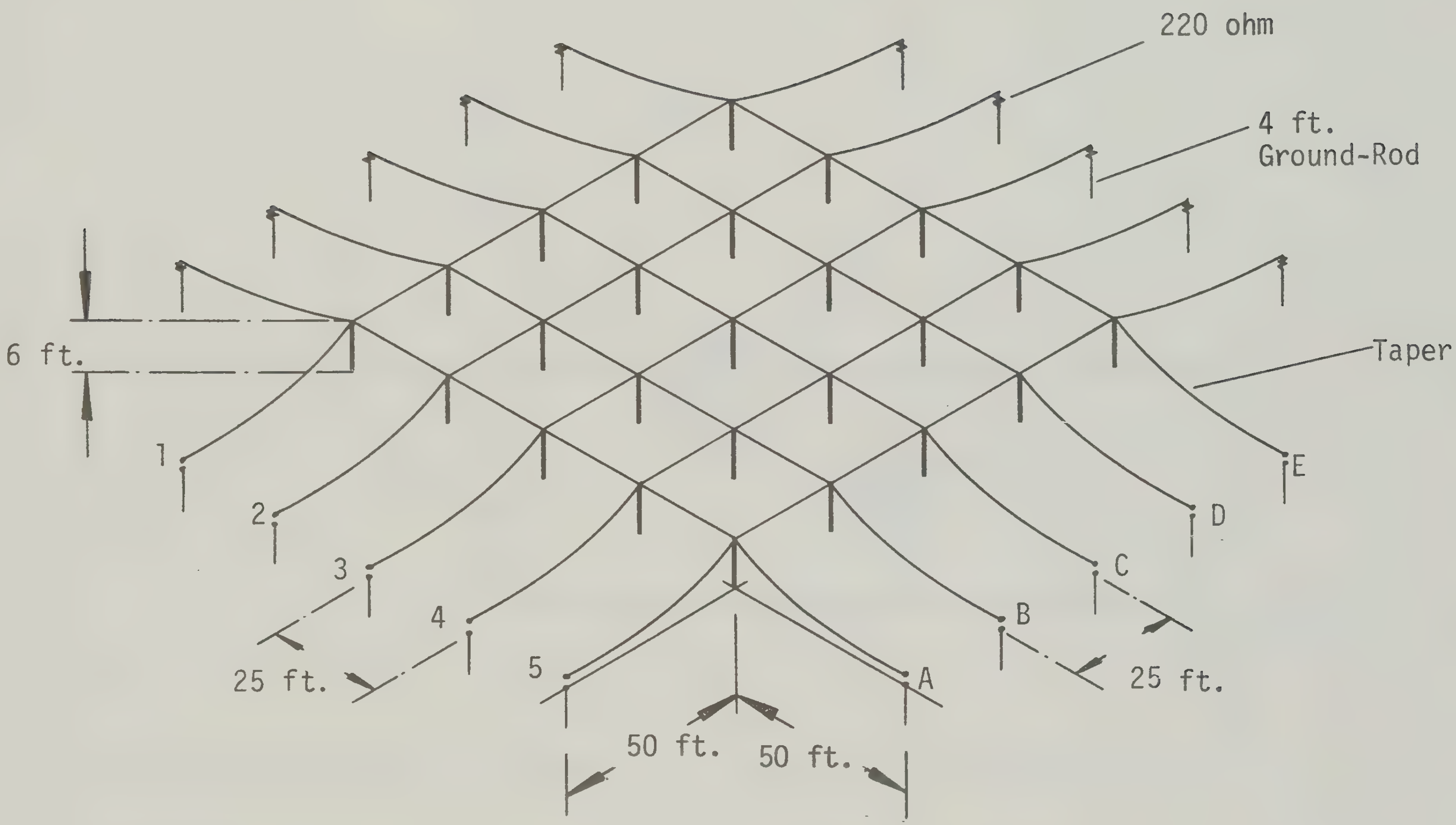

Figure 27. Wire-Grid System

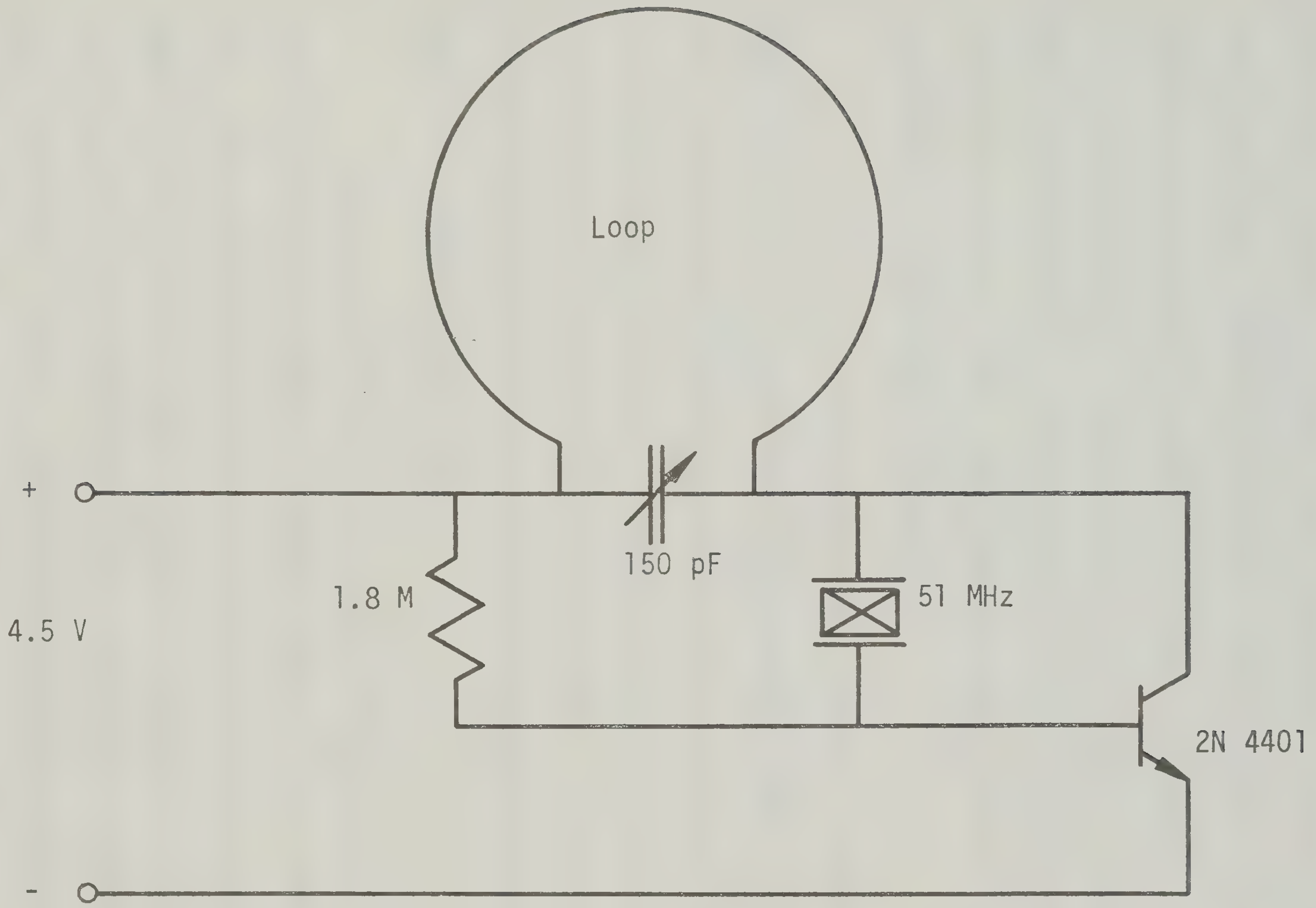

Figure 28. Small Oscillator Circuit

Since no absolute measurements of signal strength were required in this experiment, no effort was made to establish any particular output power level. The only requirement was that of obtaining a constant output. This oscillating loop was then placed within the 100 by 100-foot wire grid, illustrated in Figure 27. The Heterodyne Voltmeter, preceded by a matching network, was connected to all 10 wire lines in succession and the received signal recorded. These measurements were repeated for all possible locations and orientations of the loop. Some characteristic signal position recordings are displayed in Figure 29.

It is easily seen that it was possible to indicate in nearly all cases the position of the radiating loop within the wire grid, by noting which two orthogonal wires carried the largest signals. This method limits, however, the determination of the exact position of the loop to a square of 25 by 25 feet only. Thus, the accuracy of the system in locating the transmitter depends on the mesh dimensions chosen for the grid.

Only one ambigous reading was obtained, namely the one resulting from a transmitter located exactly in the center of one mesh with the loop positioned parallel to one wire direction. The coupling into the two wires parallel to the loop was excellent. The coupling into the perpendicular wires provided no guide to pinpoint the transmitter. Indeed, the theory developed in Chapter II showed that under these latter conditions, no signals should be present in those wires. This ambiguity is not a serious practical drawback since only

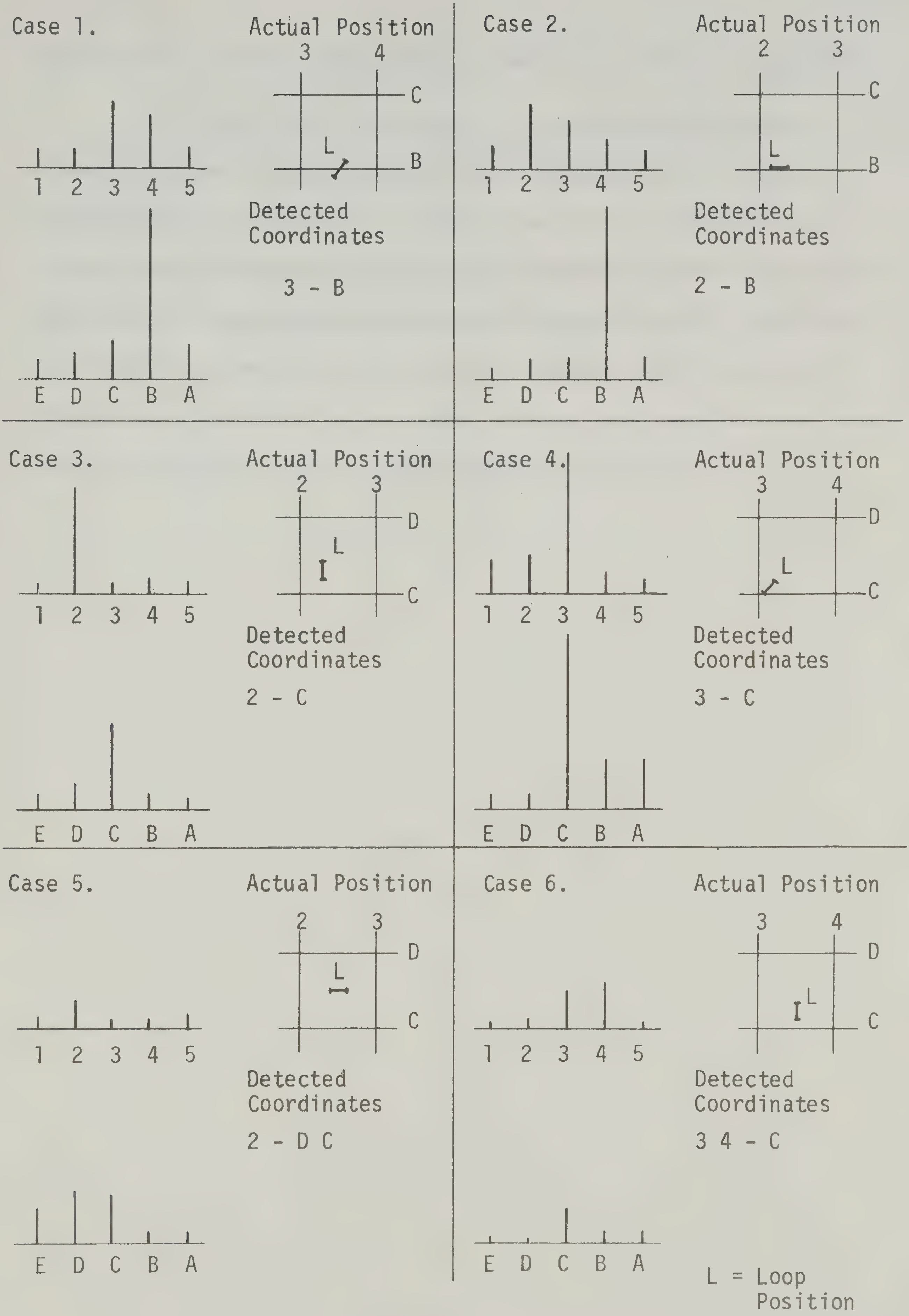

Figure 29. Typical Wire-Grid Results

rarely would a radio-tagged animal assume one unfavourable position.

It can be anticipated that in certain circumstances a wire-grid system can provide positional information on a radio-tagged animal in a simpler and cheaper way than the conventional triangulation technique using high-gain antennas. Often, only bearing information is required, such as in the current study of the cottontail rabbit presently underway at the Rochester Wildlife Centre in north- central Alberta. In this instance, the required data could be readily obtained from a simple system of radial wires.

CHAPTER IV

OMNI-DIRECTIONAL, TOWER-MOUNTED RECEIVING SYSTEM

4.1 Introduction

Radio location by means of a tower-mounted antenna is the method mainly used in today's telemetering applications. For triangulation, highly directional antennas, such as Yagi-antennas are often used.

To determine the relative efficiency of the Beverage antenna for bio-telemetric applications, a conventional tower-mounted ground-plane antenna was used for the comparison. The antenna has an omni-directional radiation pattern, that is, no received signal of any particular direction surrounding the antenna is prefered. The ground-plane antenna was tested under exactly the same physical conditions as the Beverage antenna to allow for a valid comparison.

The test system is shown in Figure 12. As in the case of the Beverage antenna, a matching network is required to bring the antenna impedance to the 50 ohms of the receiver. A 50-foot coaxial cable was used to connect the matching network located directly below the ground-plane antenna to the receiving instrument, the Heterodyne Voltmeter. The transmitting equipment was exactly the same as the one used in the Beverage antenna case. The antenna tower was extendable, so that heights of about 8, 22 and 38 feet could be utilized.

4.2 Theoretical Analysis

The transmission between two antennas is treated theoretically in Appendix A. Equation (A.51) gives the ratio of the power received to the power transmitted when antenna (1) is located at ground level and antenna (2) is located at a height, h_2 . In the present case, antenna (2) is the ground-plane antenna mounted on the tower, while antenna (1) is the transmitting loop antenna.

When the power delivered to the antenna is P_{loop} and the input impedance to the receiving system is 50 ohms, the expected rms signal voltage across the receiver may be expressed as

$$V_{rx} = (P_{loop}\ 50\ g_1\ g_2\ \eta_1\ \eta_2 \frac{R_{11}}{R_{A1}} \frac{R_{22}}{R_{A2}})^{\frac{1}{2}} \frac{|(h_2 h_o - j\ h_o^2)|}{s^2} \qquad (4.1)$$

All used variables are explained in detail in Appendix A. The following approximate values for these variables may be used:

Gain : $g_1 = 1.5$

$g_2 = 1.5$

Efficiency : $\eta_2 = 1$

$\eta_1 = 0.024$ for 29 MHz

$= 0.068$ for 51 MHz

$= 0.081$ for 91 MHz

Impedance ratio : $\frac{R_{11}}{R_{A1}} = \frac{1}{2}$, $\frac{R_{22}}{R_{A2}} = 1$

Physical height : $h = 8.1$, 22.4 and 38.8 feet

4.3 Experimental Measurements

The ground-plane antenna design, shown in Figure 30

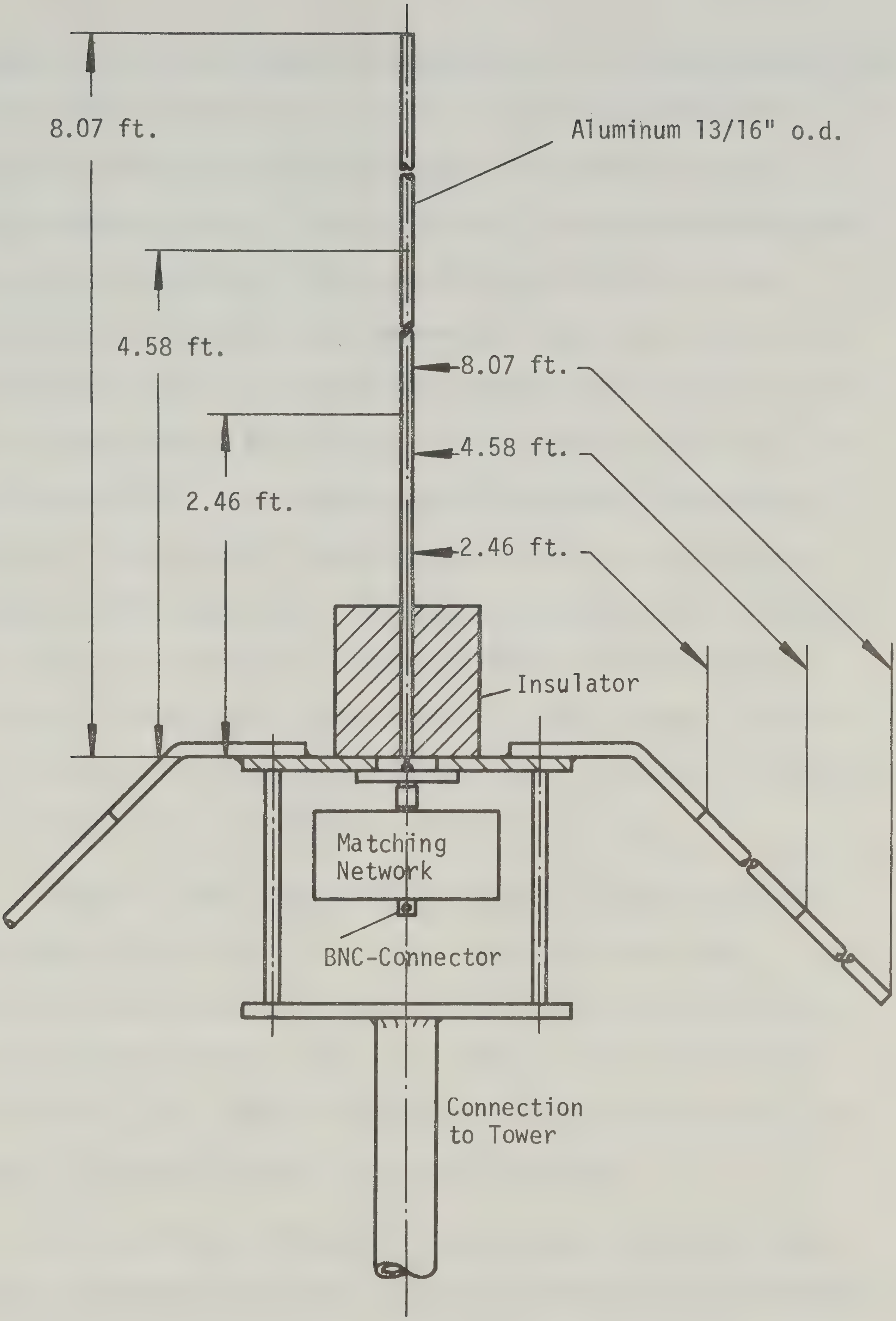

Figure 30. Ground-Plane Antenna

represents a quarter wavelength monopole above a simulated ground-plane. The ground-plane itself consists of four radial conducting arms of one-quarter wavelength, hence it no longer represents an ideal infinite conducting plane. The finite size of the ground-plane causes a tilting of the radiation field upward and away from the ground. To bring the maximum radiation back towards the horizontal plane where the loop antenna would be located, the antenna is modified by bending the four ground-plane arms at an angle of 45 degrees with respect to the horizontal [26]. The construction of the antenna represents an antenna core with conductor lengths tuned to 95 MHz, the shortest wavelength in this experiment. The antennas for the other frequencies, 51 and 95 MHz, were created by simply extending the ground-plane arms to the required quarter wavelength. For this purpose, the ends of the antenna-rod sections were equipped with a thread on the outside and joined by a short pipe connector with inside thread.

Where the input impedance of a one-half wavelength dipole antenna may be found to be 73 + j 42.5 ohms [21], the input impedance of a monopole antenna over perfect ground is given as one-half of the above, that is 36.5 + j 21 ohms. It is reasonable to expect that the input impedance for the constructed antenna will lie somewhere in between these two given limiting values.

It is further indicated in the relevant literature, that for dipole and monopole antennas, the input impedance can be varied by changing the length of the conductors [21]. By shortening the conducting rods from one-quarter wavelength, a significant reduction of the

inductance and a slight reduction of the resistive value can be obtained. Employing this knowledge for the construction of the antenna, the actual input impedance, using a 5% reduction of the conductor length, was found to be as follows:

$$Z_{in} = 19.3 + j\,12.2 \text{ ohms at } 29 \text{ MHz}$$
$$Z_{in} = 29.6 + j\,4.2 \text{ ohms at } 51 \text{ MHz}$$
$$Z_{in} = 31.0 - j\,16.2 \text{ ohms at } 95 \text{ MHz} .$$

The lowering of the inductance promised to simplify the matching network circuitry, since now mainly resistive values had to be transformed. Though the value obtained for the 95 MHz antenna shows a resistive-capacitive result, the reactance was certainly lessened.

The matching networks of the ground-plane antenna were positioned directly at the antenna terminals as shown in Figure 30. An L - C network, different for each frequency as shown in Figure 31, was used. Again, as in the case of the matching network for the Beverage antenna, the required inductors were each set in series with a variable capacitor and the tuning to 50 ohms was accomplished using the impedance meter employed earlier.

If the air capacitors and the fixed value mica capacitors are considered to be lossless, the only losses occur in the high-frequency surface resistance of the inductive air coils. It is possible to show that this value is negligible compared to the resistive portion of the actual antenna input impedance.

The overall antenna efficiency is defined as

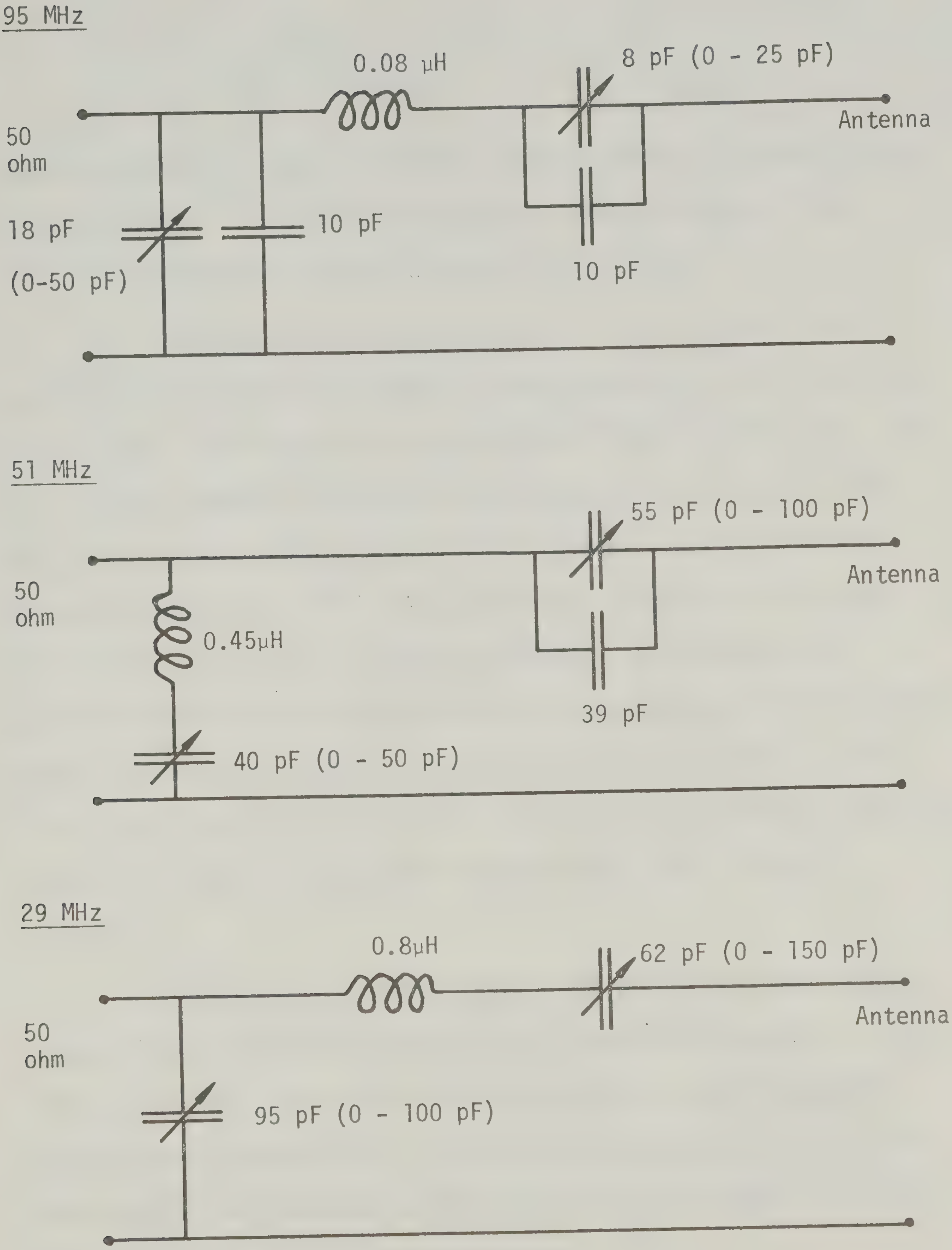

Figure 31. Matching Networks for Ground-Plane Antenna

$$\eta_1 = \frac{R_{rad}}{R_{rad} + R_{conductor}} \quad , \tag{4.2}$$

where no ground or other losses are expected from an elevated ground-plane antenna. It can thus be shown that the efficiency of the matched ground-plane antenna is approximately unity.

The actual ground-plane antenna was now elevated on an extendable metal tower and could be positioned at 8.1, 22.4 and 38.8 feet height. Two of the cases are shown on Plate 1 and Plate 2. At each height, signal transmission measurements were conducted with 500, 1000, 2000 and 4000 feet distance between loop and receiving ground-plane antenna. The loop antenna was directed at all times for maximum signal at the receiving station. To eliminate any possible errors in the instrumentation, each measurement was repeated two to three times, with the loop antenna moved about two or three feet from its previous test point. This method verified the obtained transmitted signal voltages and repeatability could clearly be affirmed.

Figures 32, 33 and 34 display the received signal values for the 8 foot and the 38 foot elevated ground-plane antenna. In all illustrated cases the actual received voltages at the Heterodyne Voltmeter were corrected for the loss which had occurred in the 50-foot coaxial cable connecting the antenna matching network and the receiving instrument. The correction was

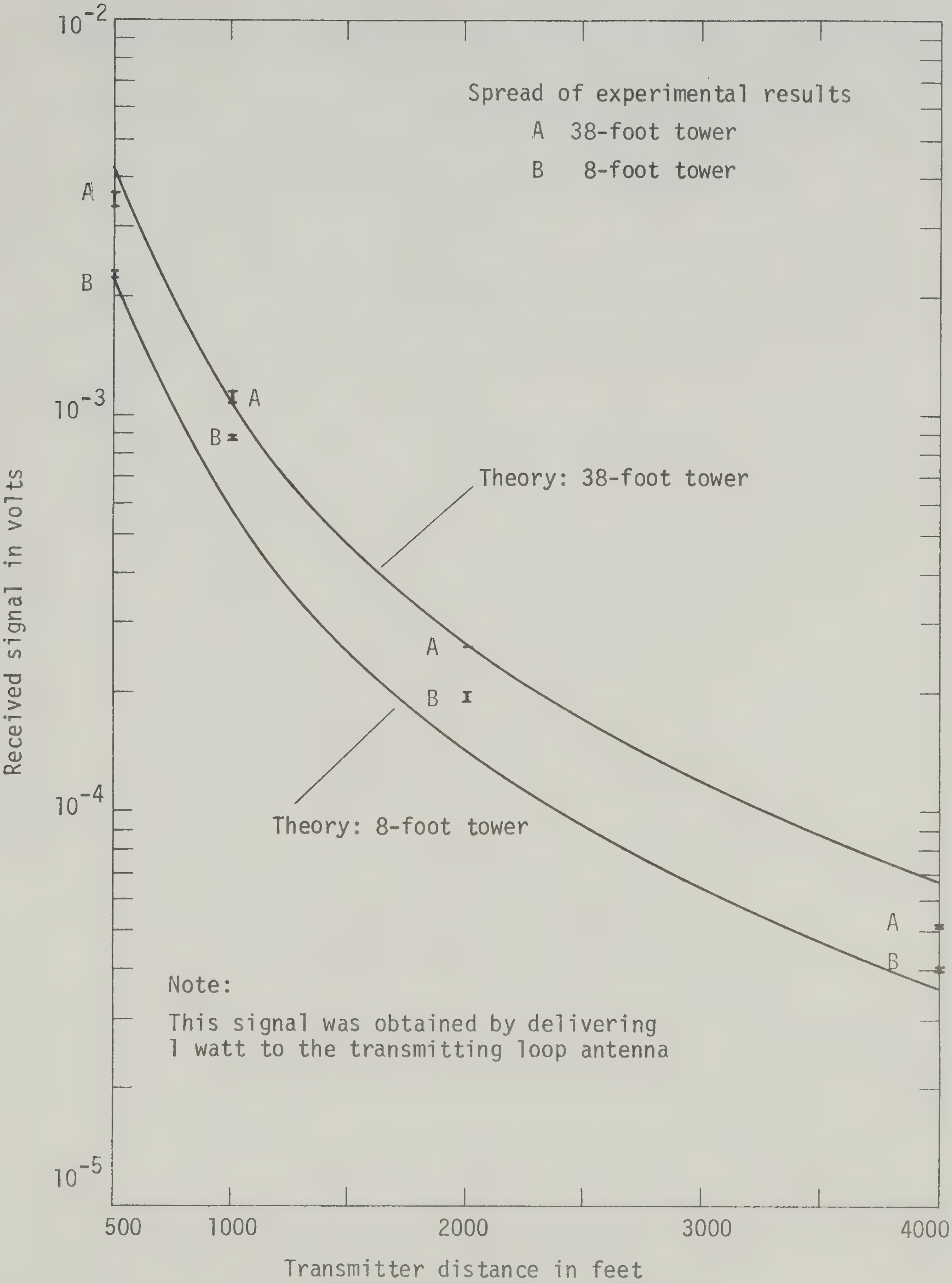

Figure 32. Received Voltage from Elevated Ground-Plane Antenna at 29 MHz

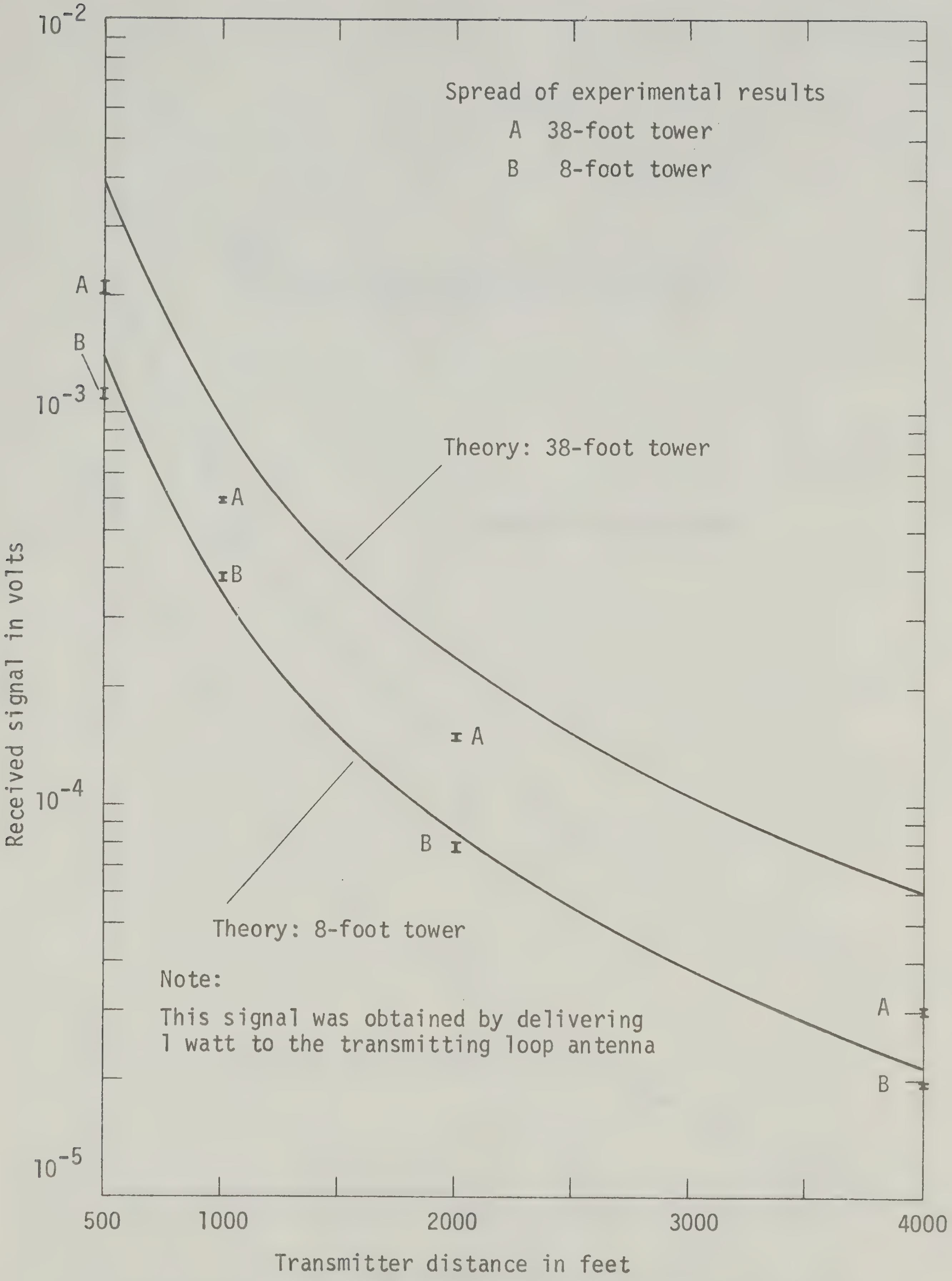

Figure 33. Received Voltage from Elevated Ground-Plane Antenna at 51 MHz

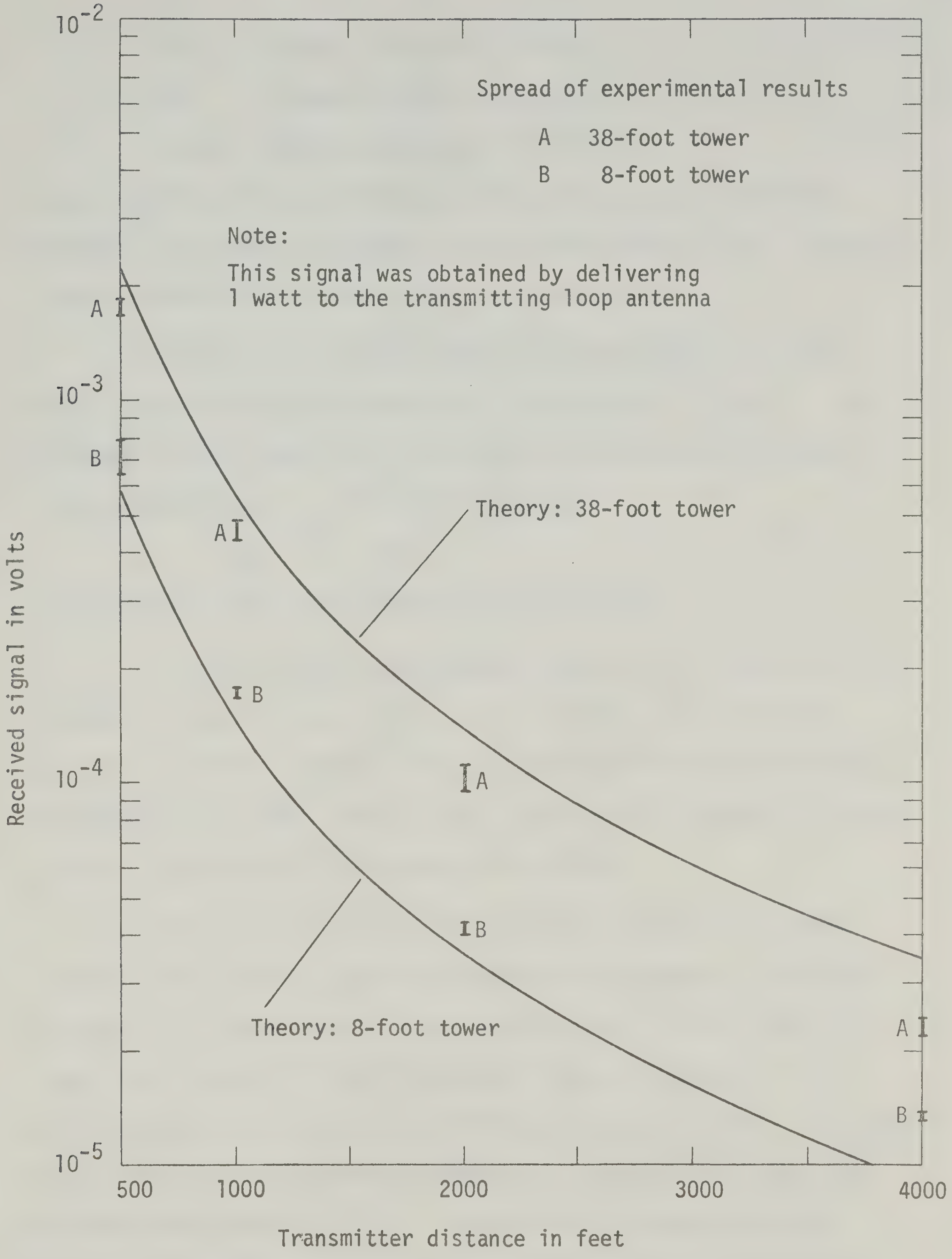

Figure 34. Received Voltage from Elevated Ground-Plane Antenna at 95 MHz

for 29 MHz a factor of 1.125,

for 51 MHz a factor of 1.336

and for 95 MHz a factor of 1.514 .

Thus, in effect, the experimental values in Figure 32, 33 and 34 represent the received voltages at the antenna terminals for a power of 1 watt delivered to the transmitting loop antenna.

To compare the experimentally received signals with the theory, equation (4.1) was employed. The variables h_2 and s were evaluated for the appropriate elevations and transmission distances. The ground constants, $\sigma_g = 0.008$ mhos/meter

and $\varepsilon_r = 15$,

were previously used and justified in Section 3.5.

Figures 32 to 34 also show the theoretically expected signal voltages at 8 and 38-foot height, at the antenna terminals. The deviations occurring between theory and experiment may be estimated to be around 6 dB at most. On the whole, however, the agreement is within 3 dB for the majority of the measurements taken.

Considering now only the theoretical curves of the three figures, it is clearly seen that the lower the frequency, the higher the received voltage, and on the other hand, the less the change of signal with increase in receiving tower height. In general, the theory predicts that as the transmission distance is doubled, the ratio between received and transmitted power will decrease by 12 dB. On the other hand, when $h_2 \gg h_o$, doubling the antenna height will provide an additional gain of 6 dB. If $h_2 \ll h_o$, the received signal is independent of h_2 . In short, the elevation of an

antenna below the value of h_o is of effectively no benefit to the transmission. In the case of the antenna heights and frequencies used, a complex overlapping of the above effects is present. However, the predicted trends are clearly established by the experimental results. At 95 MHz where h_o has its smallest value (in these experiments), there is the largest increase in signal with increasing tower height. Indeed, the measured improvement is approximately 12 dB between 8.1 and 38.8 feet. Ignoring h_o , the theoretical value would be 13.5 dB. As expected, the results at 29 MHz indicate much less improvement with increasing height - less than 6 dB in moving the antenna from 8.1 to 38.8 feet. In this case, $|h_o|$ = 22.1 feet which is comparable to the antenna elevations themselves. In all cases, the attenuation with distance agrees very closely with the theoretical value of 12 dB per octave.

In short, the experimental results verify the approximate theory developed in Appendix A.

CHAPTER V

SUMMARY AND CONCLUSIONS

5.1 Introduction

It was demonstrated in the preceeding chapters that the developed theories closely coincide with the obtained test results. Therefore, it is justifiable to employ the derived theoretical formulations for the prediction of the relative performance of the Beverage and the tower-antenna systems.

Figure 35 shows the theoretically expected received signal for various wire and tower-antenna configurations. The frequency of 51 MHz used in this figure was chosen since most of the actual tests were conducted with this frequency.

It is difficult to determine the most effective method of signal transmission from Figure 35 without first considering the theoretical dependencies and the experimental parameters used. Examination of the theory of the Beverage antenna indicates that a trade-off must be made, concerning its dimensions, between the voltage coupled to the antenna from a loop antenna and the attenuation of the coupled signal along the wire to the receiver. Equations (2.51) and (2.55) show the dependency of the mutual inductance M on the wire height used. Equation (2.46), in turn, illustrates the dependency of the coupled voltage on M and hence, the fact that as the wire height decreases, the signal coupled to the wire will increase. Moreover, as the lateral position of the loop to the wire is reduced, M, and therefore the coupled signal, will become nearly

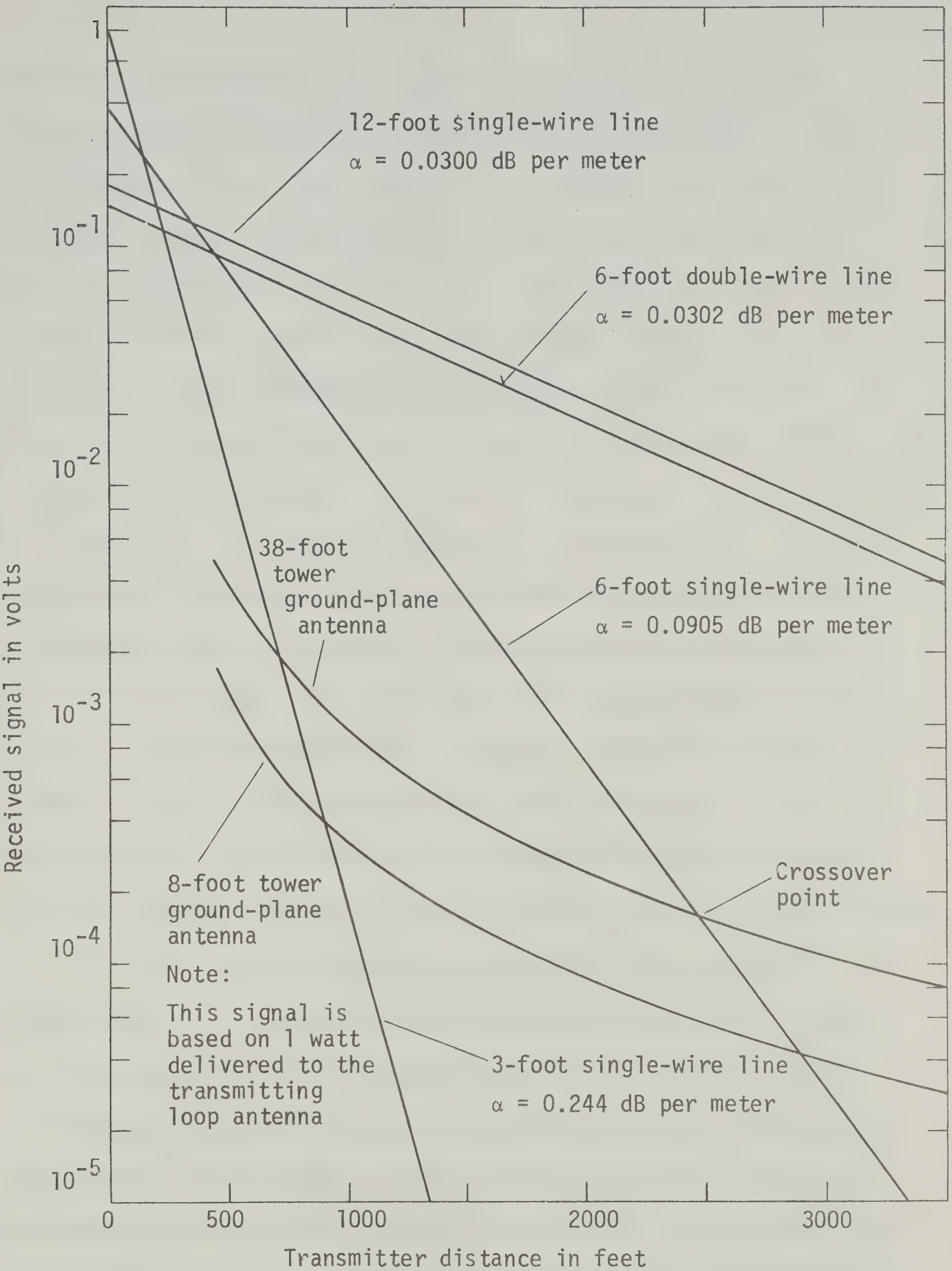

Figure 35. Systems Comparison (theoretical) at 51 MHz

inversly proportional to the height of the spanned wire. This interpretation of equation (2.46) neglects the fact that Z_o also is a variable of the wire height, h . However, this effect is only small because the relation of Z_o to h is logarithmic as seen from equations (2.14) and (2.20). The dependency of the coupled signal on the wire height would clearly suggest the use of a low-wire line, if the attenuation of the coupled signal travelling towards the receiver would not also have to be considered. The attenuation mainly depends, from equation (2.74) or (2.76) on Z_o and h , where Z_o , as earlier stated, is a function of h . As the wire height is decreased, the signal travelling along the wire will become more rapidly attenuated. Thus, except for propagation over very short distances, it is advantageous to increase the wire height as the length of the wire line is extended. Though the coupled signal to the wire will become smaller, the final value of the received signal will be larger as a comparison of signal strengths for the 3-foot, 6-foot and 12-foot wire lines (Figure 35) clearly shows.

As a relative numerical example for the experimental system used, it is interesting to note that the signal coupled to the single-wire line will decrease from 400 mV to 180 mV as the wire height is changed from 6 feet to 12 feet, as seen in Figure 35. At the same time the ground attenuation from equation (2.74) will decrease from 13.8 dB/100 feet to 4.6 dB/100 feet. As a drop of the wire height from 6 feet to 3 feet is considered, the coupled signal will rise from 400 mV to 860 mV, but the attenuation will be so severe thay beyond about 1000 feet the system becomes impractical and

the initial high signal advantage is rapidly lost.

As relatively high wires are favoured for large system ranges, h will increase towards λ. Once the height is of the order of λ, the developed theory for α, the attenuation factor, is not strictly valid. However, in this case, Kikuchi [15, 16] has indicated that even greater reductions in the attenuation can be expected than predicted here as the mode of propagation of the signal changes to a surface wave. These resulting benefits of increased wire height will, of course, be limited by practical considerations concerning construction of the antenna.

It is now interesting to see how the 8-foot and the 38-foot tower antennas compare to the Beverage antennas of different wire heights. In short, for ranges less than the respective crossover points indicated in Figure 35, the wire line delivers more received signal. Beyond these points the tower antennas will be the better choice. Whether or not the larger tower signal beyond the crossover results in an increase of effective systems range, will depend on the transmitted power, and hence, on the received noise level. This subject is explained in more detail in Section 5.3 of this chapter.

A last and interesting comparison within the different antenna systems is the result of the 6-foot double-wire antenna. This system is much better regarding the attenuation along the wire line than the system with only one wire. In fact, the 6-foot double-wire system is comparable to a single-wire of about 12-foot height. The initial low signal coupling to the double wire does not lessen

the apparent advantage regarding the line attenuation in the overall picture. Of course, it is obvious that the stringing of two wires will certainly affect the economy of a tracking system.

Moreover, the double-wire line provides orders of magnitude more signal than the tower-mounted antenna. In the present case it can be shown, using the approach outlined in Appendix A, that at a range of 3000 feet the signal received on the tower antenna can never exceed approximately 3 mV regardless of the tower height. This value at 3000 feet is at least 6 dB lower than the received voltage on the double-wire line.

5.2 Scaling the Results

It has been demonstrated that the theory and experiments of this report match each other with sufficient accuracy. The theory provided in previous chapters will, therefore, predict the received signal strength which may be expected for certain wire configurations at a specific range. Basically, there exist two equations which govern the signal transmission between the loop antenna and the receiving instrument. For the transmission by the single-wire line system, neglecting dielectric and conductor losses

$$|V_R| = \frac{\omega M}{2}\sqrt{\frac{Z_R P_{loop}}{Z_o\left(R_{loop} + \frac{(\omega M)^2}{2 Z_o}\right)}} \exp\left(- \frac{\mathrm{Real}\sqrt{\frac{j\,\omega\mu_o}{\sigma_g + j\,\omega\varepsilon_g}}}{4\,\pi\,Z_o\,h}\; z \right), \tag{5.1}$$

and for the transmission to the ground-plane antenna mounted on a tower,

$$|V_R| = \left(P_{loop}\, 50\, g_1\, g_2\, \eta_1\, \eta_2\, \frac{R_{11}}{R_{A1}}\, \frac{R_{22}}{R_{A2}}\right)^{\frac{1}{2}} \frac{|(h_2 h_o - j h_o^2)|}{s^2} \quad (4.1)\ .$$

These equations may now be used to scale the present results to other power levels and frequencies, to different wire or tower heights and to more realistic loop diameters. It should, however, be remembered that some of the variables necessary for the computation, such as R_{loop} and the antenna efficiency η, were estimated from measured data. In other words, R_{loop} and η cannot be scaled directly because their functional dependence on the parameters is not known.

Consider rewriting equation (3.10) as

$$\eta_1 = \frac{R_{A1}}{R_{loop\ 1}} \quad . \tag{5.2}$$

Since the measured values of efficiency were small at all frequencies it is apparent that $R_{loop\ 1} >> R_{A1}$. Hence,

$$R_{loop\ 1} = R_{A1} + R_{loss\ 1} \approx R_{loss\ 1} \quad . \tag{5.3}$$

The loss resistance, $R_{loss\ 1}$, accounts for copper losses in the antenna as well as for the loss in the conducting ground in the vicinity of the loop. For small loops close to the ground, the ground loss is always orders of magnitude larger than the copper loss, and hence $R_{loss\ 1}$ and $R_{loop\ 1}$ can be expected to be relatively independent of the loop diameter. Thus, assuming σ_g and ε_g are unchanged, the results at 29, 51 and 95 MHz can be scaled to smaller loop diameters by using the existing values of $R_{loop\ 1}$ and by calculating the efficiency from equation (5.2) using the theoretical

expression, $R_{A1} = 2R_{11}$. The functional dependence of R_{11} on the loop diameter is given by equation (3.2).

In order to scale the results to different frequencies it is desirable to first measure η_1 at the new frequency. However, between 29 and 95 MHz first order estimates of η_1, for an 8-inch diameter loop, can be made simply by interpolating between the values measured in this study, assuming σ_g and ε_g are unchanged. R_{loop} at the new frequency can then be determined as described in Chapter III.

5.3 Relative Systems Range

As the results of a variety of calculations based on equations (4.1) and (5.1) of Section 5.2 are evaluated, it becomes quite clear that it is impossible to select one of the two antenna systems as always being superior to the other. More specific requirements such as the system's range and sensitivity are also of importance. To illustrate the relative transmission properties of the system, the following example will be helpful.

Let the power delivered to a loop antenna of 1 inch diameter be 10^{-3} watts at a frequency of 51 MHz. These data represents realistically the case of a small radio-tagged rodent. The loop antenna efficiency of this system can be calculated as described in Section 5.2 to be

$$1.84 \times 10^{-3} \ \% \ .$$

This value is consistent with an empirically estimated efficiency given

by Cochran [4]. For a loop antenna surrounding flesh, he gives

$$\eta = 0.65 \ 10^{-4} \ (\text{freq}_{\text{MHz}} - 20) \ d^{3.5} \ \% \ , \tag{5.4}$$

where d is the loop diameter in inches. In the present case, the above expression will yield

$$2.02 \times 10^{-3} \ \% \ .$$

It must be noted that the efficiency of 1.84×10^{-3} % results from a loop antenna which does not surround flesh. However, as an experimental result, the two values compare satisfactorily.

Figure 36 shows the calculated received voltages for a 38-foot tower-mounted ground-plane antenna and a 6-foot high single-wire Beverage antenna, using the earlier specified variables. It is easily seen that there exists a critical transmission distance, where at a crossover point the received signal of both systems possess the same value.

The system's noise level will set a limit up to which a specific signal can clearly be distinguished. Let the noise level for the chosen system be 3×10^{-7} volts, a value which is quite typical for a receiving system operating in this frequency range. With this limitation on the signal strength, the critical transmitting distance is obviously extended by using the Beverage antenna.

Considering a noise level below the signal strength at the crossover point will certainly favour the use of the tower-mounted receiving antenna. At the crossover point, the slope of the signal

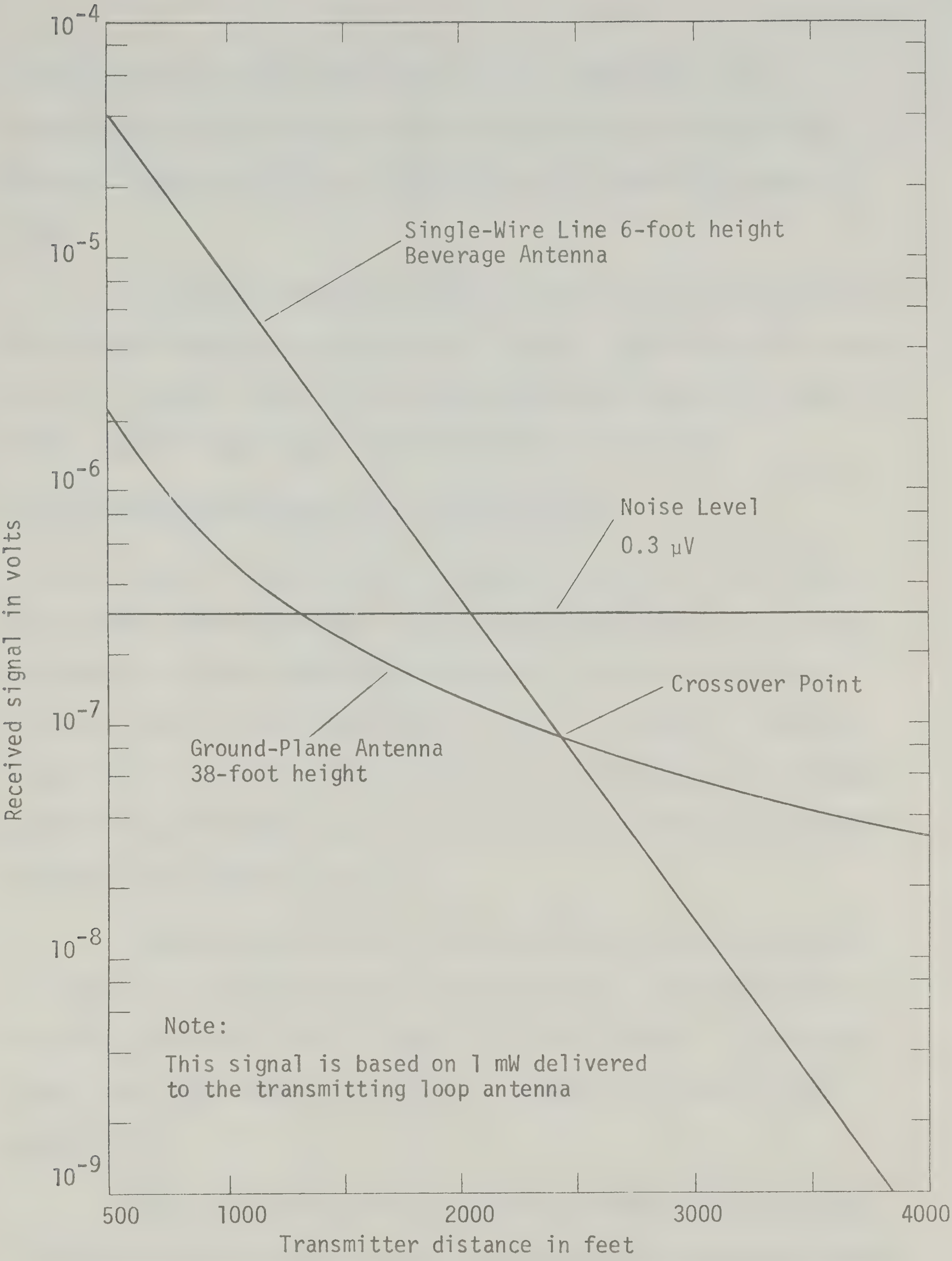

Figure 36. Systems Comparison (practical) at 51 MHz

strength curve for the tower antenna shows significantly less attenuation per transmitting distance than the one of the Beverage antenna. The possible initial advantage of the Beverage antenna is lost.

It should be realized that selecting the ideal antenna system for all applications is not possible. However, the theories developed here for the tower, loop and Beverage antenna will permit a relatively simple systems comparison - one of the goals of this work.

5.4 Wire-Grid System versus Directional Antenna

Consider the problem of finding the direction from which a transmitting source radiates. In a conventional system this is done by mounting a highly directional antenna on a tower of sufficient height to provide the desired range. Provision is made to remotely rotate this antenna to obtain omni-directional coverage. In addition, controlling and indicating devices are necessary to provide continuous readout of the antenna orientation.

Alternatively several Beverage antennas may be arranged as in Figure 37. Depending on the surrounding area, supporting poles or existing trees may be used to keep the wires in place. At the center-point, a multiple switch can be used to locate the signal-carrying antenna wire.

The cost of the number of Beverage antennas participating in this star configuration can be illustrated by the following example. For a one-mile reception radius, allowing at 0.5 miles radius a

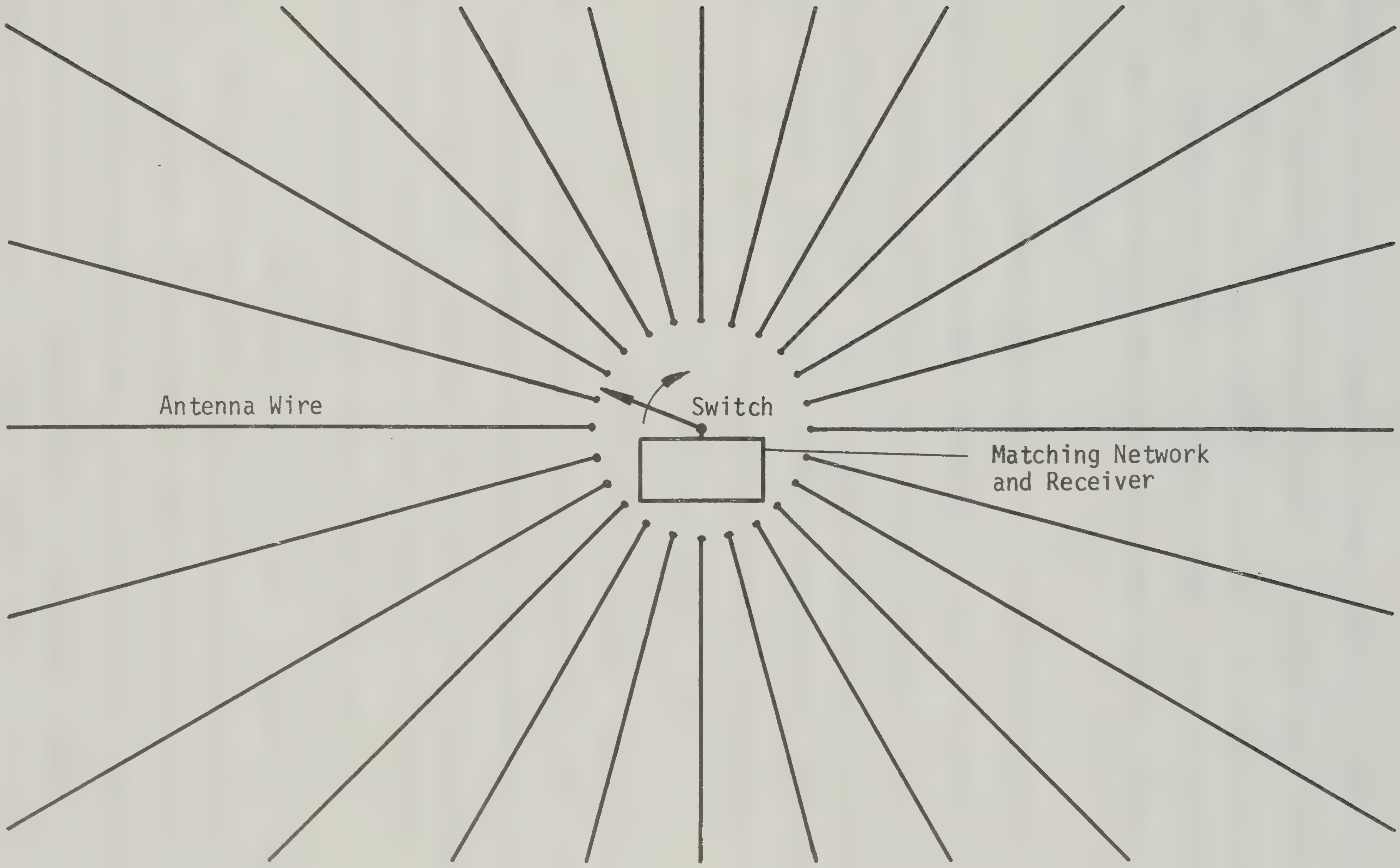

Figure 37. Wire-Star System

separation of the Beverage antennas of about 100 feet, a total of about 166 single wires would be required. An estimation of the wire costs, neglecting even the installation, results in a price of about $15 per 1000 feet for a total of about $13,000. This sum is at least five times the investment necessary for a tower-antenna system of similar capabilities.

Using the Beverage antenna for a smaller sized area will reduce the involved investment drastically, whereas the costs of a tower-antenna system will stay approximately the same as before. This characteristic will make it possible to find some point at which the wire-antenna system will be the most economical one. The result will be that the economy of the Beverage antenna system is restricted to short ranges when area coverage is required.

This restriction does not apply for special applications where only a few wires have to be installed. One use of this kind of system is the monitoring of a small area, as for example a salt lick or a water hole. As pointed out previously, such an application would involve a small overhead grid attached to a long Beverage antenna leading back to some convenient monitoring location.

Often the exact location of an animal is required. In this case several directional tower-mounted antenna systems are usually used to triangulate on the animal. However, when small areas are to be covered the wire-grid systems illustrated in Figures 27 and 38 are not only more economical, but they can provide a more accurate determination of position. As seen in Chapter III, the grid spacing

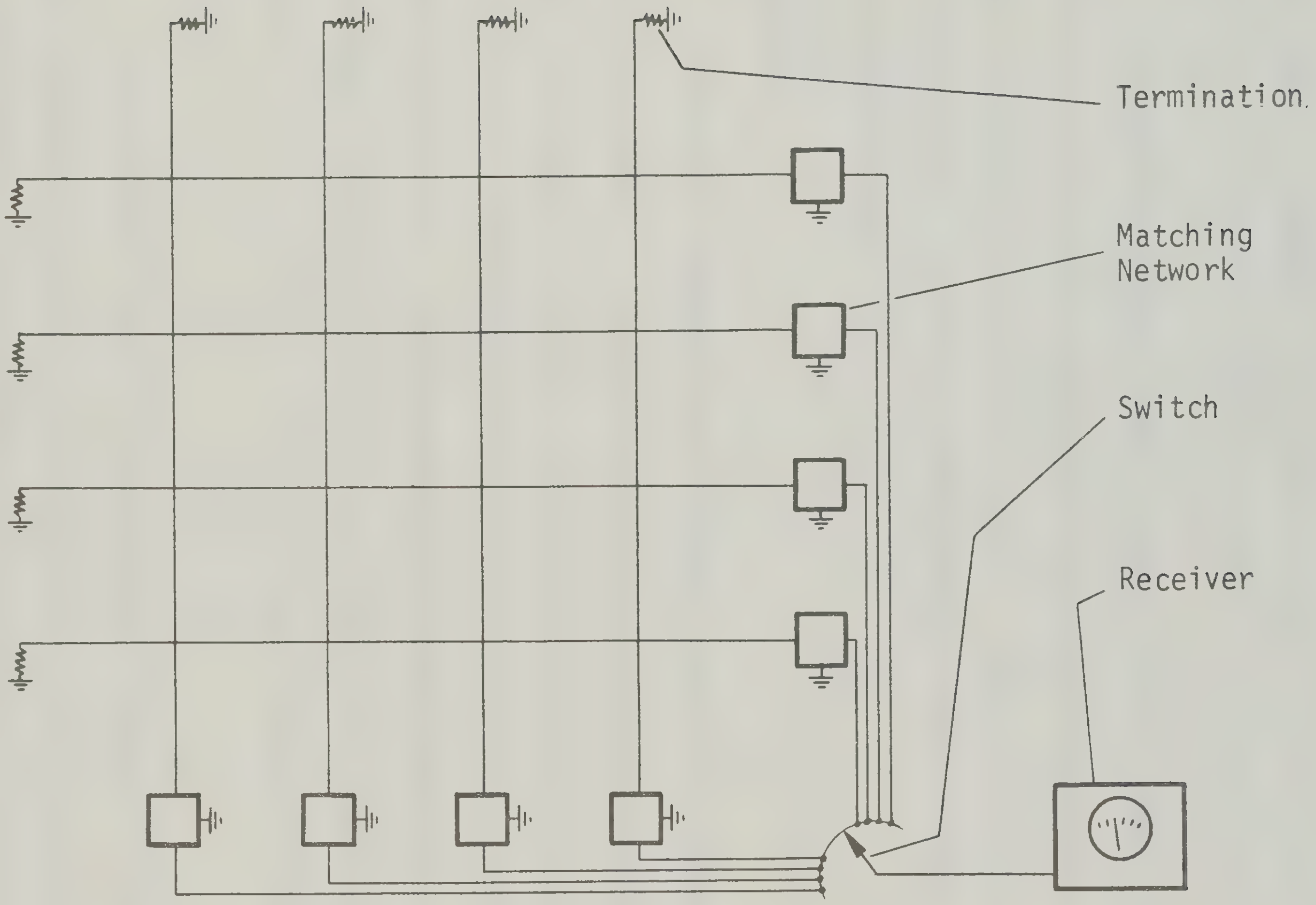

Figure 38. Wire-Grid Locating System

determines the location accuracy. Spacings as small as 5 feet by 5 feet are definitely practical. On the other hand directional antennas suitable for this application rarely have angular resolutions of better than ± 5 degrees. At a range of 500 feet the resulting uncertainty in the position of the transmitter is greater than ± 80 feet.

The author believes that a system like that shown in Figure 38 represents one of the best uses for the Beverage antenna in biotelemetry. For this small system, low cost, accurate results, easy construction and use, as well as independence of loop orientations are the relative merits.

5.5 Conclusions

The previous chapters and sections show the development of a theory by which means it is possible to evaluate the advantages of the Beverage antenna system relative to a tower-mounted antenna system. In general, it was found that neither of the systems was superior to the other in all cases. The tower-mounted antenna seems to be better for large-range telemetry. The Beverage antenna and the wire-grid configurations derived from it offer better performance for small area coverage.

A wide range of uses for the wire-grid method is possible. The author estimates, that as long as the grid area is within the size of up to about 500 by 500 feet, the construction cost will stay within tolerable limits. This restriction does not exclude the possibility that several small grid areas of special interest, such as salt licks or water holes, might be connected by a single-wire line to a larger

system over distances of more than 500 feet. Such a scheme would permit the use of very low power long-life transmitter packages on the animals. Then only when they used the area would a signal be coupled to the line. Further, by using somewhat lower frequencies, it is to be expected that the grid system will prove valuable for the tracking of burrowing animals below the ground surface. The first application of the presented theory is already in progress with the construction of a wire-grid system for the observation of red backed voles in the Northwest Territories of Canada.

With the orientation of man towards the exploration, protection and restoration of the environment, the Beverage antenna system will undoubtedly find further applications in the future.

REFERENCES

1. Adams, L., and Smith, W.C., "Wildlife Telemetry", National Telemetering Conference Proceedings, p. 2-3, 1964.

2. Craighead, F.C. Jr. and Craighead, J.J., "Tracking Grizzly Bears", Bio-Science, vol. 15, p. 88, Feb. 1965.

3. Mackay, R.S., Bio-Medical Telemetry, p. 57, J. Wiley and Sons, Inc., 1970.

4. Slater, L.E., Bio-Telemetry, p. 149, The Macmillan Co., 1963.

5. Beverage, H.H., Rice, C.W., Kellog, E.W., "The Wave Antenna", A.I.E.E., vol. 42, p. 258, March 1923.

6. Eckersley, T.L., "The Beverage Aerial", The Electrician, vol. 92, p. 39, Jan. 11, 1924.

7. Manneback, C., "Radiation from Transmission Lines", Jour. A.I.E.E., vol. 42, p. 95, Feb. 1923.

8. Manneback, C., "Radiation from Transmission Lines - Continued Discussions", Jour. A.I.E.E., vol. 42, p. 1362, Dec. 1923.

9. Storer, J.E., and King, R., "Radiation Resistance of a Two-Wire Line", Proc. I.R.E., vol. 39, p. 1408, Nov. 1951.

10. Jenssen, M., "On Radiation from Overhead Transmission Lines", Proc. I.E.E., vol. 97, part III, p. 166, May 1950.

11. Knight, P., "Propagation Coefficient of the Beverage Aerial", Proc. I.E.E., vol. 119, p. 821, July 1972.

12. Wise, W.H., "Propagation of High-Frequency Currents in Ground Return Circuits", Proc. I.R.E., vol. 22, p. 522, April 1934.

13. Walmsley, T., "Distribution of Radiation Resistance in Open Wire Radio Transmission Lines", Phil. Magazine and Jour. of Science, vol. 12, p. 392.

14. Carson, J.R., "Wave Propagation in Overhead Wires with Ground Return", Bell Tech. Jour., vol. 5, p. 539, Oct. 1926.

15. Kikuchi, H., "Electromagnetic Fields on an Infinite Wire above a Plane Earth at High Frequencies", Bull. Electrotech. Lab. (Tokyo), vol. 21, no. 6, p. 439, June 1957. - In Japanese -

16. Kikuchi, H., "Wave Propagation along an Infinite Wire above the Ground in the High-Frequency Region", Bull. Electrotech. Lab. (Tokyo), vol. 21, no. 1, p. 49, Jan. 1957. - In English -

17. Pollaczek, F., "Ueber die Felder der Wechselstromleitung mit Erde und der Horizontalantenne", Electrische Nachrichten Technik Berlin, vol. 4, p. 295, July 1927 and p. 515, Dec. 1927.

18. Pollaczek, F., "Ueber das Feld einer unendlich langen wechselstromdurchflossenen Einfachleitung", Electrische Nachrichten Technik Berlin, vol. 3, p. 339, Sept. 1926.

19. Harrison, C.W., Jr., "The Response of a Terminated Two-Wire Line Suspended in Air Above a Semi-Infinite Dissipative Medium and Excited by a Plane-Wave RF Field Generated in Free Space", Transact. I.E.E.E., vol. EMC - 11, p. 149, Nov. 1969.

20. Wait, J.R., "On the Impedance of Long Wire Suspended Over the Ground", Proc. I.R.E., vol. 49, p. 1576, Oct. 1961.

21. Jordan, E.C., Balmain, K.G., Electromagnetic Waves and Radiating Systems, Prentice Hall, Inc., 1968.

22. Saha, J.N., "The Radio Interference Field of an Overhead Transmission Line", Transact. I.E.E.E., vol. EMC - 13, p. 38, Nov. 1971.

23. Ramo, S., Whinnery, J.R., Van Duzer, T., "Fields and Waves in Communication Electronics", John Wiley & Sons, Inc., 1965.

24. Tyras, G., Radiation and Propagation of Electromagnetic Waves, Academic Press, 1969.

25. Jasik, H., Antenna Engineering Handbook, McGraw-Hill, 1961.

26. Kraus, J.D., Antennas, McGraw-Hill, 1950.

27. Schelkunoff, S.A., Friis, H.T., Antennas, Theory and Practice, John Wiley & Sons, Inc., 1952.

28. Libby, L.L., "Special Aspects of Balanced Shielded Loops", Proc. I.R.E., vol.34 , p. 641, Sept. 1946.

29. H.W. Sams & Co., Inc., Reference Data for Radio Engineers, 1969.

30. Reich, H.J., Ordung, P.R.,Kraus, H.L., Skalnik, J.G., Microwave Theory and Techniques, D. Van Nostrand Company, Inc., 1953.

31. Bullington, K., "Radio Propagation at Frequencies Above 30 Megacycles", Proc. I.R.E., vol. 35, p. 1122, Oct. 1947.

32. Burrows, C.R., "Radio Propagation Over Plane Earth - Field Strength Curves", Bell System Tech. Journal, vol. 16, p. 45, Jan. 1937.

33. Norton, K.A., "The Propagation of Radio Waves over the Surface of the Earth and in the Upper Atmosphere", Proc. I.R.E., vol. 24, p. 1367, Oct. 1936, vol. 25, p. 1203, Sept. 1937.

APPENDIX A

POWER TRANSFER BETWEEN TWO ANTENNAS

It is the intention of this appendix to develop a theory for the power transfer between two elevated antennas including the ground effects on the radio wave propagation.

The principal effect of the plane earth on the propagation of radio waves is indicated by the following equation [31, 32, 33]:

$$\overline{E}_a = \overline{E}_o \left[1 + R\, e^{j\Delta} + (1 - R)\, F\, e^{j\Delta}\right] \quad . \tag{A.1}$$

The three terms represent the direct, reflected and the surface wave respectively. $\overline{E}_o$ is the electric field of the particular antenna used, as it would be in free space but with the same terminal current as in the actual situation. R describes the ground reflection coefficient and, F, the surface-wave attenuation factor. Δ is the phase difference due to wave path inequalities as explained on the following pages.

Additional terms could be added to the equation, accounting for induction fields and secondary effects of the ground. The actual fields, however, are expected to vary by up to several dB due to experimental errors and nonideal conditions in any case.

Since the above equation is developed mainly for the purpose of relating it to experimental results, one may neglect these second-order terms.

Figure 39 shows how the direct wave, reflected wave and surface wave are propagated in a two medium space of air and earth. Both antennas are considered as having vertically polarized electric fields.

For the ground with loss, the intrinsic impedance and the propagation constant are, respectively,

$$\eta_g = \sqrt{\frac{j\omega\mu}{\sigma_g + j\omega\varepsilon_g}} \qquad \text{(A.2)}$$

and

$$k_g = \sqrt{\omega^2 \mu \varepsilon_g - j\omega \mu \sigma_g} \quad . \qquad \text{(A.3)}$$

For the air space,

$$\eta_a = \sqrt{\frac{\mu_o}{\varepsilon_o}} \qquad \text{(A.4)}$$

and

$$k_a = \sqrt{\omega^2 \mu_o \varepsilon_o} \quad . \qquad \text{(A.5)}$$

For all practial purposes the ground is non-magnetic and so,

$$\mu = \mu_o \quad . \qquad \text{(A.6)}$$

Figure 40 shows the vertically polarized E-field at the ground level, as it is transmitted into the ground and reflected back into space. It is possible to show for this case, that the ground reflection coefficient, R , is given by

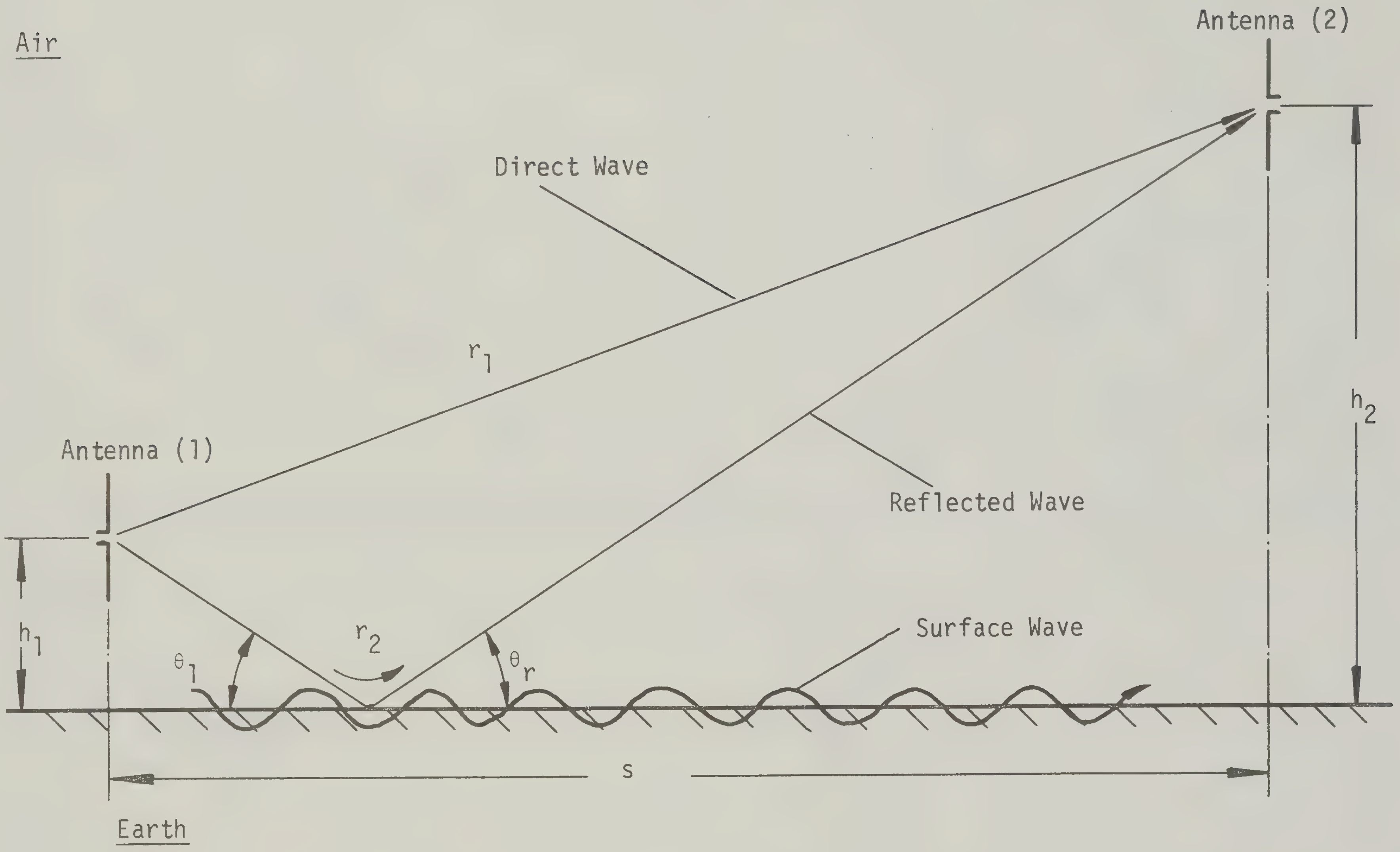

Figure 39. Antenna Transmission

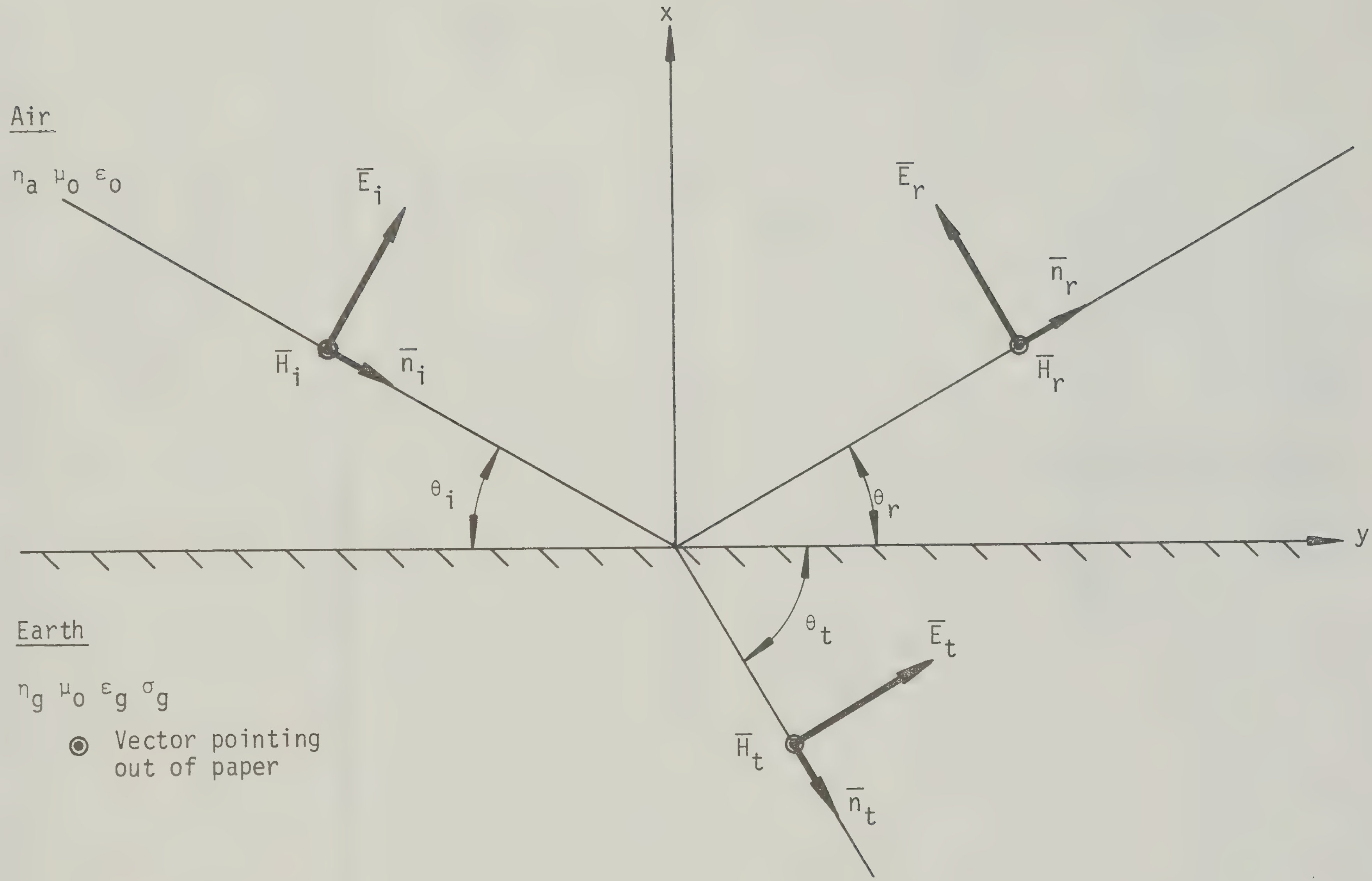

Figure 40. Reflected Vertically Polarized E-Wave

$$R = \frac{\overline{H}_r}{\overline{H}_i} = \frac{\eta_a \sin\theta_i - \eta_g \sin\theta_t}{\eta_a \sin\theta_i + \eta_g \sin\theta_t} \tag{A.7a}$$

and

$$R = \frac{(\varepsilon_r - jX)\sin\theta_i - \sqrt{(\varepsilon_r - jX) - \cos^2\theta_i}}{(\varepsilon_r - jX)\sin\theta_i + \sqrt{(\varepsilon_r - jX) - \cos^2\theta_i}} \quad , \tag{A.7b}$$

where

$$\varepsilon_r = \frac{\varepsilon_g}{\varepsilon_o} \tag{A.8}$$

and

$$X = \frac{\sigma_g}{\omega\varepsilon_o} \quad . \tag{A.9}$$

Referring to Figure 39, when $h_1 + h_2 << s$,

$$\sin\theta_i = \theta_i \tag{A.10}$$

and

$$\cos^2\theta_i = 1 \quad . \tag{A.11}$$

This assumption proves to be accurate for the final result within one percent.

By defining,

$$Z = \frac{\sqrt{(\varepsilon_r - 1) - jX}}{\varepsilon_r - jX} \tag{A.12}$$

and using the above approximations, equation (A.7b) can be written as

$$R = \frac{\theta_i - Z}{\theta_i + Z} \quad . \tag{A.13}$$

E.C. Jordan and K.G. Balmain [21] state the surface wave attenuation function as

$$F = 1 - j\sqrt{\pi\omega}\ e^{-\omega}\ \mathrm{erfc}\,(j\sqrt{\omega}\,) \tag{A.14}$$

for a vertical polarized E-field, where

$$\omega = \frac{-jk_a\, r_2\, u^2(1 - u^2 \cos^2\theta_i)}{2} \left[1 + \frac{\sin\theta_i}{u\sqrt{1-u^2\cos^2\theta_i}} \right]^2 , \tag{A.15}$$

$$u^2 = \frac{1}{\varepsilon_r - jX} \tag{A.16}$$

and

$$\mathrm{erfc}\,(j\sqrt{\omega}\,) = \frac{2}{\sqrt{\pi}} \int_{j\sqrt{\pi}}^{\infty} e^{-v^2}\, dv \quad . \tag{A.17}$$

Using the previous approximations, equation (A.15) yields

$$\omega = \frac{-j\, k_a\, r_2\, u^2}{2} \quad . \tag{A.18}$$

The error function, equation (A.17), can be expressed by its asymptotic expansion,

$$\mathrm{erfc}(x) \approx \frac{e^{-x^2}}{\sqrt{\pi}\, x} \left(1 - \frac{1}{2x^2} + \frac{1\cdot 3}{(2x^2)^2} - \frac{1\cdot 3\cdot 5}{(2x^2)^3} + \ldots\right) . \tag{A.19}$$

For the range of the experimental comparison planned, the

third and higher order terms of the expansion may be neglected. Including these terms affects the final expressions for the power transfer by an amount smaller than the experimental errors inherent in such a comparison.

Equation (A.14) thus becomes, using equation (A.18) and (A.19),

$$F = -j \frac{\lambda}{2\pi r_2 u^2} \quad . \tag{A.20}$$

Or, when $\varepsilon_g >> \varepsilon_o$ it is $u^2 = Z^2$, and so

$$F = -j \frac{\lambda}{2\pi r_2 Z^2} \quad . \tag{A.21}$$

Referring to Figure 39, the phase difference resulting from the inequality of the propagation paths is defined as

$$\Delta = k (r_2 - r_1) \quad . \tag{A.22}$$

For the purpose of this report, only the signal transmission from an antenna directly at ground level has to be considered, which will result in

$$h_1 = 0 \tag{A.23}$$

and consequently,

$$\Delta = 0 \quad . \tag{A.24}$$

Equation (A.1) may now be rewritten with the aid of equations (A.13), (A.20) and (A.24) as

$$\overline{E}_a = \overline{E}_o \left[\frac{2\theta_i}{\theta_i + Z} + \left(\frac{2\,Z}{\theta_i + Z} \right) \left(-j \frac{\lambda}{2\pi\, r_2\, Z^2} \right) \right] . \tag{A.25}$$

But, for the range of the experimental values,

$$\theta_i << Z \tag{A.26}$$

and

$$r_2 \approx s \quad . \tag{A.27}$$

Thus, with the introduction of the minimum effective antenna height as

$$h_o = \frac{\lambda}{2\pi Z} \quad , \tag{A.28}$$

equation (A.25) will change to

$$\overline{E}_a = \overline{E}_o \, \frac{4\pi}{\lambda s} \left[h_2\, h_o - j\, h_o^{\,2} \right] . \tag{A.29}$$

Use has been made of the fact that when $h_1 + h_2 << s$,

$$\theta_i = \frac{h_1 + h_2}{s} = \frac{h_2}{s} \tag{A.30}$$

when $h_1 = o$.

It is now possible to calculate the received power at antenna (2), the receiving antenna, in terms of the power delivered to

antenna (1), the transmitting antenna.

The power density in watts per unit area created by antenna (1) at the position of antenna (2) is obtained from Poynting's Theorem as

$$p_2 = \frac{1}{2} \frac{|\bar{E}_a|^2}{\eta_a} , \tag{A.31}$$

where the intrinsic impedance of free space is

$$\eta_a = 120 \pi . \tag{A.32}$$

Therefore,

$$p_2 = \frac{1}{2} \frac{|\bar{E}_o|^2}{\eta_a} \frac{|\bar{E}_a|^2}{|\bar{E}_o|^2} = p_2' \frac{|\bar{E}_a|^2}{|\bar{E}_o|^2} \tag{A.33}$$

where p_2' is the power density that would be produced by the antenna if it were situated in free space, carrying the same current as in the actual location.

Now the free-space gain of an antenna may be defined as [26]

$$g = \frac{4\pi s^2 p}{P_r} , \tag{A.34}$$

where P_r is the radiated power from the antenna, and p is the power density produced by the antenna at some specified location, a distance s from the antenna. Thus,

$$p_2' = \frac{g_1 P_{r1}}{4\pi s^2} \tag{A.35}$$

and g_1 is the gain of antenna (1) in the direction of the receiving antenna (2). P_{r1} is the power radiated from antenna (1) assuming it is located in free space, and s is the distance between the transmitting and receiving antennas.

This radiated power is given in terms of the rms antenna terminal current as

$$P_{r1} = I^2 R_{11} \quad , \tag{A.36}$$

where R_{11} is the radiation resistance of the transmitting antenna (1) in free space, referred to the antenna terminals. Also, if P_{tx} is the power delivered to the antenna (1) in its actual location near the ground,

$$P_{tx} = I^2 (R_{A1} + R_{loss\ 1}) \; , \tag{A.37}$$

where R_{A1} represents the radiation resistance of antenna (1) in the presence of the ground, referred to the antenna terminals, and $R_{loss\ 1}$ is the summation of conductor and ground losses in antenna (1), referred to the antenna terminals.

Hence, using equations (A.36) and (A.37),

$$P_{r1} = P_{tx} \frac{R_{11}}{R_{A1} + R_{loss\ 1}} \tag{A.38}$$

which may be substituted into equation (A.33) with the aid of equation (A.35), to give

$$p_2 = \frac{g_1}{4\pi s^2} \; P_{tx} \; \frac{|\bar{E}_a|^2}{|\bar{E}_o|^2} \; \frac{R_{11}}{R_{A1}} \; \eta_1 \quad , \tag{A.39}$$

where η_1 is the actual radiation efficiency of antenna (1) and is defined as

$$\eta_1 = \frac{R_{A1}}{R_{A1} + R_{\text{loss }1}} \quad . \tag{A.40}$$

Finally, the received power at antenna (2) may be expressed in terms of p_2 as indicated in Figure 41.

The equivalent generator represents the open voltage induced across the terminals $a - b$ of the receiving antenna by the incident electric field. The impedance R_{in} is the sum of the radiation resistance of antenna (2) in the presence of the ground, that is R_{A2}, and the conductor and ground loss resistances referred to the terminals, so that,

$$R_{in} = R_{A2} + R_{\text{loss }2} \; . \tag{A.41}$$

The power received by a matched-receiving system is given by

$$P_{rx} = \frac{1}{8} \; \frac{|\bar{V}_{oc}|^2}{R_{in}} \quad . \tag{A.42}$$

Multiplying and dividing by p_2 from equation (A.31) will result in

$$P_{rx} = p_2 \, \frac{1}{4} \, \eta_a \; \frac{|\bar{V}_{oc}|^2}{|\bar{E}_a|^2} \; \frac{1}{R_{in}} \quad . \tag{A.43}$$

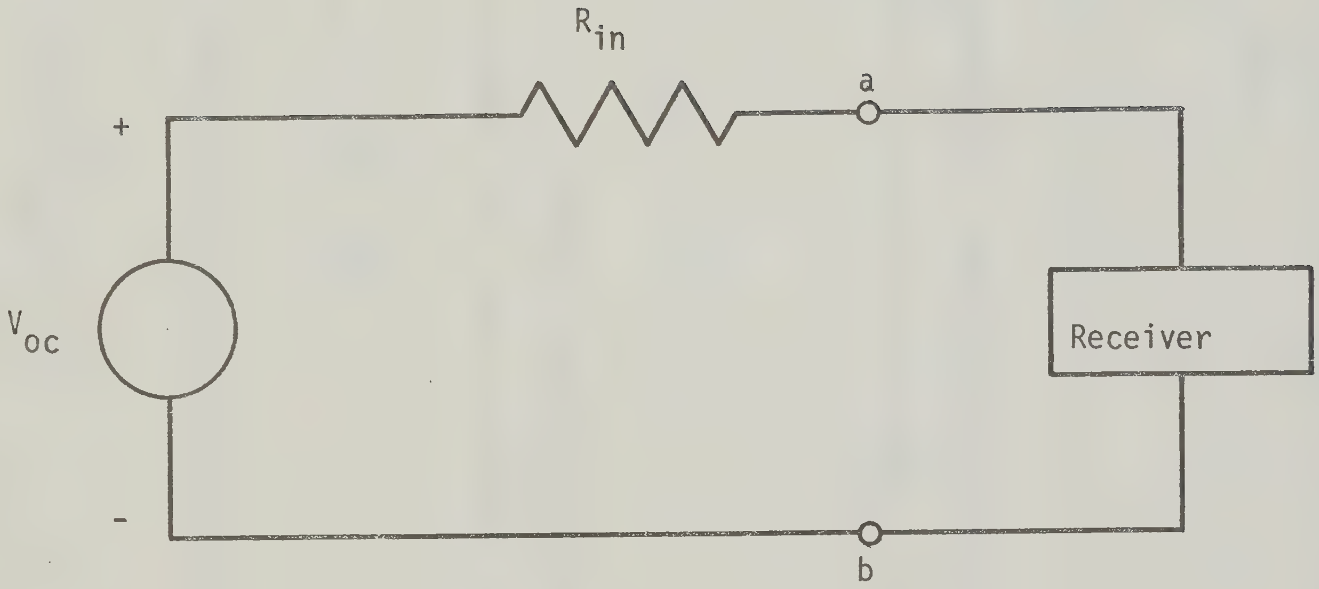

Figure 41. Receiving System

However,

$$|\overline{V}_{oc}|^2 = C\ |\overline{E}_a|^2 \tag{A.44}$$

where C is a constant that depends on the type and orientation of the antenna. Thus,

$$P_{rx} = p_2 \frac{1}{4}\ \eta_a\ \frac{C}{R_{in}} \ . \tag{A.45}$$

If R_{22} represents the radiation resistance of antenna (2) in free space, referred to the antenna terminals, it can be shown [26], that the quantity,

$$\frac{1}{4}\ \eta_a\ \frac{C}{R_{22}} = \frac{\lambda^2 g_2}{4\pi} \ . \tag{A.46}$$

In this case g_2 is the free space gain of antenna (2) in the direction of antenna (1). Hence, equation (A.45) becomes

$$P_{rx} = p_2 \frac{\lambda^2 g_2}{4\pi}\ \frac{R_{22}}{R_{in}} \ . \tag{A.47}$$

Defining the receiving efficiency of antenna (2) as

$$\eta_2 = \frac{R_{A2}}{R_{A2} + R_{loss\ 2}} \ , \tag{A.48}$$

equation (A.47) may be written as

$$P_{rx} = p_2 \frac{\lambda^2 g_2}{4\pi} \frac{R_{22}}{R_{A2}} \eta_2 \quad . \tag{A.49}$$

Finally, the use of equation (A.39) permits the expression of the power transfer between the two antennas in the form

$$\frac{P_{rx}}{P_{tx}} = \left(\frac{\lambda}{4\pi s} \right)^2 g_1 \, g_2 \, \eta_1 \, \eta_2 \frac{R_{11}}{R_{A1}} \frac{R_{22}}{R_{A2}} \frac{|\bar{E}_a|^2}{|\bar{E}_o|^2} \quad . \tag{A.50}$$

Thus, from equation (A.29),

$$\frac{P_{rx}}{P_{tx}} = \frac{1}{s^4} g_1 \, g_2 \, \eta_1 \, \eta_2 \frac{R_{11}}{R_{A1}} \frac{R_{22}}{R_{A2}} |(h_2 h_o - j \, h_o^2)|^2 \quad . \tag{A.51}$$

B30068